FLUORESCENCE STUDIES OF AROMATIC MOLECULES IN MICELLES

A thesis submitted to the
Australian National University
for the degree of
Doctor of Philosophy

by

KHUANGA

CANBERRA, A.C.T.

July 1976

The material presented in this thesis is my own original work, except where reference is made to the work of others. The following papers have been published in the course of this work:

U Khuanga, Ben K. Selinger and Rod McDonald, 1976. "A Study of Surfactant Micelles with a Fluorescent Probe", *Aust. J. Chem.* 29, 1.

U Khuanga, Rod McDonald and Ben Selinger, 1976. "Excited State Processes in Surfactant Micelles", *Theodor Förster Memorial Issue, Z. Physik. Chem. N.F.* 101 (in press).

U Khuanga, Rod McDonald and Ben Selinger, 1976. "Fluorescence Studies of Protolytic Reactions in Micelles". Accepted for presentation at the Tenth Australian Spectroscopy Conference, August, Perth, W.A.

Khuanga

KHUANGA

ACKNOWLEDGEMENTS

My thanks go to Dr. Ben Selinger and Dr. Rod McDonald for their guidance and encouragement throughout the course of this work. I thank my fellow students: Dr. Phil Nott, Jim O'Brien, Chris Harris and Alan Hinde for their help and co-operation.

My thanks also to Dr. Andrew Watkins for many useful discussions and Professor Bryan Henry for his advice. My gratitude to Professor Ian Ross for his help and hospitality. I am grateful for the assistance provided by the technical staff of the Chemistry Department, Australian National University.

I thank Miss Norma Chin for her competence in typing this thesis. My gratitude to my wife, Mawii, for her understanding and support.

Finally, I should like to thank the Socialist Republic of the Union of Burma, and the Colombo Plan Award Scheme of the Australian Government for the Scholarship to carry out this work.

C O N T E N T S

LIST OF FIGURES

LIST OF TABLES

CHAPTER 1

INTRODUCTION

Surfactants are amphiphilic, organic or organometallic compounds. Amphiphilic substances, or amphiphiles, are molecules possessing distinct regions of hydrophobic and hydrophilic character. When amphiphilic molecules are dissolved in water they can achieve segregation of their hydrophobic portions from the solvent by self-aggregation. The aggregated products, known as micelles, consist of a hydrocarbon core with polar groups at the surface which serve to maintain the solubility of the amphiphile in water. The state of knowledge about micellization has been discussed over the years by the following authors [Shinoda, Nakagawa, Tamamushi and Isemura 1963; Shinoda 1967; Schick 1967; Elworthy, Florence and Macfarlane 1968; Jungermann 1970; Tanford 1973; Fendler and Fendler 1975].

As well as being important compounds in the pharmaceutical and detergent industries, surfactant molecules are analogous to the lipids present in biological membranes. Thus the understanding of micellar systems can provide models for studying the more complicated biological macromolecules. Surfactant molecules normally contain a strongly hydrophilic head group and one long hydrocarbon tail, but lipids may have one or more (most often two) hydrocarbon tails attached to the head group. This thesis is concerned only with the amphiphile molecules which have one hydrocarbon tail attached to the polar head group. The

application of the techniques outlined in this thesis to those micelles formed by amphiphile molecules which have two hydrocarbon tails attached to the polar head group may be profitable for the further understanding of lipid systems. Despite the research which has been carried out in the field of surfactants, there remains much to be learned about the micellization process.

The physical properties of micelles, such as the size, shape and charge, have been investigated with techniques such as light scattering, ultracentrifugation, diffusion, viscosity and X-ray diffraction. The ability of micelles to dissolve hydrocarbons and other hydrophobic substances makes it possible to insert aromatic molecules inside the micelles. Thus the spectroscopic studies of aromatic molecules in micelles provides a widely-used technique for the investigation of micellar systems.

The position of the solubilizate in the micelle can be determined from a study of changes in the ultraviolet absorption spectra — for example, the wavelength of maximum absorption, and the vibrational fine structure of several aromatic solubilizates. A resemblance between the absorption spectra of the solubilizate in the micellar phase and that in polar solvents is generally interpreted as implying a polar environment for the substrate in the micelle [Riegelman, Allawala, Hrenoff and Strait 1958]. Conversely, a similarity between the absorption spectrum in the micellar solution and that in nonpolar solvents seems to indicate that the substrate is solubilized in a hydrocarbon-like environment [Riegelman *et al.* 1958]. The ultraviolet and visible absorption spectroscopic studies also provide a simple and useful technique for the determination of the critical micelle concentration (CMC) of surfactants. The CMC of a surfactant is

extracted from a plot of the absorbance of an appropriate dye against the concentration of the surfactant [Corrin and Harkins 1946a and 1946b].

The site of incorporation of solubilizates in micellar systems has also been investigated with proton nuclear magnetic resonance spectroscopy. Since both nuclear magnetic resonance frequencies (chemical shifts) and line widths are dependent on the molecular environment of the nuclei, changes in these parameters for solubilizates and surfactants as a function of concentration can provide precise information on the location of a solubilizate with respect to the micellar nuclei. In addition, comparison of the chemical shifts of a solubilizate in micellar systems with those in polar and nonpolar solvents can be used to obtain information on the nature of the environment of the solubilizate [Eriksson 1963; Eriksson and Gillberg 1966]. Similar information on the location of substrates in micellar systems can be obtained using electron spin resonance spectroscopy [Hamilton and McConnell 1968; Griffith and Waggoner 1969]. The combined data obtained by PMR and absorption spectroscopy not only establishes the average solubilization sites but also indicates the nature of the environment of the micellar solubilization site.

The development of new experimental techniques has played a major role in the advances made in the understanding of molecular spectra and the decay of molecular luminescence. At this stage of development, it is possible not only to detect minute changes in the excited state of molecules through the absorption and emission of electromagnetic radiation but also to monitor picosecond events in the excited states of aromatic molecules. A combination of steady state fluorescence and time dependent fluorescence studies provide a powerful technique to investigate the excited state of polyatomic molecules and

the formation of complexes by them. The fluorescence excitation and emission spectra, the quantum yields and decay times of polyatomic molecules are the parameters which are solvent dependent; hence, they provide information on the microenvironment of the solute molecules.

Since hydrocarbon chains of surfactant molecules are not fluorescent at usable wavelengths, micellar systems may be investigated using fluorescent probes, which are molecules containing suitable chromophores that are soluble in the micelle. The fluorescent probe technique involves inserting the fluorescent solute in the required media, observing the changes in the fluorescence parameters and finally interpreting the state of the local environment of the solute. Studies of fluorescent probes in micellar systems can be carried out in order to obtain information on the viscosity, size, oxygen content, and polarity of the micelle interior. Alternatively, changes in fluorescence intensities, lifetimes, quantum yields, and quenching rates as compared to aqueous solution or homogeneous organic solvent can be considered to be micellar effects on excited state reaction. Basic to the utilization of fluorescent probes is the requirement that the excited states be sufficiently long-lived to interact with their immediate environment prior to their decay. The lifetime of the excited state in fluorescence measurements is of the order of nanoseconds, and the dependence on the solvent properties can be used for investigation of micellar aqueous system.

Aromatic molecules such as naphthalene, methylanthracene, anthracene, pyrene and perylene have been used as fluorescent probes by various investigators [Förster and Selinger 1964; Shinitzky, Dianoux, Gitler and Weber 1971; Almgren 1972; Hautala and Turro 1972; Hautala, Schore and Turro 1973; Patterson and Vieil 1973; Chen, Grätzel and

Thomas 1974]. The general conclusions are: that the interior of a micelle resembles an aliphatic hydrocarbon solvent [Shinitzky *et al.* 1971]; that naphthalene molecules are solubilized in the interior of micelles [Almgren 1972]; that the distribution of naphthalene molecules between micelles and the aqueous phase depends on the surfactant concentrations [Hautala *et al.* 1973]; that anthracene is solubilized at the CTAB-water (CTAB — cetyltrimethylammonium bromide) interface whereas perylene resides in the micellar interior [Patterson *et al.* 1973]; that the effective concentration of oxygen is different in the interior of different micelles [Hautala *et al.* 1973].

The fast photophysical properties of complex formation in the excited state have been widely studied in fluorescence decay spectroscopy. These excited state complexes are described by such parameters as fluorescence intensities, emission frequencies, quantum yields, decay times, rate of formation and rate of dissociation. These parameters are sensitive to the microenvironment of the complex and therefore they may be useful as fluorescent probes for the investigation of micellar systems. However, the rate of formation of the complex must be significantly faster than the rate of formation and breaking up of micelles so that a micelle can be treated as a microsolvent.

The pyrene excimer was first used by Förster and Selinger [1964] as a fluorescent probe to estimate the micelle size from the ratio of the steady state intensities of the excimer to the monomer fluorescence. Since then this probe has been widely used to calculate the micelle size of sodium dodecyclsulphate [Hauser and Klein 1972]; to investigate the nature of the interior of the cationic micelles and to estimate the oxygen concentration in the micelles [Dorrance and Hunter 1972] and to estimate the viscosity of the micelle interior [Pownall and

Smith 1973].

Information on the distribution of charged particles in micellar aqueous systems has been obtained from studies of the influence of a micelle on protolytic reactions [Tong and Glesmann 1957; Klein and Hauser 1975]. However, the effect of surfactant on the acid-base equilibrium deserves more detailed study.

The use of the fluorescence parameters of aromatic molecules and those of some excited state complexes as fluorescent probes to investigate micellar systems is a recent occurrence and further refinement is possible in the experimental techniques. This thesis is mainly concerned with the fluorescence studies of some aromatic molecules and their excited state processes in surfactant micelles.

CHAPTER 2

FLUORESCENCE DECAY SPECTROSCOPY

This chapter describes the experimental techniques used to measure the fluorescence spectra and fluorescence lifetimes of some aromatic molecules in homogeneous and micellar solutions. In particular the spectrofluorimeter used to record the fluorescence spectra and the time correlated single photon counting instrument used to measure the decay of molecular fluorescence are described. The detailed treatment of the spectra and the decay curves is presented. The purification of chemicals and the preparation of surfactant solutions are also described.

2.1 THE SPECTROFLUORIMETER

The spectrofluorimeter used in this study has been described elsewhere [McDonald 1972]. Since all the fluorescence spectra presented in this thesis have been recorded with the spectrofluorimeter, a description of the instrument in its present form is given below.

The instrument is schematically shown in Figure 2.1. The excitation source is a Wotan XBO 150 watt xenon lamp. The lamp housing is connected to a fan which removes the ozone (a health hazard) produced by the lamp. The lamp is prevented from overheating by circulating water through a copper coil which is wound around the inside of the housing. Excitation wavelengths are selected by a Bausch & Lomb high

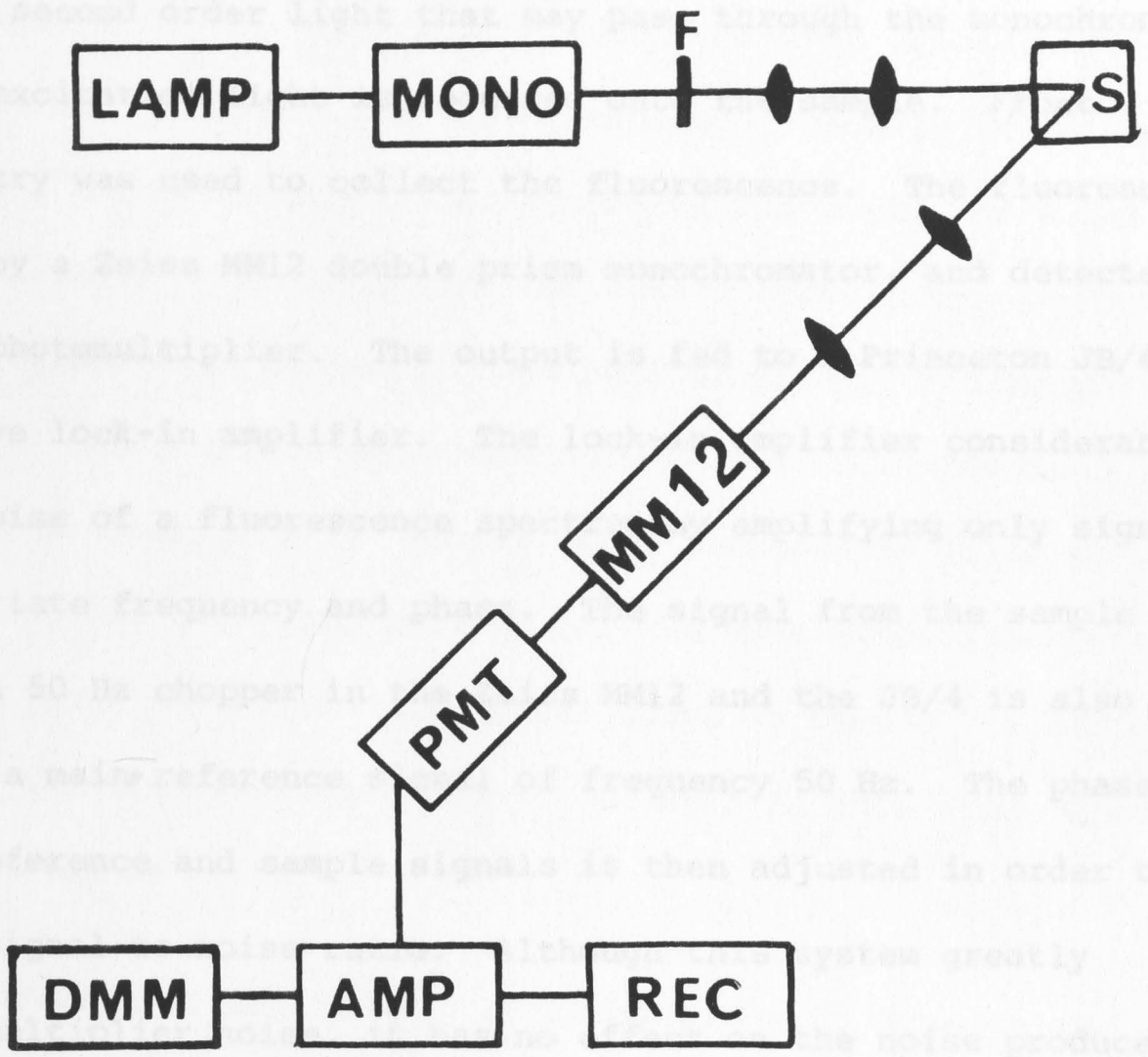

Figure 2.1. A schematic representation of the spectrofluorimeter.

LAMP — Wotan XBO 150 watt Xe lamp.

MONO — Bausch & Lomb UV-visible monochromator.

F — UG11 filter.

MM12 — Zeiss MM12 double prism monochromator.

PMT — EMI 6256B photomultiplier.

AMP — Princeton JB/4 phase sensitive lock-in amplifier.

REC — Vom 7 recorder.

DMM — Digital multimeter (Keithley).

intensity monochromator. A filter (usually a UG11 for this study) is placed in the light path after the Bausch & Lomb monochromator in order to absorb any second order light that may pass through the monochromator. The selected excitation light is focussed onto the sample. Front surface geometry was used to collect the fluorescence. The fluorescence was analysed by a Zeiss MM12 double prism monochromator, and detected by an EMI 6256B photomultiplier. The output is fed to a Princeton JB/4 phase sensitive lock-in amplifier. The lock-in amplifier considerably reduces the noise of a fluorescence spectrum by amplifying only signals of the appropriate frequency and phase. The signal from the sample is modulated by a 50 Hz chopper in the Zeiss MM12 and the JB/4 is also supplied with a mains reference signal of frequency 50 Hz. The phase between the reference and sample signals is then adjusted in order to maximise the signal-to-noise ratio. Although this system greatly reduces photomultiplier noise, it has no effect on the noise produced before the analysing monochromator, such as noise due to the fluctuations in the intensity of the lamp.

2.1.1 Correction of Fluorescence Spectra

Fluorescence spectra recorded by any spectrofluorimeter require correction because the spectral response of the analysing system is non-linear with wavelength. It has been suggested that the spectrum should be corrected for variations in photomultiplier sensitivity, spectrometer dispersion and any light losses in any other optical components through which the emission passes before detection [Chapman, Förster, Kortüm, Lippert, Melhuish, Nebbia and Parker 1963]. The non-linear response with wavelength of the spectrofluorimeter used in this

work is due to the lower sensitivity of the photocathode S13 of the EMI 6256B photomultiplier at longer wavelengths and the greater dispersion of the quartz prisms of the Zeiss MM12 monochromator at shorter wavelengths. The overall response has been measured previously [Wilairat 1966; Nott 1971] using the spectra of compounds for which corrected spectra are available. To produce the correction curve given in Figure 2.2 Nott has used benzene, biphenyl, naphthalene, BBD (2,5-Diphenyl-1,3,4-Oxadiazole) and perylene and compared with the corresponding spectra given by Berlman [1971]. As the curve obtained by Wilairat [1966] is reproducible over long periods for the same monochromator and photomultiplier [Nott 1971], the correction curve in Figure 2.2 has been used to correct the fluorescence spectra presented in this study whenever it is essential to do so.

The uncorrected spectrum as recorded by a Vom 7 recorder is converted to digital form with a DMAC pencil follower. The paper tape output from DMAC is read into the Univac 1108 computer. The x-axis data is converted to linear wavenumber from the conversion curve shown in Figure 2.3. This curve is approximated by a quintic polynomial over the range 14000 - 40000 cm^{-1} (7143 - 2500 Å) [Hinde 1975]. The correction curve (Figure 2.2) is also approximated by a quartic polynomial over the range 18950 - 37200 cm^{-1} (5277 - 2688 Å) and extrapolated up to 15000 cm^{-1} (6667 Å) [Hinde 1975]. Multiplication of each point on each spectrum by this function on a linear wavenumber axis yields a spectrum in which the ordinate is proportional to quanta of energy per wavenumber interval as suggested by Chapman *et al.* [1963].

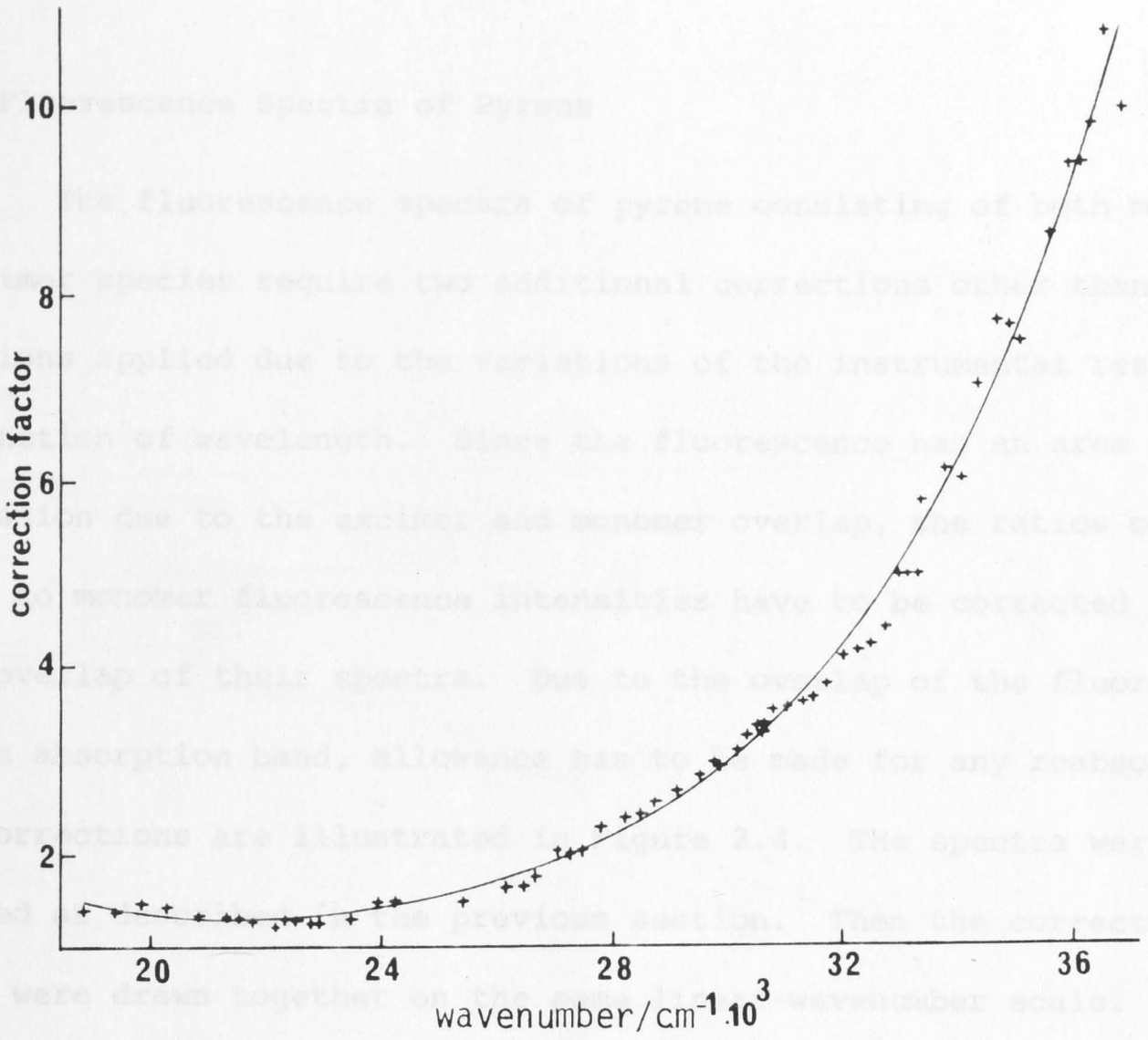

Figure 2.2. The correction curve for correcting the fluorescence spectra. (X) Nott [1971] and (—) Hinde [1975].

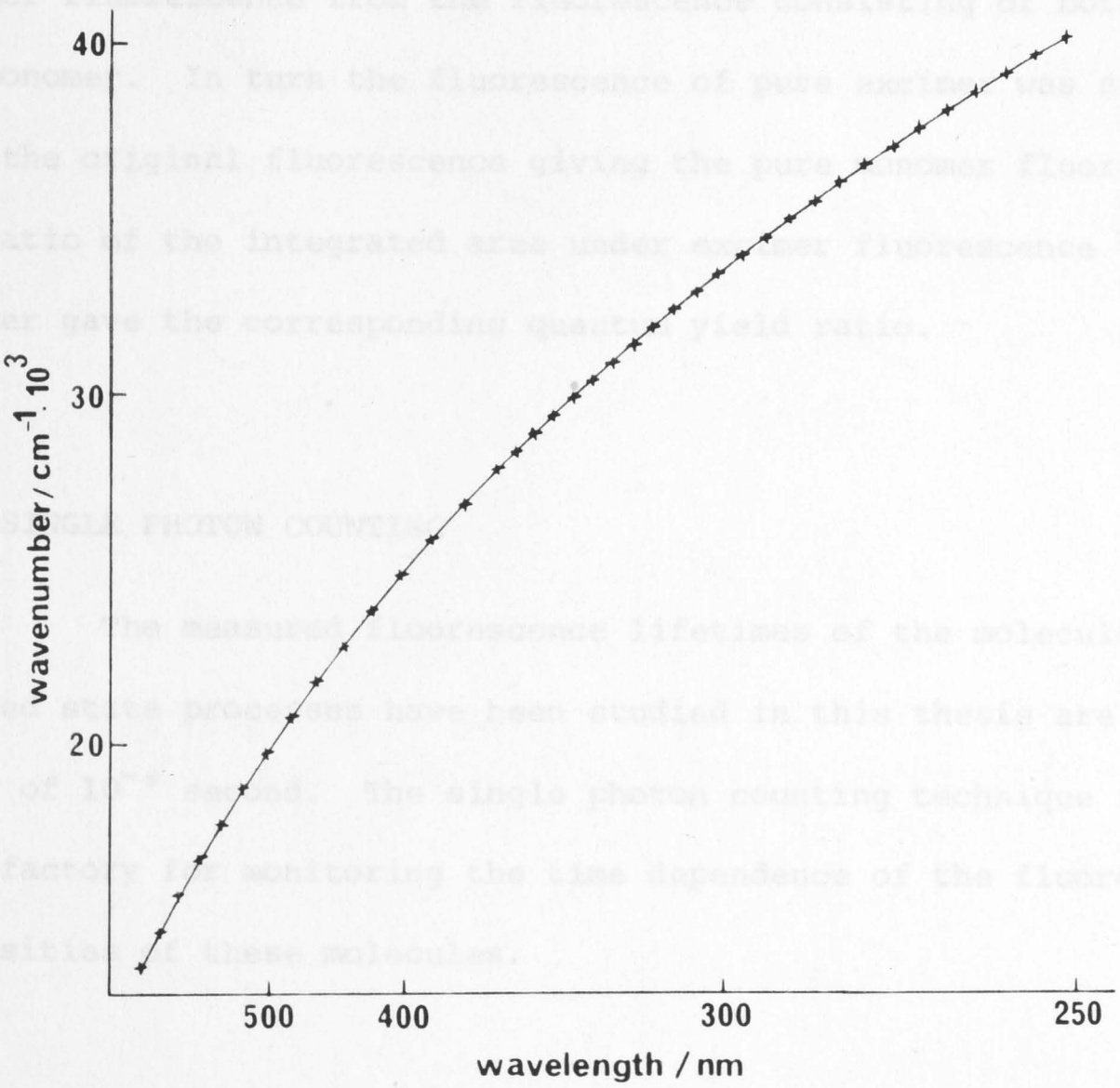

Figure 2.3. The curve to convert wavelength scale to linear wavenumber scale.

2.1.2 Fluorescence Spectra of Pyrene

The fluorescence spectra of pyrene consisting of both monomer and excimer species require two additional corrections other than the corrections applied due to the variations of the instrumental response as a function of wavelength. Since the fluorescence has an area where the emission due to the excimer and monomer overlap, the ratios of excimer to monomer fluorescence intensities have to be corrected for the mutual overlap of their spectra. Due to the overlap of the fluorescence with the absorption band, allowance has to be made for any reabsorption. These corrections are illustrated in Figure 2.4. The spectra were first corrected as described in the previous section. Then the corrected spectra were drawn together on the same linear wavenumber scale. The intensities of excimer fluorescence at each point on the linear wavenumber scale were obtained by subtracting the contribution of pure monomer fluorescence from the fluorescence consisting of both excimer and monomer. In turn the fluorescence of pure excimer was subtracted from the original fluorescence giving the pure monomer fluorescence. The ratio of the integrated area under excimer fluorescence to that of monomer gave the corresponding quantum yield ratio.

2.2 SINGLE PHOTON COUNTING

The measured fluorescence lifetimes of the molecules whose excited state processes have been studied in this thesis are of the order of 10^{-8} second. The single photon counting technique is therefore satisfactory for monitoring the time dependence of the fluorescence intensities of these molecules.

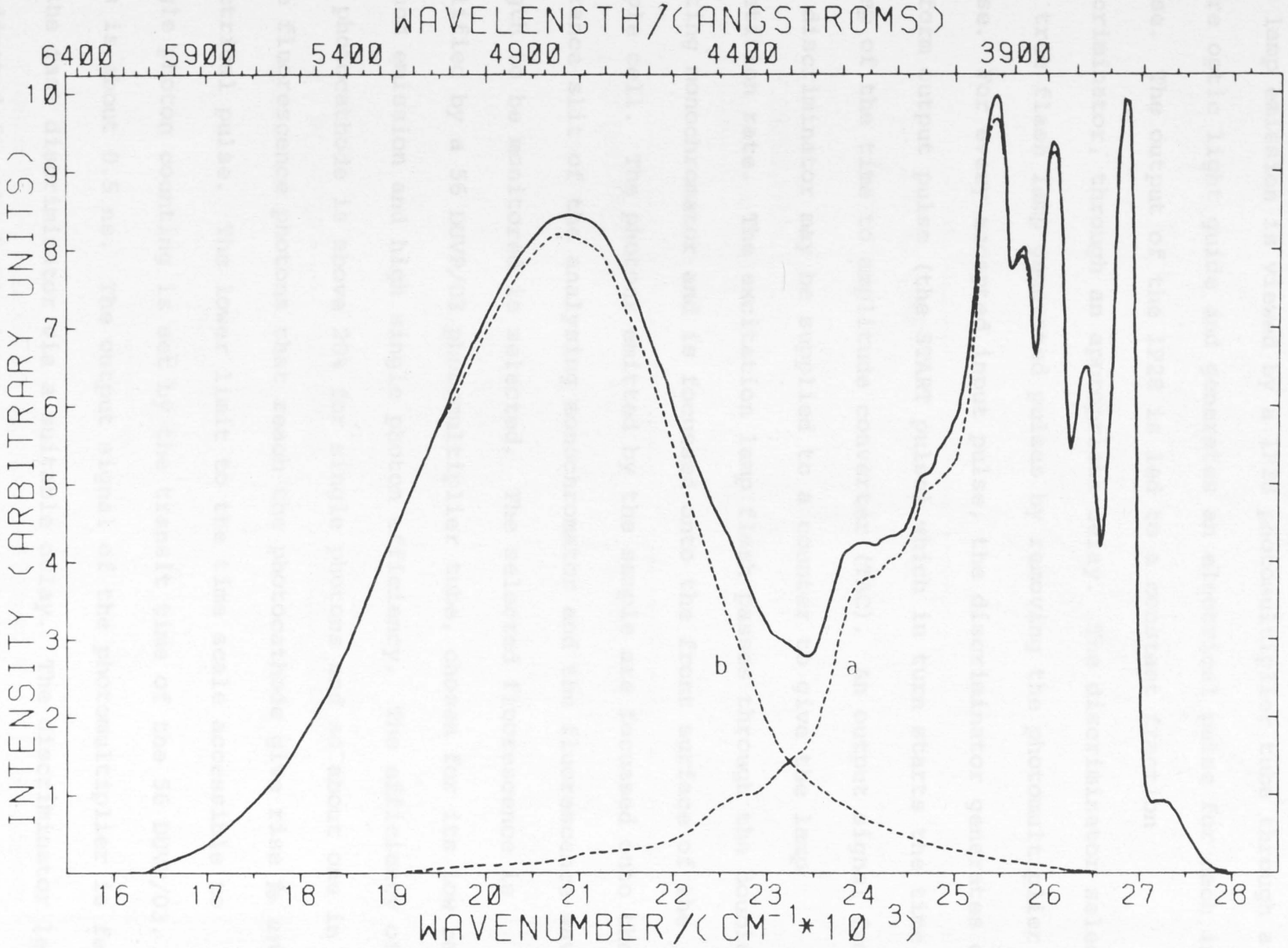

Figure 2.4. Corrected fluorescence spectra of pyrene in 0.1 mol l^{-1} SDS.
------ (a) fluorescence due to the monomer.
------ (b) fluorescence due to the excimer.

The instrument used for this study is schematically represented in Figure 2.5. The flash lamp repetition rate is 10 kHz. The lamp emission is viewed by a 1P28 photomultiplier tube through a fibre optic light guide and generates an electrical pulse for each input pulse. The output of the 1P28 is led to a constant fraction discriminator, through an appropriate delay. The discriminator selects the true flash lamp generated pulses by removing the photomultiplier noise. For every accepted input pulse, the discriminator generates one uniform output pulse (the START pulse) which in turn starts the time sweep of the time to amplitude converter (TAC). An output signal from the discriminator may be supplied to a counter to give the lamp repetition rate. The excitation lamp flash passes through the double grating monochromator and is focussed onto the front surface of the sample cell. The photons emitted by the sample are focussed onto the entrance slit of the analysing monochromator and the fluorescence wavelength to be monitored is selected. The selected fluorescence is amplified by a 56 DUVP/03 photomultiplier tube, chosen for its low background emission and high single photon efficiency. The efficiency of the photocathode is above 20% for single photons and so about one in five fluorescence photons that reach the photocathode give rise to an electrical pulse. The lower limit to the time scale accessible to single photon counting is set by the transit time of the 56 DUVP/03. This is about 0.5 ns. The output signal of the photomultiplier is fed to the fast discriminator via a suitable delay. The discriminator level is adjusted for the best signal-to-noise ratio. For every input pulse accepted, the discriminator generates a standard output pulse which is fed to the stop input of the TAC. A discriminator output may be supplied to a counter to give the total number of STOP pulses per second.

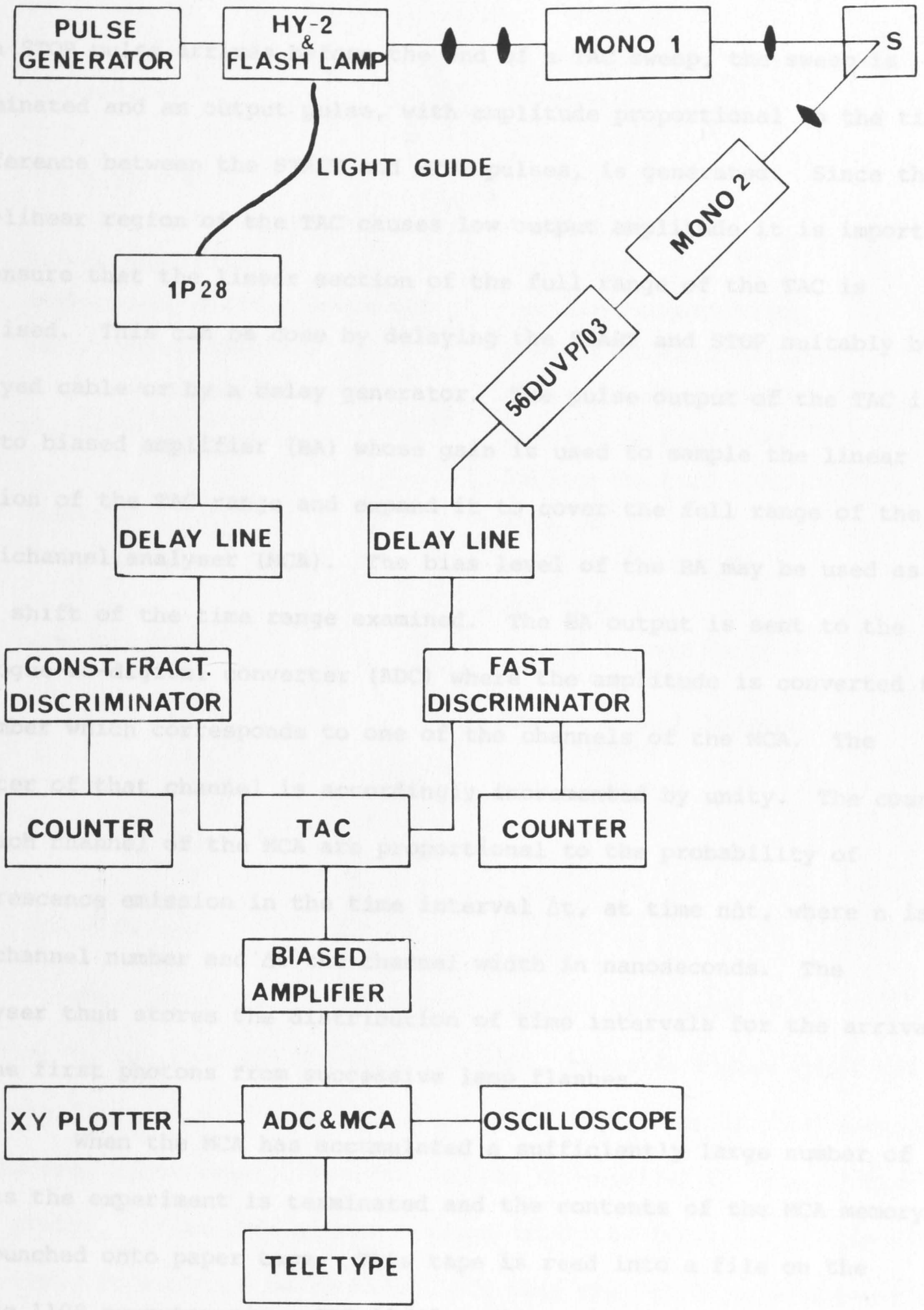

Figure 2.5. Schematic representation of the single photon counting instrument.

If a STOP pulse arrives before the end of a TAC sweep, the sweep is terminated and an output pulse, with amplitude proportional to the time difference between the START and STOP pulses, is generated. Since the non-linear region of the TAC causes low output amplitude it is important to ensure that the linear section of the full range of the TAC is utilised. This can be done by delaying the START and STOP suitably by delayed cable or by a delay generator. The pulse output of the TAC is fed to biased amplifier (BA) whose gain is used to sample the linear section of the TAC range and expand it to cover the full range of the multichannel analyser (MCA). The bias level of the BA may be used as a zero shift of the time range examined. The BA output is sent to the analogue-to-digital converter (ADC) where the amplitude is converted to a number which corresponds to one of the channels of the MCA. The counter of that channel is accordingly incremented by unity. The counts in each channel of the MCA are proportional to the probability of fluorescence emission in the time interval Δt, at time $n\Delta t$, where n is the channel number and Δt the channel width in nanoseconds. The analyser thus stores the distribution of time intervals for the arrival of the first photons from successive lamp flashes.

When the MCA has accumulated a sufficiently large number of events the experiment is terminated and the contents of the MCA memory are punched onto paper tape. This tape is read into a file on the Univac 1108 computer via a PDP 11/45 peripheral computer.

The commercially available components of the lifetime apparatus are listed below.

Voltage stabiliser	Stabilac SP3000
High voltage supply	DEL Electronics PSC 10-10-1
Stabilised power supply	Fluke 415B

Nim bin	Ortec 401A
Discriminators	Ortec 417
	Ortec 463
Delay generator	Ortec 416A
Time-to-amplitude converter	Ortec 437A
Biased amplifier	Ortec 408
Analogue-to-digital converter	Hewlett-Packard 5416B
Multichannel analyser	Hewlett-Packard 5422B
Display oscilloscope	Hewlett-Packard 5431B
Counters	Hewlett-Packard 5321
	Hewlett-Packard 5381A
Teletype	AS R 33
Photomultiplier tubes	Philips 56 DUVP/03
	RCA 1P28
Monochromators	Bausch & Lomb "high intensity"
	Bausch & Lomb "double grating"
Thyratron	EG & G HY-2

2.2.1 Pulse Pile-Up

When using the single photon counting technique it is important to consider the photon count rate, since at higher count rates the probability of more than one photon arriving within the TAC sweep time becomes significant. The TAC records the arrival in time of the first photon. If another photon arrives after the first during the TAC sweep time, it will not be recorded, and thus the TAC is biased towards early arriving photons. This phenomenon is termed "pulse pile-up". This pulse pile-up distorts the true fluorescence decay curve. It can be demonstrated on the oscilloscope display that the decay curves show obvious reduced lifetime once the pulse pile-up becomes significant.

It is necessary to work at a low P/F (photon count rate)/(flash repetition rate) ratio to eliminate this distortion. The photons arriving at the photocathode within a particular time interval follows a Poisson distribution with the following statistics:

$$P(x) = \frac{\mu^x e^{-\mu}}{x!}, \qquad (2.1)$$

where μ is the mean number of photons which arrive during a TAC sweep time after a lamp flash and $P(x)$ is the probability of x photons being detected after a flash.

For $$\mu = P/F = 0.02 \qquad (2.2)$$

$$P(\geqslant 2) = 0.0002 . \qquad (2.3)$$

Under this condition, the probability of more photons arriving after the first within the TAC sweep time is negligible and so the decay curve is undistorted. A photon count rate as low as 200 counts s^{-1} is required to fulfil this condition at a lamp repetition rate of 10 kHz. For a Poisson distribution the standard error in estimating the mean number of counts in a particular time interval, when expressed as a percentage error, is $100\ N^{-\frac{1}{2}}$, where N is the number of counts accumulated in a MCA channel. For $N = 10^4$, the error is 1%. In practice, therefore, counts of the order of 10^4 are required in the channels at the peak of the decay curve and lengthy periods are required to obtain an acceptable fluorescence decay profile.

The problem of pulse pile-up can be overcome by using a pile-up inspector which rejects the TAC output for a first photon arrival if a second photon arrives within the TAC range. The pile-up inspector built in this laboratory [Goodwin and Nicholls 1972] is used in

conjunction with the single photon counting instrument. A schematic representation of the apparatus used to correct for pile-up is given in Figure 2.6.

The performance of the pile-up inspector has been investigated recently [Harris 1975]. The resolution of the pile-up inspector is limited to the pulse-pair resolution of the fast discriminator, and pulses from the 56 DUVP/03 which are separated by less than 10 ns give only a single standardised pulse from this discriminator. It was reported that the limitation of a 10 ns resolution time resulted in the maximum acceptable ratio of P/F, for which the error in the number of counts in a channel is of the same order as the random Poisson error, varying with the TAC range chosen. Acceptable ratio of P/F values are given in Table 2.1 for various TAC ranges.

Table 2.1

Maximum acceptable P/F ratio for different TAC ranges.[1]

Effective TAC Ranges[2] (μs)	Maximum P/F[3] (%)	Photon Counts/s
0.025	0.5	50
0.050	1.0	100
0.100	2.0	200
0.200	4.0	400
0.250	5.0	500
0.400	8.0	800
0.500	10.0	1000
1.000	20.0	2000

[1] Harris [1975].

[2] These numbers are arrived at by combining the bias amplifier gain of 2 and the TAC range.

[3] Flash repetition rate, F = 10 kHz.

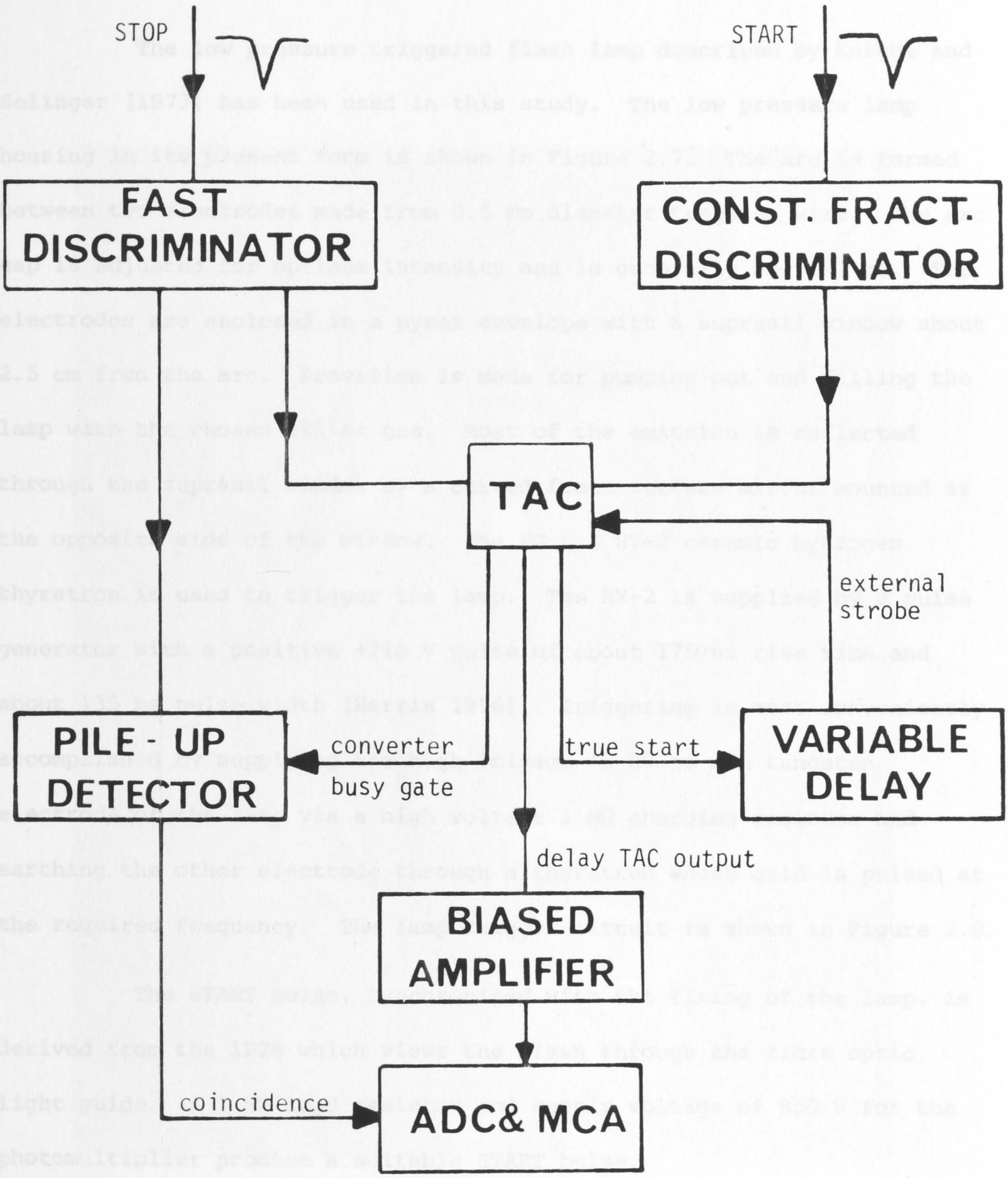

Figure 2.6. Schematic representation of the apparatus used to correct for pile-up.

2.2.2 The Pulsed Light Source

The low pressure triggered flash lamp described by Knight and Selinger [1973] has been used in this study. The low pressure lamp housing in its present form is shown in Figure 2.7. The arc is formed between two electrodes made from 0.5 mm diameter tungsten wire. The arc gap is adjusted for optimum intensity and is generally about 3 mm. The electrodes are enclosed in a pyrex envelope with a suprasil window about 2.5 cm from the arc. Provision is made for pumping out and filling the lamp with the chosen filler gas. Most of the emission is reflected through the suprasil window by a curved front surface mirror mounted at the opposite side of the window. The EG & G HY-2 ceramic hydrogen thyratron is used to trigger the lamp. The HY-2 is supplied by a pulse generator with a positive +210 V pulse of about 175 ns rise time and about 135 ns pulse width [Harris 1976]. Triggering is most conveniently accomplished by supplying the high voltage +8 kV to one tungsten electrode of the lamp via a high voltage 1 MΩ charging resistor and earthing the other electrode through a thyratron whose grid is pulsed at the required frequency. The lamp trigger circuit is shown in Figure 2.8.

The START pulse, synchronised with the firing of the lamp, is derived from the 1P28 which views the flash through the fibre optic light guide. A 1 MΩ load resistor and supply voltage of 950 V for the photomultiplier produce a suitable START pulse.

The spectral output of the low pressure lamp is determined by the filler gas. Although various other filler gases have been tried at a pressure of less than 1 atmosphere, the most useful (in terms of intensity and spectral versatility) appear to be air, nitrogen, hydrogen and deuterium [Knight and Selinger 1973]. The air filled flash lamp has

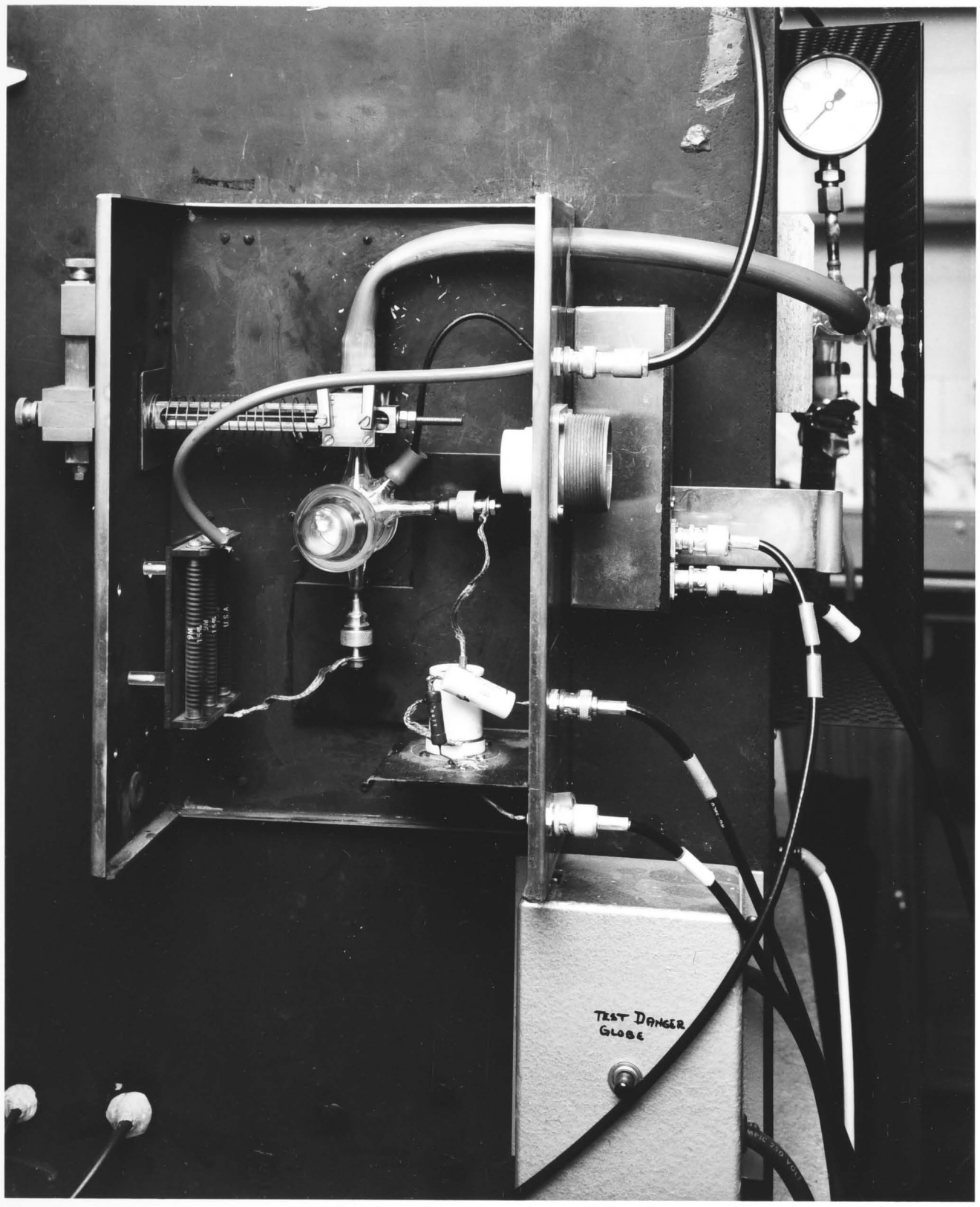

Figure 2.7 The low pressure lamp housing

been found satisfactory for this study. The spectral output of the air flash lamp is shown in Figure 2.9. The spectrum consists of intense bands, the most prominent being at 316, 337 and 358 nm. The decay curve for the 337 nm band is given in Figure 2.10. The build-up of a longer lived emission from the flash lamp as a result of prolonged use is prevented by cleaning the electrodes periodically.

2.2.3 Techniques

The typical experimental conditions used to obtain fluorescence lifetimes in this study were as follows:

Air flash lamp

High voltage (anode voltage)	8 kV
Repetition rate	10 kHz
Discriminator level	110 mV
Power supply 1P28 (cathode voltage)	-950 V
Pressure	0.4 atmosphere
Arc gap	3 mm
Pulse width	~ 4 ns FWHM

Detection system

Excitation band pass (Bausch & Lomb "double grating")	2 nm
Fluorescence band pass (Bausch & Lomb "high intensity")	10 nm
56 DUVP/03	
Cathode voltage	-2.4 kV
Gain	3×10^8
Discriminator level	170 mV
Dark pulse†	~ 20 counts s^{-1}

† The tube dark pulse rate is reduced on "pump out", that is, leaving the high voltage applied to the tube (in the dark) when not in use and on cooling the photocathode to reduce thermal photon emission. At -5 °C the average dark pulse is usually 20 counts s^{-1}. After prolonged cooling, condensation may occur on the tube. This can be prevented by blowing dry nitrogen over the tube.

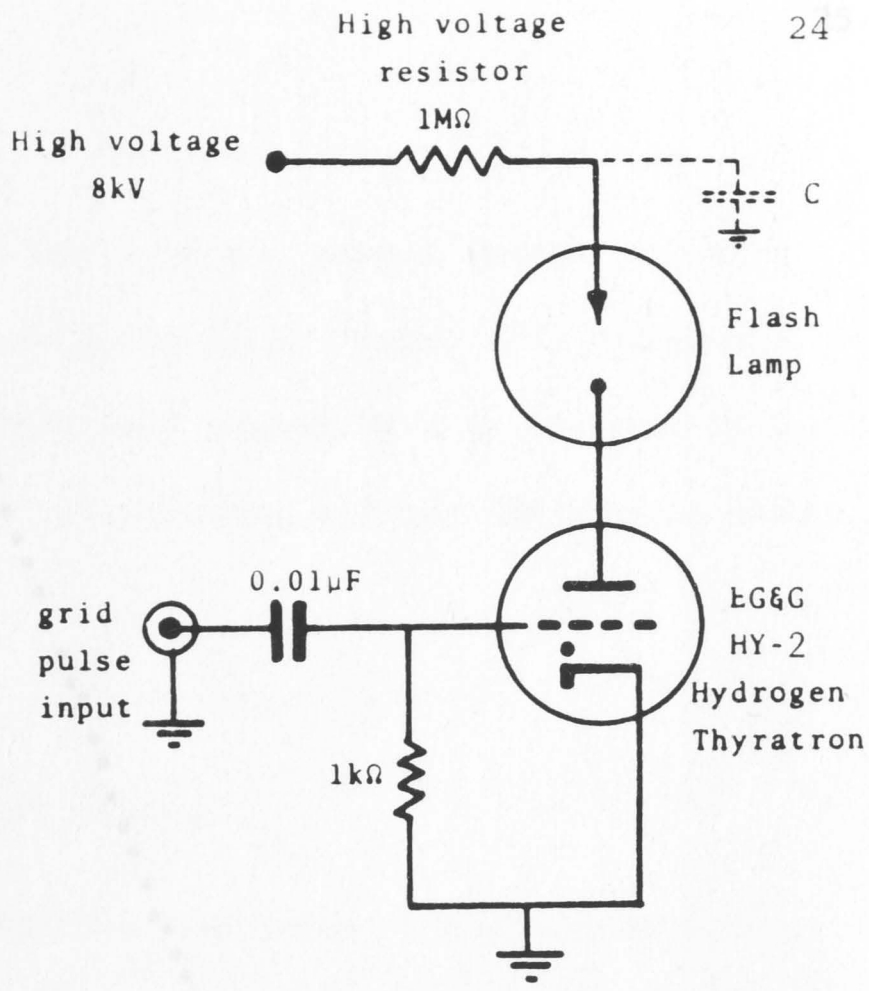

Fig. 2.8. Low pressure flash lamp trigger circuit. High voltage resistor is a Victoreen type HPX. The complete unit is enclosed in a fully shielded housing to prevent RF pick-up by the detection system. C can be stray or added capacitance. [After Knight and Selinger 1973.]

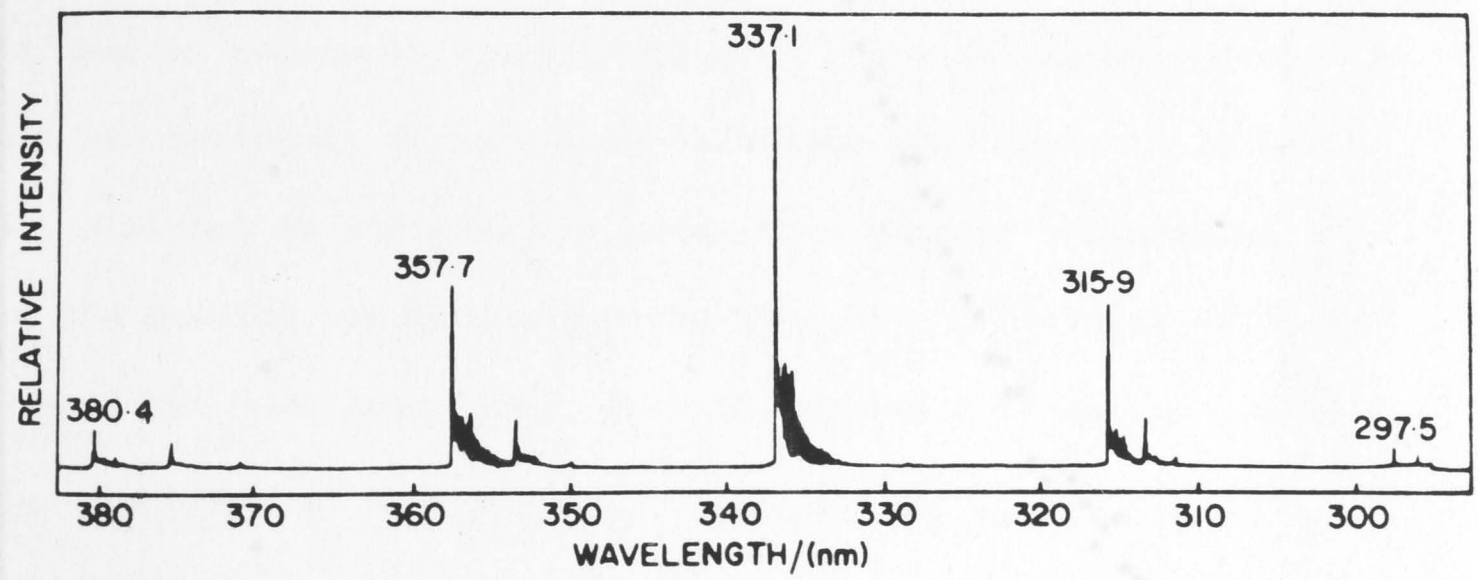

Figure 2.9a. Spectral output of the air flash lamp. [After Knight and Selinger 1973.]

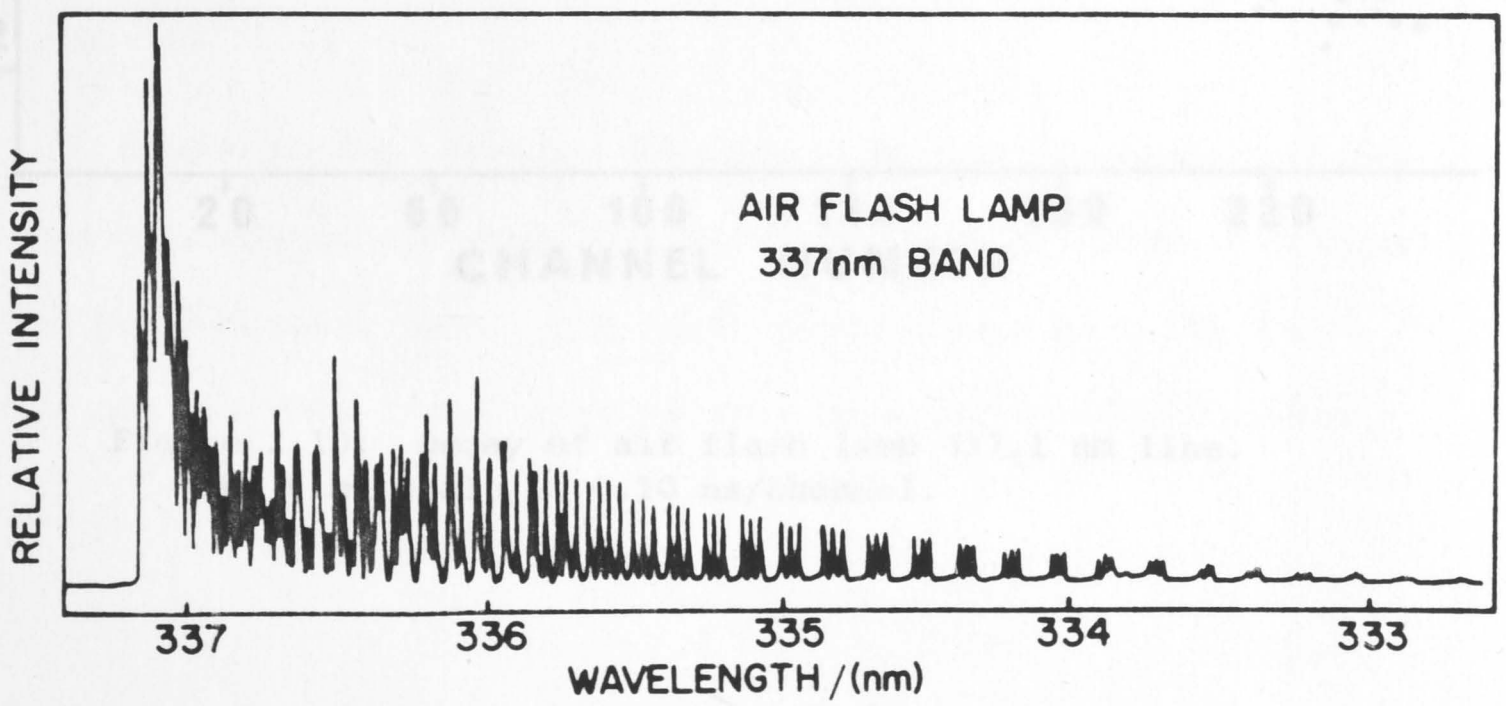

Figure 2.9b. The 337.1 nm band group measured at high resolution (photoelectric recording). [After Knight and Selinger 1973.]

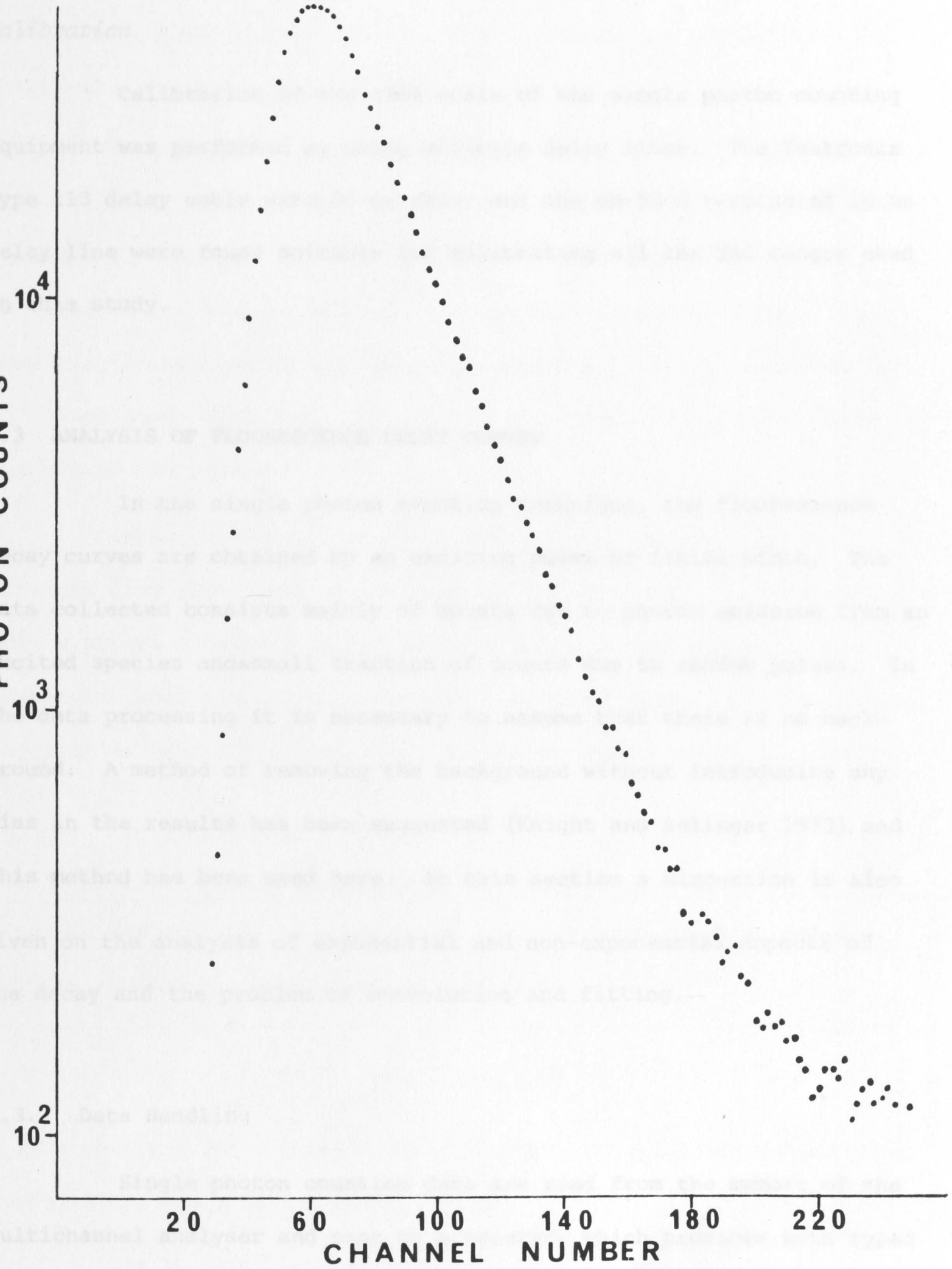

Figure 2.10. Decay of air flash lamp 337.1 nm line.
The time scale is 0.10 ns/channel.

Calibration

Calibration of the time scale of the single photon counting equipment was performed by using accurate delay lines. The Tektronix type 113 delay cable with 60 ns delay and the GR-50 Ω terminated 10 ns delay line were found suitable for calibrating all the TAC ranges used in this study.

2.3 ANALYSIS OF FLUORESCENCE DECAY CURVES

In the single photon counting technique, the fluorescence decay curves are obtained by an exciting pulse of finite width. The data collected consists mainly of counts due to photon emission from an excited species and a small fraction of counts due to random pulses. In the data processing it is necessary to assume that there is no background. A method of removing the background without introducing any bias in the results has been suggested [Knight and Selinger 1973] and this method has been used here. In this section a discussion is also given on the analysis of exponential and non-exponential aspects of the decay and the problem of convoluting and fitting.

2.3.1 Data Handling

Single photon counting data are read from the memory of the multichannel analyser and sent to a teletype which produces both typed copy and punched paper tape. The paper tape is read on a PDP 11/45 computer and the data transferred to file on a Univac 1108 computer.

Interactive terminals are used to edit the data, for preparing programmes and for executing them.

The single photon counting apparatus is set up with the stop pulse suitably delayed, so that the time profile of the decay curve is recorded in channels 20 - 255. The mean of the counts in channels 1 - 19, accepted as the mean background, is subtracted from the data. The remaining counts are plotted semi-logarithmically by the computer onto 10" graph paper with $\log_{10}$ (counts) on the y-axis and channel number of the MCA of the x-axis.

When the data is clearly exponential, the slope of the straight line plot gives an estimate of the lifetime; if it is not, some *a priori* knowledge of the decay process is required before a meaningful analysis can be performed. Whatever decay law is selected, the plot is used for calculating initial estimates of the parameters.

2.3.2 Exponential and Non-Exponential Decay

The decay of molecular fluorescence is a random process which in many cases leads to an expression of the form

$$I(t) = A\, e^{-t/\tau} . \qquad (2.4)$$

A is a constant for a particular measurement of the fluorescence decay curve, I(t), and τ is the mean lifetime.

If it is assumed that the excitation pulse is a delta pulse, the probability density function I(k), k = 1,2,...,n, can be treated as an undistorted estimate of I(t). n is the number of data points (MCA channels). For each value of k, I(k) represents a single estimate of the mean of a Poisson distribution of counts for the channel.

Where the semi-log plot of the data indicates the decay is clearly exponential, initial estimates for the lifetime and pre-exponential factor are obtained from the plot's slope and intercept respectively. The computer then performs a non-linear least squares fit to the data using equation (2.4), with the reduced chi-square, χ^2_ν, the parameter minimised.

$$\chi^2_\nu = \frac{1}{\nu} \sum_t \frac{[I(t) - I^0(t)]^2}{I^0(t)} , \qquad (2.5)$$

where $I(t)$ is the original data;

$I^0(t)$ the function fitted to the data for the parameters A, τ;

t the channel number;

and $\nu = n-\gamma-1$ the number of degrees of freedom left after fitting "n" points with γ parameters.

If the fitted function is a good approximation to the data, then the value of the reduced chi-square should on the average be unity. Using the accepted 5% level of significance, this means that for 200 - 210 data points χ^2_ν must be less than or equal to 1.17.

The application of this reasoning may be illustrated in terms of real experimental data. The decay of the fluorescence of 2-methyl-naphthalene in sodium dodecyl sulphate (SDS) is shown in Figure 2.11. The results obtained for fitting a single exponential (equation 2.4) are also given in the figure.

The fitting of a single exponential to decay data is a straightforward procedure involving the minimisation of a function of two variables, A and τ. However, the problem becomes exceedingly difficult for the non-exponential decay data. A non-exponential fluorescence decay curve may be composed of a sum of many exponentials.

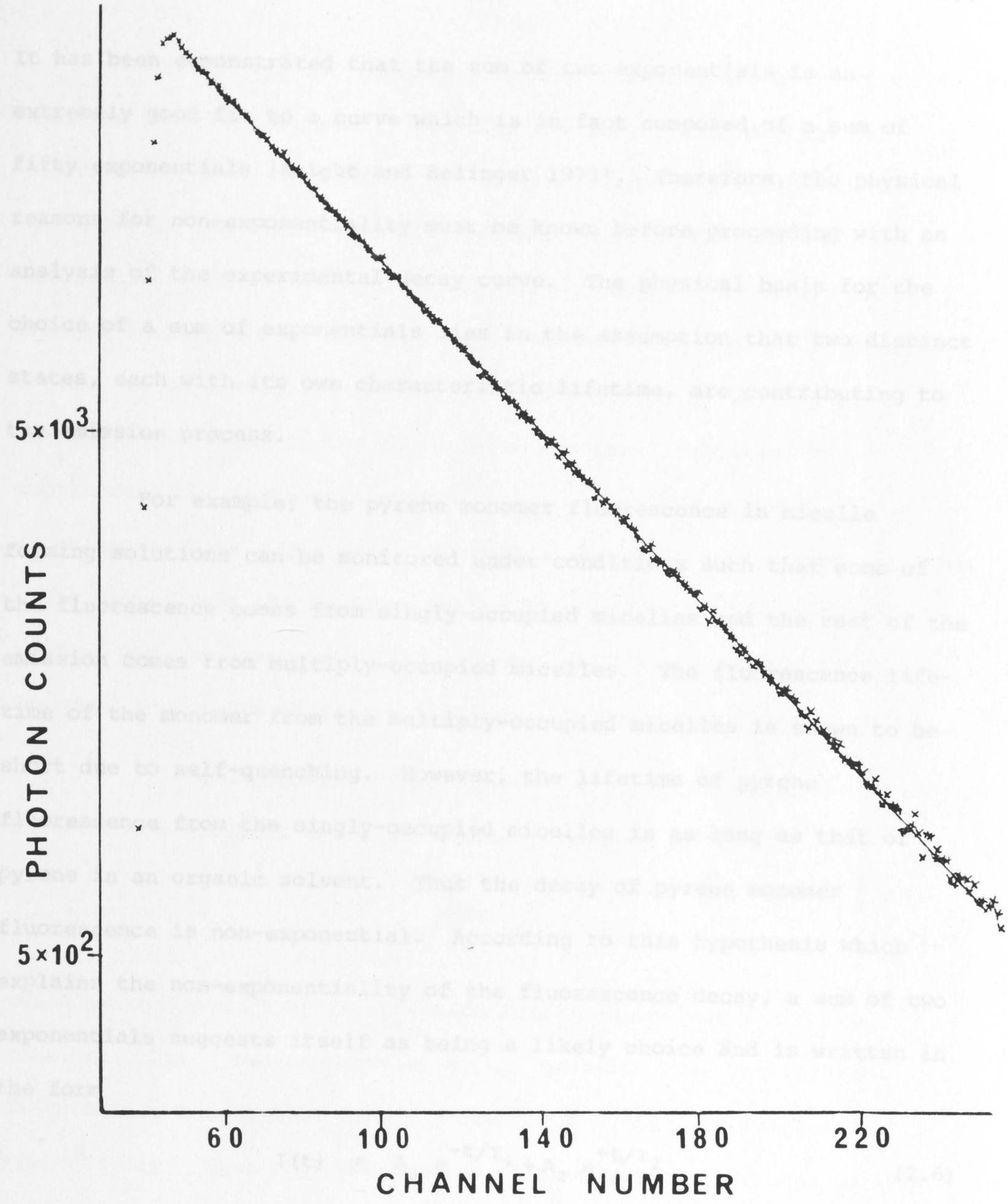

Figure 2.11. The decay of 3×10^{-3} mol l^{-1} 2-methylnaphthalene fluorescence in 0.1 mol l^{-1} SDS. The solid line, a single exponential with A = 48250 and τ = 52.8 ns, is the fit to the experimental data points (x). $\chi^2_\nu = 1.05$.

It has been demonstrated that the sum of two exponentials is an extremely good fit to a curve which is in fact composed of a sum of fifty exponentials [Knight and Selinger 1973]. Therefore, the physical reasons for non-exponentiality must be known before proceeding with an analysis of the experimental decay curve. The physical basis for the choice of a sum of exponentials lies in the assumption that two distinct states, each with its own characteristic lifetime, are contributing to the emission process.

For example, the pyrene monomer fluorescence in micelle forming solutions can be monitored under conditions such that some of the fluorescence comes from singly-occupied micelles and the rest of the emission comes from multiply-occupied micelles. The fluorescence lifetime of the monomer from the multiply-occupied micelles is shown to be short due to self-quenching. However, the lifetime of pyrene fluorescence from the singly-occupied micelles is as long as that of pyrene in an organic solvent. Thus the decay of pyrene monomer fluorescence is non-exponential. According to this hypothesis which explains the non-exponentiality of the fluorescence decay, a sum of two exponentials suggests itself as being a likely choice and is written in the form

$$I(t) = A_1 e^{-t/\tau_1} + A_2 e^{-t/\tau_2}, \qquad (2.6)$$

where τ_1 and τ_2 are the lifetimes of the two decay components weighted by the constants A_1 and A_2. As is the case for fitting one exponential, when a sum of two exponentials is fitted the computer performs a non-linear fit to the data with the reduced chi-square, χ^2_ν, the parameter minimised.

To fit the two exponentials the estimates are taken from the semi-log plot of the decay. Firstly, the longer lifetime and its corresponding pre-exponential are estimated from the linear section of the decay in the later channels. This is done by fitting a single exponential decay between Lim 1 and Lim 2. Lim 1 and Lim 2 are the channel numbers of the MCA where the fit started and ended respectively. A best fit is chosen from different fits obtained by varying Lim 1. Secondly, the decay of the short-lived species is obtained by subtracting the calculated counts $I(k)_{cal}$ † from the original experimental data. The remaining counts are plotted on a semi-log scale whose slope gives the estimate of the lifetime of the short-lived species and the intercept gives the estimate of the pre-exponential factor. Treatments of the results are illustrated in Figure 5.12.

The contribution of an exponential decaying component of fluorescence decay to the fluorescence intensity is

$$\int_0^\infty A\, e^{-t/\tau}\, dt = A\tau \qquad (2.7)$$

which is the product of the pre-exponential factor and the decay constant. For a two-exponential decay (equation 2.6) the relative fluorescence intensities from the two species are $A_1\tau_1$ and $A_2\tau_2$ respectively. Thus the contribution of each component can be compared by using the ratio $A_1\tau_1/A_2\tau_2$.

---

† $I(k)_{cal} = A_1\, e^{-t/\tau_1}$ which is obtained by fitting between Lim 1 and Lim 2. That is, $I(k)_{cal}$ is the count contributed by the long-lived species.

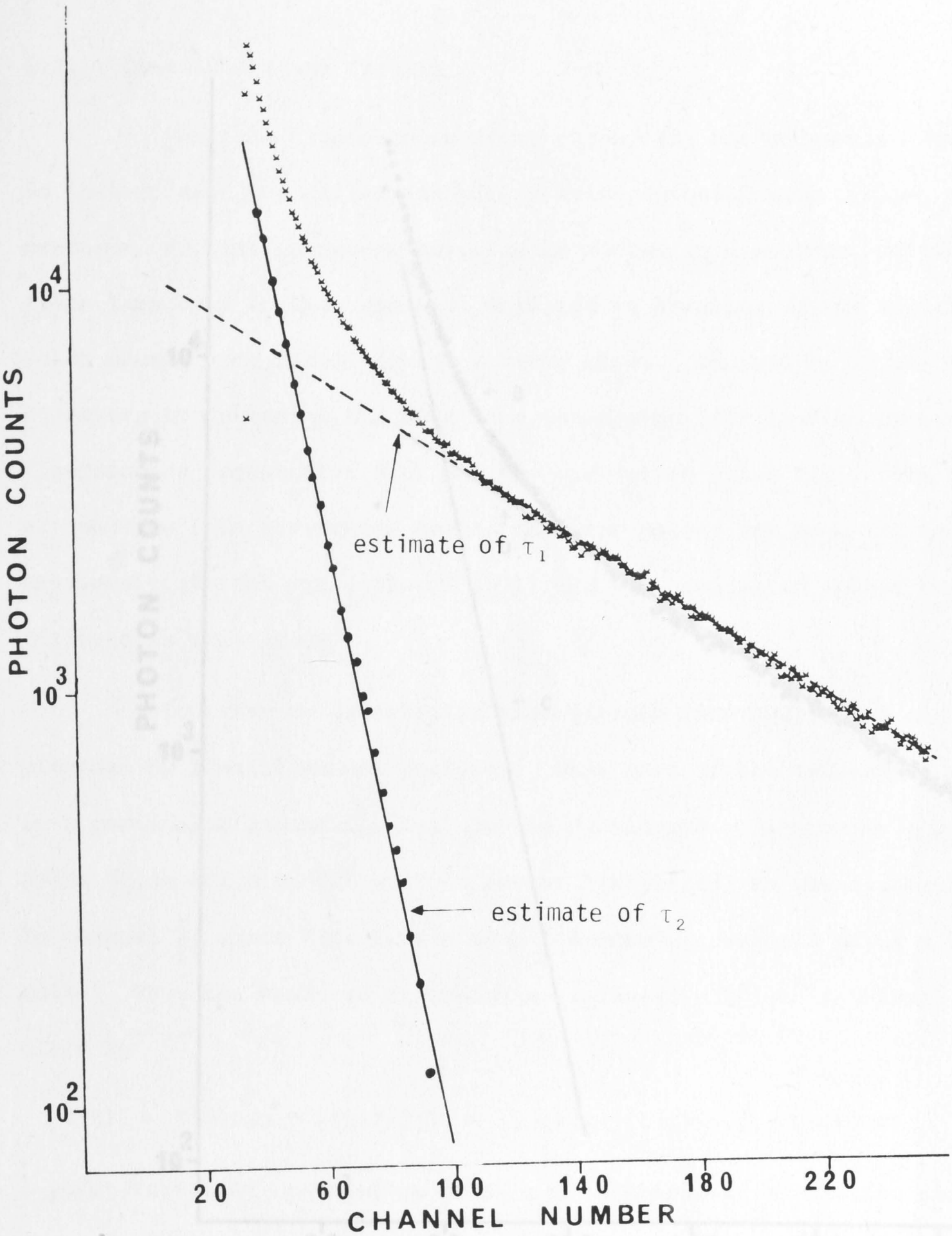

Figure 2.12(a). The decay of monomer fluorescence of 1.5×10^{-3} mol l^{-1} pyrene in 0.1 mol l^{-1} SDS. (x) experimental data and (---) single exponential, which is subtracted from (x), giving the decay of the short-lived fluorescence (•).

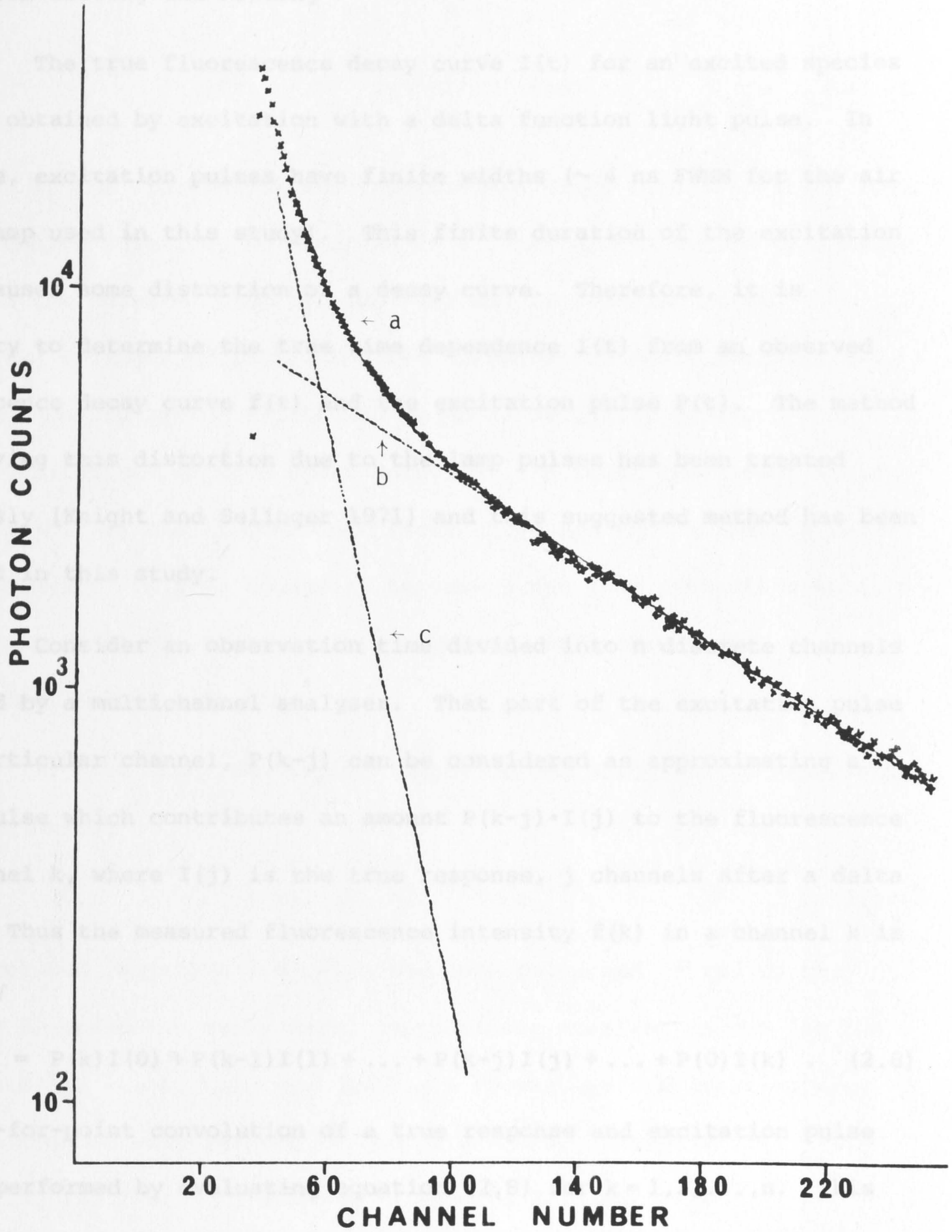

Figure 2.12(b). The decay of monomer fluorescence (x) of 1.5×10^{-3} mol l^{-1} pyrene in 0.1 mol l^{-1} SDS. The solid line (a) represents the sum of the two components (b) and (c).

τ_1 = 386 ns; A_1 = 11,830

τ_2 = 54.2 ns; A_2 = 620,000

χ^2_ν = 2.44.

2.3.3 Convoluting and Fitting

The true fluorescence decay curve I(t) for an excited species is that obtained by excitation with a delta function light pulse. In practice, excitation pulses have finite widths (~ 4 ns FWHM for the air flash lamp used in this study). This finite duration of the excitation pulse causes some distortion of a decay curve. Therefore, it is necessary to determine the true time dependence I(t) from an observed fluorescence decay curve f(t) and the excitation pulse P(t). The method of removing this distortion due to the lamp pulses has been treated previously [Knight and Selinger 1971] and this suggested method has been followed in this study.

Consider an observation time divided into n discrete channels provided by a multichannel analyser. That part of the excitation pulse in a particular channel, P(k-j) can be considered as approximating a delta pulse which contributes an amount $P(k-j)\cdot I(j)$ to the fluorescence in channel k, where I(j) is the true response, j channels after a delta pulse. Thus the measured fluorescence intensity f(k) in a channel k is given by

$$f(k) = P(k)I(0) + P(k-1)I(1) + \ldots + P(k-j)I(j) + \ldots + P(0)I(k) \quad . \qquad (2.8)$$

A point-for-point convolution of a true response and excitation pulse can be performed by evaluating equation (2.8) for $k = 1,2,\ldots,n$. This can be expressed by the convolution sum:

$$f(k) = \sum_{j=0}^{k} P(k-j)I(j) \; ; \qquad k = 1,2,\ldots,n \; . \qquad (2.9)$$

The ideal experiment would involve data collection in an infinite number of channels during the interval of observation, and the convolution of the function P(t) and I(t) in terms of the convolution

integral:

$$f(t) = \int_0^t P(t - t')I'(t)dt' \quad . \qquad (2.10)$$

If the lifetime of the fluorescence decay is sufficiently long, the excitation pulse may be regarded as a close approximation to a delta pulse and the measured fluorescence f(t) may be regarded as an undistorted estimate of I(t). For the lifetimes of short duration the distortion caused by the excitation pulse is naturally greater. In measuring lifetimes of such short duration, the ideal experiment would involve measuring the fluorescence decay curve and the excitation pulse simultaneously. This is necessary because flash lamp characteristics, which are a function of gas purity, electrode environment and temperature, change with time.

In this study the excimer decay curves which can be expressed by the equation:

$$I'(t) = B(e^{-\lambda_1 t} - e^{-\lambda_2 t}) \qquad (2.11)$$

are convoluted (equation 2.9) with the lamp pulse and fitted to the observed fluorescence decay data. Approximate starting values for the parameters λ_1, λ_2, B, Lim 1 and Lim 2 are chosen and the least squares sum is minimised with respect to the parameters. Examples of convoluting and fitting are shown in Figures 2.13 and 2.14.

A practical difficulty is the accumulation of the lamp pulse as it was during the collection of the fluorescence data. To measure both pulse and decay curves simultaneously, one would need two separate detection systems. It is however possible to collect the lamp before and after the decay curve is accumulated and this was done for the present study. The less accurate values for the shorter lifetimes (see

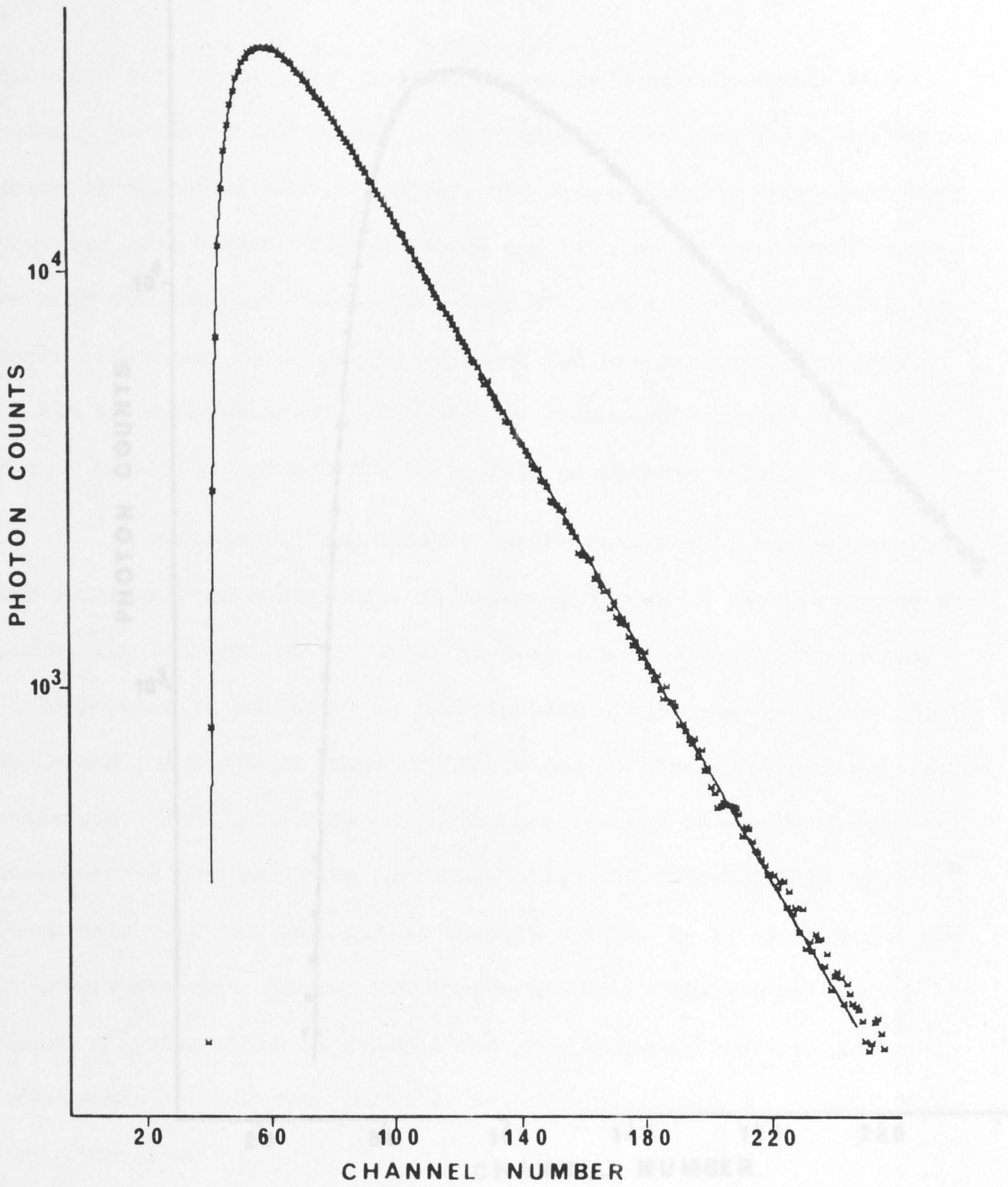

Figure 2.13. The decay of excimer fluorescence of 10^{-3} mol l^{-1} pyrene in 0.05 mol l^{-1} SDS and 0.1 mol l^{-1} NaCl aqueous solution. (—) the resultant fitted to the experimental data (x) after convolution.

τ_1 = 67 ns;

τ_2 = 20 ns;

χ^2_ν = 1.61.

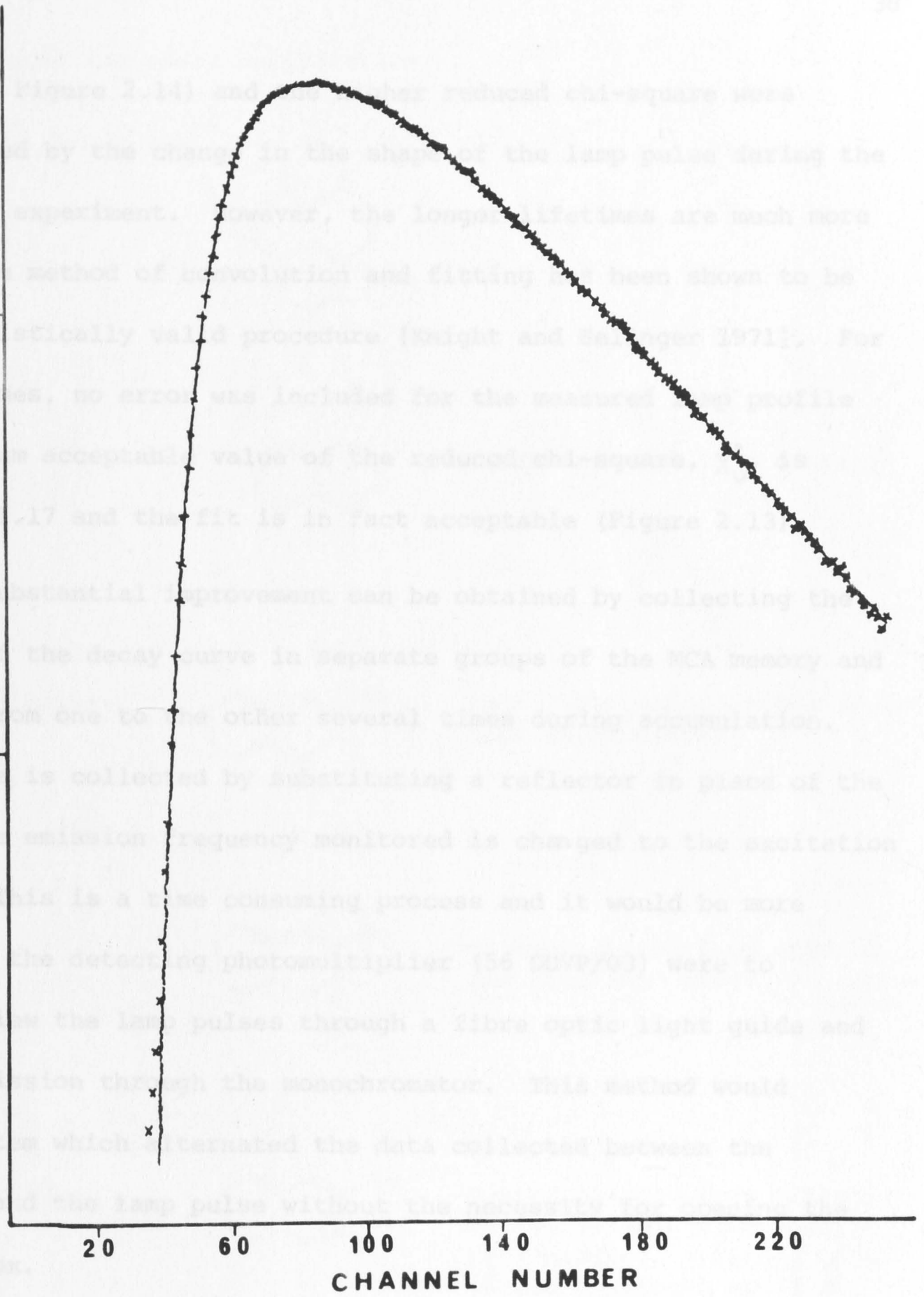

Figure 2.14. The decay of 2-naphtholate anion fluorescence in water. (—) convoluting and fitted to the experimental data (x).

τ_1 = 9.31 ns;

τ_2 = 3.87 ns;

χ^2_ν = 5.80.

Table 5.9 and Figure 2.14) and the higher reduced chi-square were probably caused by the change in the shape of the lamp pulse during the course of the experiment. However, the longer lifetimes are much more accurate. The method of convolution and fitting has been shown to be the only statistically valid procedure [Knight and Selinger 1971]. For longer lifetimes, no error was included for the measured lamp profile and the maximum acceptable value of the reduced chi-square, χ^2_ν, is greater than 1.17 and the fit is in fact acceptable (Figure 2.13).

A substantial improvement can be obtained by collecting the lamp pulse and the decay curve in separate groups of the MCA memory and alternating from one to the other several times during accumulation. The lamp pulse is collected by substituting a reflector in place of the sample and the emission frequency monitored is changed to the excitation wavelength. This is a time consuming process and it would be more convenient if the detecting photomultiplier (56 DUVP/03) were to alternately view the lamp pulses through a fibre optic light guide and the sample emission through the monochromator. This method would require a system which alternated the data collected between the fluorescence and the lamp pulse without the necessity for opening the light tight box.

2.4 MATERIALS AND SAMPLE HANDLING

Organic solvents were "spectroquality" grade from Matheson, Coleman & Bell. These were tested to ensure that they gave no detectable fluorescence, and then used without further purification. Solutes and surfactants were treated by the following methods.

2.4.1 Chemicals and their Purification

Pyrene 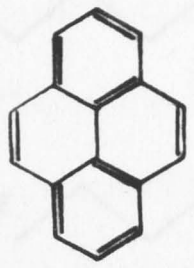 zone refined.

Naphthalene 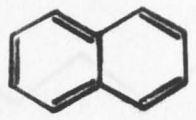 recrystallised from ethanol.

2-methylnaphthalene 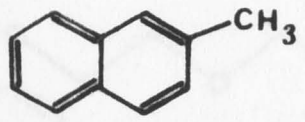

Koch-light Laboratories (Pure) used as received.

2-naphthol 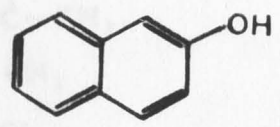

recrystallised from ethanol and then from water.

1-cyanonaphthalene 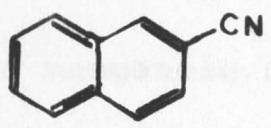

recrystallised from ethanol; recrystallised from methyl-cyclohexane; sublimed under vacuum collected at 77 K.

p-chloroiodobenzene 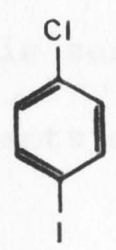

chromatographed using a silica gel column with cyclohexane as eluting solvent.

SODIUM STEARATE

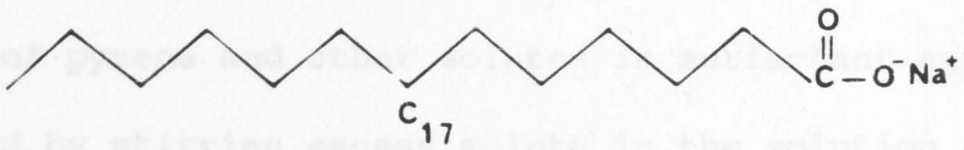

SODIUM DODECYL SULPHATE

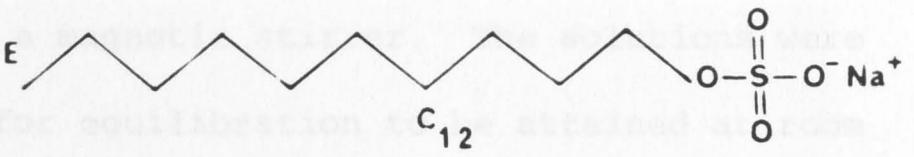

CETYL DIMETHYLBENZYLAMMONIUM CHLORIDE

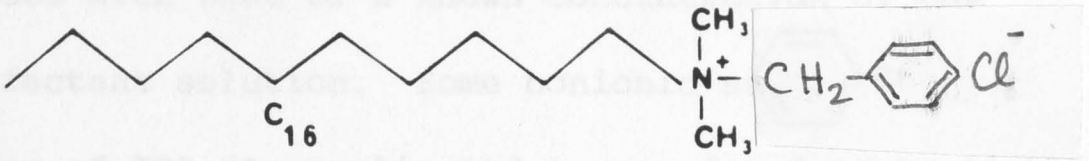

POLYOXYETHYLENE DIISOBUTYL PHENOL TRITON X100

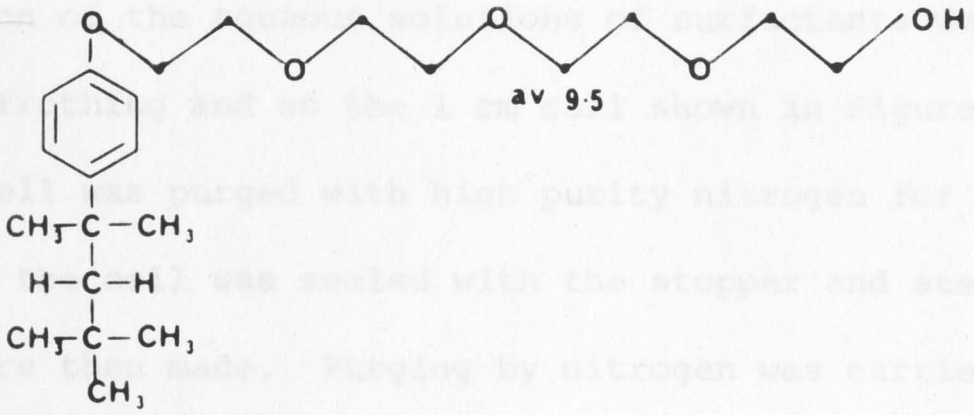

POLYOXYETHYLENE ALCOHOL TERIC 12A23

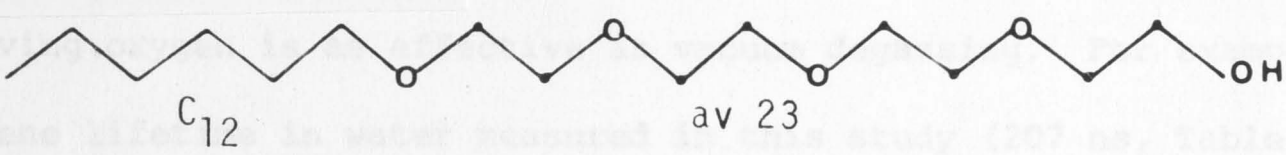

Sodium chloride and manganese chloride have negligible absorbance at wavelengths longer than 300 nm at the concentrations used. Sodium dodecyl sulphate (SDS) was recrystallised three times from ethanol. Cetyldimethylbenzylammonium chloride (CDBA) fluka (pure), Triton-X100 and Teric (ICI) nonionic surfactants were used without further purification. The surfactants commonly available are shown above.

2.4.2 Sample Handling

The samples of pyrene and other solutes in surfactant aqueous solutions were prepared by stirring excess solute in the solution at 50 °C for 5 - 10 hours using a magnetic stirrer. The solutions were allowed to stand overnight for equilibration to be attained at room temperature and then were filtered. Concentrations were determined by comparing the absorbances with that of a known concentration of the solute in the same surfactant solution. Some nonionic surfactants supplied by the courtesy of ICI (Australia Ltd.) were found to be light sensitive and the solutions were protected from light at all times.

Deoxygenation of the aqueous solutions of surfactants was difficult because of frothing and so the 1 cm cell shown in Figure 2.15 was designed. This cell was purged with high purity nitrogen for about half an hour and then the cell was sealed with the stopper and steady state measurements were then made. Purging by nitrogen was carried out during the experiments of transient lifetime measurements. This method of removing oxygen is as effective as vacuum degassing. For example, the pyrene lifetime in water measured in this study (207 ns, Table 5.7) is in very good agreement with the literature value of 206 ns obtained by vacuum degassing [Geiger and Turro 1975].

2.5 OTHER MEASUREMENTS

The absorption spectra were recorded using the Cary 14H spectrometer. High temperature fluorescence measurements were done by circulating thermostatted water through a copper coil which was wound around inside the cell holder housing. Using this cell holder measurements were possible up to 75 °C.

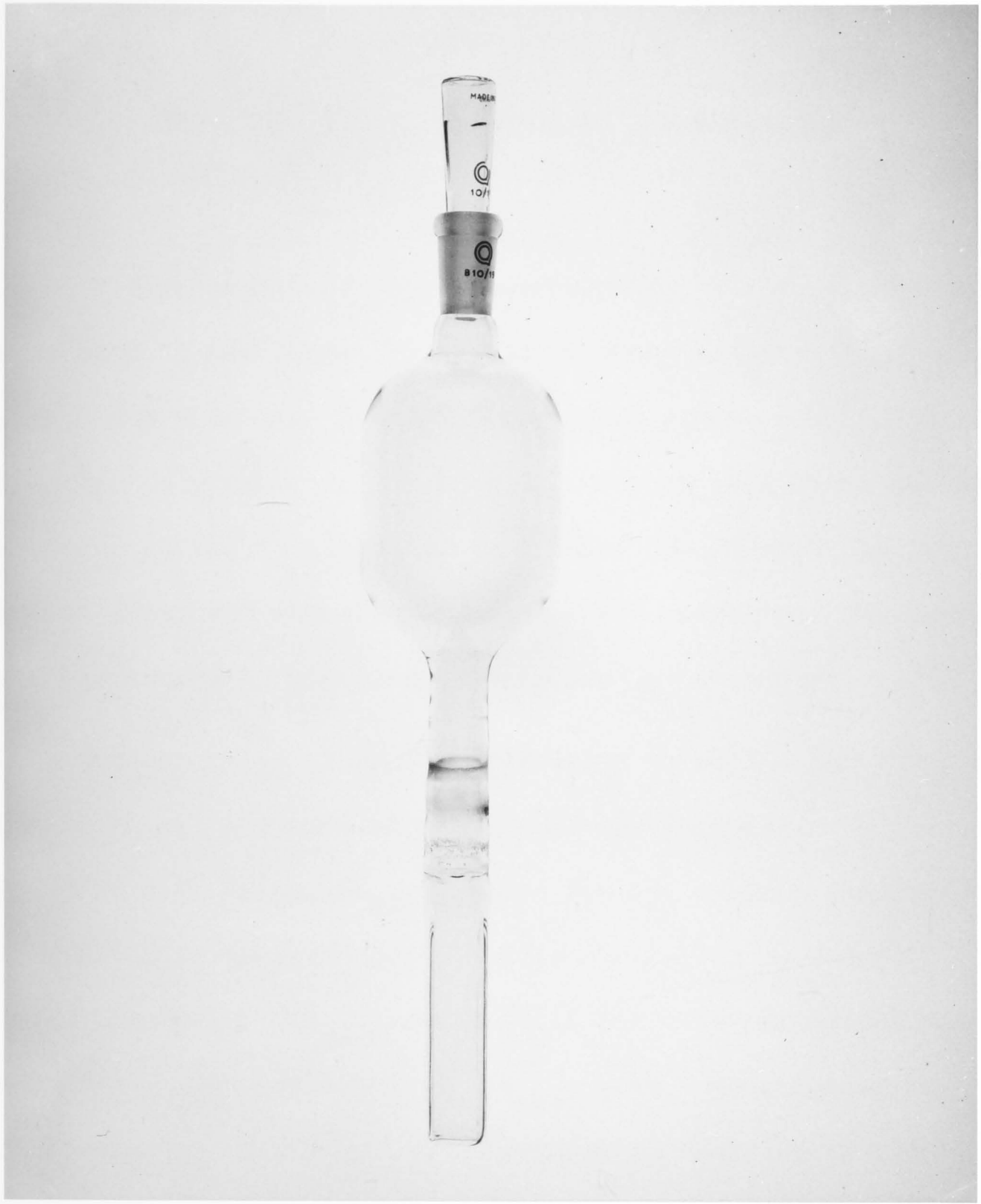

Figure 2.15 The 1 cm cell for fluorescence measurements

CHAPTER 3

EXCITED STATE PROCESSES IN SOLUTION

This chapter describes the mechanisms of some excited state processes such as the formation of excimers and exciplexes and protolytic reactions which are used as fluorescent probes within micelles. The fluorescence parameters involved in these excited state processes are sensitive to their environment and hence can be expected to provide information about the micelle structure. For comparison the behaviour of these parameters in homogeneous solution is presented.

The mechanism of excimer formation is well established but it is relevant to collate some of the equations characterising the excimer process. The time delay (Δt_{max}) needed for the excimer concentration to reach a maximum is both viscosity and concentration dependent. Therefore, this time delay (Δt_{max}) can be used for determining the viscosity of the solvent. The variation of (Δt_{max}) with concentration will be used to examine the distribution of solutes in micelles in Chapter 5. The relevant equations relating various fluorescence decay parameters are introduced. In Chapter 5 the effect of quenching on a fluorescence spectrum consisting of both excimer and monomer emission will be used to investigate the statistical distribution of the solute in micelles. The effect of quencher on the ratio of excimer to monomer fluorescence intensities, (ϕ'/ϕ), is examined in normal homogeneous solvents. The magnitude of ϕ'/ϕ assumed under different limiting conditions is

considered. Excimer formation of pyrene, 2-methylnaphthalene and 1-cyanonaphthalene will be used as fluorescent probes in Chapter 5. The effect of oxygen (as a quencher) on their (ϕ'/ϕ) ratio and the nature of the decay of their excimer and monomer fluorescence in organic solvent are examined in this chapter.

The kinetics of exciplex formation are very similar to those of excimer formation and a detailed treatment is not necessary here. However, the dependence of emission frequency and quantum yield on solvent polarity is an important characteristic of exciplexes and is discussed in Section 3.2. The red shift of the emission frequency of exciplex as an indicator of the high polarity of the interior of micelles is treated in Chapter 5.

The use of 2-naphthol as a fluorescent probe will be discussed in Chapter 5. The distribution of 2-naphthol as ROH^* and RO^{-*} forms between micellar-phase and aqueous phase will be examined using the fluorescence spectrum and the decay of the fluorescence of the probe. The protolytic reaction of 2-naphthol in pure water is summarised in this chapter and the nature of the excited state equilibrium is examined.

3.1 EXCIMERS

Excimer formation occurs upon collision of an electronically excited pyrene molecule with a molecule in its ground state and was discovered by Förster and Kasper [1955]. A dilute solution of pyrene ($< 5 \times 10^{-5}$ mol l^{-1}) has a structured fluorescence spectrum which is the mirror image of the absorption band. At higher concentration a new structureless fluorescence band appears at the longer wavelengths. As the concentration of pyrene is increased, the fluorescence intensity of

the new band increases at the expense of the normal fluorescence. No corresponding absorption band is observed for the new fluorescence. This new band was attributed to emission from excited dimers (later called "excimer" [Stevens and Hutton 1960]) of pyrene molecules. Following the discovery of excimer formation for pyrene, a large number of aromatic compounds have been found to exhibit excimer fluorescence in solution. These results have been reviewed by Förster [1969]. Data on excimer formation has been collected by Birks [1970a]. A review by Birks [1970b] and a book by Parker [1968a] have also dealt with the subject of excimer formation in solution. During the past five years the study of the subject has been carried out on various compounds using an interesting variety of techniques, including time-resolved spectroscopy.

Time resolved spectra of the pyrene excimer have been measured by Yoshihara and Kasuya [1971]. The time-resolved fluorescence spectrum of 3.2×10^{-3} mol l^{-1} pyrene in cyclohexane shows that, after a 5 ns delay, the monomer fluorescence is more intense than that of the excimer. The excimer fluorescence increases in intensity with time while the monomer emission intensity decreases. After 100 ns delay, the fluorescence spectrum of the same solution of pyrene is mainly that of the excimer with much reduced monomer emission. These results indicate that the monomer fluorescence decays monotonically while the excimer fluorescence increases from zero at $t = 0$, reaches a maximum and thereafter decays. This is consistent with the decay of pyrene excimer observed at a fixed wavelength.

The excimer emission of dibenzofuran has been reported by Horrocks and Brown [1970]. Thermodynamic data for the excimer formation were later obtained by Pinion, Minn and Filipescu [1971]. Excimer

formation with substituted fluorene was also reported. The dibenzofuran excimer has been re-examined by Nott and Selinger [1972]. They reported that ϕ'/ϕ is not affected by the addition of oxygen and that the monomer and the excimer have similar lifetime of 9.0 and 9.5 ns respectively.

Excimer formation by quinoline and isoquinoline in ethanol solution has been reported by Blaunstein and Gant [1973]. However, no excimer emission has been observed in non-polar solvent. No fluorescence was detected from quinoline in n-heptane, whereas fluorescence from quinoline in ethanol was readily observed. The extinction coefficient of the first absorption band of quinoline and isoquinoline increases with increasing solvent polarity. The appearance of excimers in the polar solvent was explained by the increase in the extinction coefficient of the first absorption band causing an enhanced probability of excimer formation.

3.1.1 Reaction Kinetics

The consideration of the fluorescence emission, the radiationless deactivation of the electronically excited monomer and of the excimer, and the dissociation of the excimer leads to the following reaction scheme [Förster and Kasper 1955; Döller and Förster 1962].

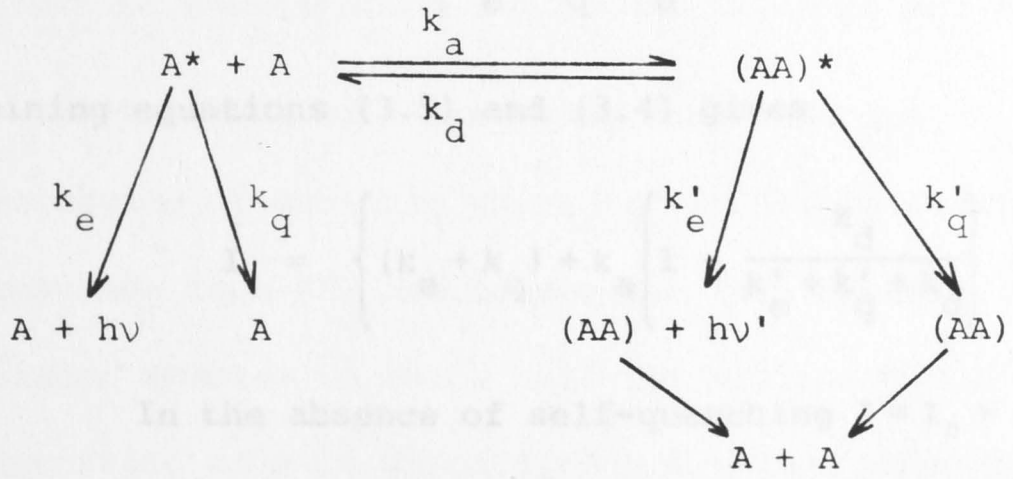

(3.1)

where: A is an aromatic molecule in the ground state,

A^* is an electronically excited molecule in the first singlet state,

$(AA)^*$ is an excimer in the first excited singlet state,

k_e and k'_e are rate constants for radiative decay processes,

k_q and k'_q are rate constants for radiationless decay processes,

k_a and k_d are association and dissociation rate constants, respectively.

Case I: Steady-State Irradiation

If I = the intensity of light in einstein l^{-1} s^{-1} absorbed by A, then from the reaction scheme,

$$\frac{d[A^*]}{dt} = I - \{k_e + k_q + k_a[A]\}[A^*] + k_d[(AA)^*] \qquad (3.2)$$

and

$$\frac{d[(AA)^*]}{dt} = k_a[A^*][A] - \{(k'_e + k'_q + k_d)[(AA)^*]\} . \qquad (3.3)$$

For continuous, uniform irradiation $[A^*]$ = constant and $[(AA)^*]$ = constant. That is, $d[A^*]/dt = 0$ and $d[(AA)^*]/dt = 0$. Then equations (3.2) and (3.3) become

$$I = \{k_e + k_q + k_a[A]\}[A^*] - k_d[(AA)^*] \qquad (3.4)$$

and

$$[(AA)^*] = \frac{k_a[A^*][A]}{k'_e + k'_q + k_d} . \qquad (3.5)$$

Combining equations (3.5) and (3.4) gives

$$I = \left\{(k_e + k_q) + k_a\left(1 - \frac{k_d}{k'_e + k'_q + k_d}\right)[A]\right\}[A^*] . \qquad (3.6)$$

In the absence of self-quenching $I = I_0 = (k_e + k_q)[A^*]$ and the

quantum yield of monomer fluorescence ϕ_0 is given by

$$\phi_0 = \frac{k_e[A^*]}{I_0} = \frac{k_e}{k_e + k_q} .$$

In the presence of self-quenching the monomer quantum yield ϕ is given as

$$\phi = \frac{k_e}{\left\{(k_e + k_q) + k_a\left(1 - \frac{k_d}{k'_e + k'_q + k_d}\right)[A]\right\}} ;$$

$$\therefore \frac{\phi_0}{\phi} = 1 + \frac{k_a[A]\ (k'_e + k'_q)}{(k_e + k_q)(k'_e + k'_q + k_d)} \qquad (3.7)$$

which may be written as

$$\frac{\phi_0}{\phi} = 1 + \frac{k_a[A]\tau}{1 + k_d\tau'} , \qquad (3.8)$$

where $\tau = 1/(k_e + k_q)$, and represents the lifetime of the monomer in the absence of self-quenching, and $\tau' = 1/(k'_e + k'_q)$, and represents the lifetime of the excimer in the absence of dissociation. Equation (3.8) can be written as

$$\frac{\phi_0}{\phi} = 1 + K[A] \qquad (3.9)$$

which is a Stern-Volmer equation for self-quenching. The Stern-Volmer constant K is a function of k_a, τ and the relative magnitudes of the rate constants of deactivation and dissociation of the excimer.

The mean self-quenching concentration, C_h, is the concentration of quencher which halves the intensity of monomer fluorescence from A*, and causes the fluorescence intensity of the associated species to reach half its maximum value. That is, C_h is the concentration of A at which $\phi_0/\phi = 2$. Thus equation (3.7) gives

$$C_h = \frac{k_e + k_q}{k_a} \cdot \frac{k'_e + k'_q + k_d}{k'_e + k'_q} . \qquad (3.10)$$

Case II: Transient Reaction Kinetics

A molecule A is promoted to its first excited singlet state by excitation with a δ-function light flash at $t = 0$ producing an initial concentration of excited monomer molecules, [A*]. This excited monomer A* may form species (AA)* upon collision with an unexcited molecule A. Thus after the flash has ceased, the decay of A* and (AA)* follow. At a subsequent time t after the excitation the rate equations, obtained from the reaction scheme (3.1), are as follows

$$\frac{d[A^*]}{dt} = k_d[(AA)^*] - \{k_e + k_q + k_a[A]\}[A^*] \qquad (3.11)$$

$$\frac{d[(AA)^*]}{dt} = k_a[A^*][A] - \{k'_e + k'_q + k_d\}[(AA)^*] . \qquad (3.12)$$

These can be written as

$$\frac{d[A^*]}{dt} = - n[A^*] + k_d[(AA)^*] \qquad (3.13)$$

$$\frac{d[(AA)^*]}{dt} = - n'[(AA)^*] + k_a[A][A^*] , \qquad (3.14)$$

where

$$n = k_e + k_q + k_a[A] \quad \text{and} \quad n' = k'_e + k'_q + k_d . \qquad (3.15)$$

The time dependences of fluorescences of both excited species are given by the time dependences of the concentrations of A* and (AA)*. These can be obtained by solving the two simultaneous differential equations (equations 3.13 and 3.14), and applying the initial conditions at $t = 0$, to produce

$$[A^*] = \frac{[A^*]_0}{\lambda_2 - \lambda_1}\left\{(\lambda_2 - n)\ e^{-\lambda_1 t} + (n - \lambda_1)\ e^{-\lambda_2 t}\right\} \qquad (3.16)$$

$$[(AA)^*] = \frac{k_a [A^*][A^*]_0}{\lambda_2 - \lambda_1}\left\{e^{-\lambda_1 t} - e^{-\lambda_2 t}\right\}, \qquad (3.17)$$

where $[A^*]_0$ = concentration of A at $t = 0$ and

$$\lambda_{1,2} = \tfrac{1}{2}\left\{(n + n') \mp [(n' - n)^2 + 4k_d k_a [A]]^{\frac{1}{2}}\right\} . \qquad (3.18)$$

The intensity of monomer fluorescence (per initially excited molecule) at time t is

$$I(t) = k_e \frac{[A^*]}{[A^*]_0} . \qquad (3.19)$$

Therefore, the monomer fluorescence intensity at any time t is given by equations (3.16) and (3.19) as

$$I(t) = \frac{k_e}{\lambda_2 - \lambda_1}\left\{(\lambda_2 - n)\ e^{-\lambda_1 t} + (n - \lambda_1)\ e^{-\lambda_2 t}\right\} . \qquad (3.20)$$

The intensity of excimer fluorescence at time t is

$$I'(t) = k'_e \frac{[(AA)^*]}{[A^*]_0} \qquad (3.21)$$

or

$$I'(t) = \frac{k'_e k_a [A]}{\lambda_2 - \lambda_1}\left\{e^{-\lambda_1 t} - e^{-\lambda_2 t}\right\} . \qquad (3.22)$$

The total quantum yield of monomer fluorescence is given by

$$\phi = \int_0^\infty I(t)dt . \qquad (3.23)$$

Using the value of I(t) and integration yields

$$\phi = \frac{k_e/(k_e + k_q)}{1 + [A]/C_h} \qquad (3.24)$$

or

$$\phi = \frac{\phi_0}{1 + [A]/C_h} . \qquad (3.25)$$

The total quantum yield of excimer fluorescence is given by

$$\phi' = \int_0^\infty I'(t)dt \ . \tag{3.26}$$

Using the value of I'(t) and integration gives

$$\phi' = \frac{k'_e/(k'_e + k'_q)}{1 + C_h/[A]} \tag{3.27}$$

or

$$\phi' = \frac{\phi'_0}{1 + C_h/[A]} \ . \tag{3.28}$$

Equations (3.25) and (3.28) give an important relation between monomer and excimer fluorescence

$$\frac{\phi'}{\phi} = \frac{\phi'_0[A]}{\phi_0 C_h} \ . \tag{3.29}$$

Using the values of C_h, ϕ'_0 and ϕ_0

$$\frac{\phi'}{\phi} = [A]\,\frac{k'_e}{k_e} \cdot \frac{k_a}{k'_e + k'_q + k_d} \ . \tag{3.30}$$

From equation (3.18), it is worth noting that λ_1 and λ_2 are functions of concentration, [A]. In order to obtain all the rate constants from the measurement of λ_1 and λ_2 as a function of concentration, it is useful to consider the following limiting conditions:

(1) At low concentration, $[A] \to 0$

$$\lambda_1 = k_e + k_q = \frac{1}{\tau_{monomer}} \tag{3.31a}$$

$$\lambda_2 = k'_e + k'_q + k_d = n' \ . \tag{3.31b}$$

(2) At high concentrations, $[A] \to \infty$

$$\lambda_1 = k'_e + k'_q = \frac{1}{\tau'_{excimer}} \tag{3.32a}$$

$$\lambda_2 = k_e + k_q + k_a[A] + k_d = n + k_d \qquad (3.32b)$$

$$\frac{\partial \lambda_2}{\partial [A]} = k_a \ . \qquad (3.32c)$$

The combination of the measurements of λ_1 and λ_2 and quantum yields of the monomer and excimer fluorescence gives all the rate constants in the reaction scheme [Birks, Dyson and Munro 1963].

In order to calculate the four rate constants k_a, k_d, $(k_e + k_q)$ and $(k'_e + k'_q)$, it is sufficient to measure λ_1 and λ_2 as a function of concentration [Hauser and Klein 1973]. For simplicity, let

$$n = k_e + k_q \quad \text{and} \quad n' = k'_e + k'_q \ . \qquad (3.33)$$

Then at all concentrations

$$\lambda_1 + \lambda_2 = n + n' + k_d + k_a[A] \qquad (3.34)$$

and

$$\lambda_1 \cdot \lambda_2 = n(n' + k_d) + n'k_a[A] \ . \qquad (3.35)$$

A plot of $(\lambda_1 + \lambda_2)$ against [A] gives a slope of k_a and an intercept of $n + n' + k_d$. Similarly $(\lambda_1 \cdot \lambda_2)$ plotted against [A] gives a slope of $n'k_a$ and an intercept of $n(n' + k_d)$. Thus, the rate constants k_a, k_d, n and n' can be calculated.

Förster and Kasper [1955] found that the half-value concentrations for pyrene excimer formation increased with solvent viscosity, indicating that the excimer formation was diffusion-controlled. The rate of a diffusion-controlled reaction is generally determined from the combination of the Smoluchowski equation [Smoluchowski 1917]

$$k = 4 \times 10^{-3}\ \pi\sigma N(D_A + D_{A^*}) \ , \qquad (3.36)$$

where σ is the encounter cross-section, D_A and D_{A^*} are the diffusion coefficients of A and A* and N is Avogadro's number, with the Stokes-Einstein equation

$$D = \frac{RT}{6\pi\gamma\eta} \tag{3.37}$$

on the assumption that $\sigma_{AA^*} = 2\gamma$. The result is the expression most often used to calculate the rate of diffusion of solute molecules through a solvent of viscosity η:

$$k = \frac{8RT}{3000\ \eta} . \tag{3.38}$$

A more rigorous approach gives the expression [Osborne and Porter 1965; Stevens and Dubois 1966]

$$k = \frac{8RT}{2000\ \eta} . \tag{3.39}$$

The agreement between k_a and the rate constant calculated for diffusion has also shown that excimer formation is a diffusion-controlled collision process [Birks, Dyson and Munro 1963]. Both k_a and C_h therefore depend on the viscosity of the solvent.

Because of the diffusion process involved in the formation of an excimer, there is often a measurable time delay for the excimer concentration to build up to a maximum. This time delay is obtained by differentiating equation (3.22) with respect to "t" and equating to zero which gives

$$\Delta t_{max} = \frac{ln(\lambda_1/\lambda_2)}{\lambda_2 - \lambda_1} . \tag{3.40}$$

As λ_1 and λ_2 are a function of concentration, [A], (equation 3.18), Δt_{max} is also concentration dependent. This effect is illustrated in Figure 3.1.

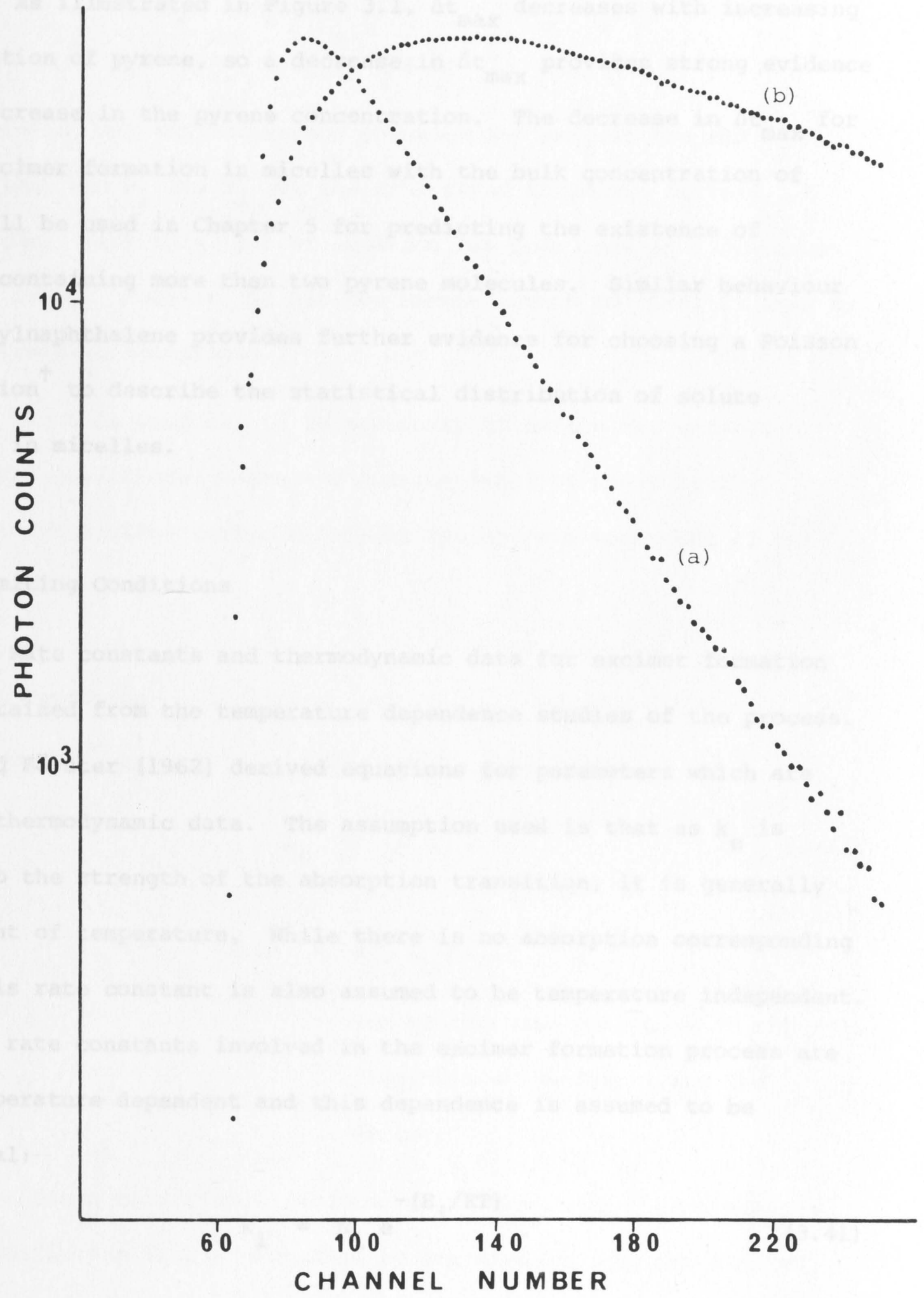

Figure 3.1. Fluorescence decay curves for pyrene excimer in cyclohexane at room temperature.

(a) 10^{-2} mol l^{-1}; (b) 10^{-3} mol l^{-1}.

The time scale is 1.0 ns/channel.

As illustrated in Figure 3.1, Δt_{max} decreases with increasing concentration of pyrene, so a decrease in Δt_{max} provides strong evidence for an increase in the pyrene concentration. The decrease in Δt_{max} for pyrene excimer formation in micelles with the bulk concentration of pyrene will be used in Chapter 5 for predicting the existence of micelles containing more than two pyrene molecules. Similar behaviour of 2-methylnaphthalene provides further evidence for choosing a Poisson distribution† to describe the statistical distribution of solute molecules in micelles.

3.1.2 Limiting Conditions

Rate constants and thermodynamic data for excimer formation can be obtained from the temperature dependence studies of the process. Döller and Förster [1962] derived equations for parameters which are used for thermodynamic data. The assumption used is that as k_e is related to the strength of the absorption transition, it is generally independent of temperature. While there is no absorption corresponding to k'_e, this rate constant is also assumed to be temperature independent. The other rate constants involved in the excimer formation process are often temperature dependent and this dependence is assumed to be exponential:

$$k_i = N_i \, e^{-(E_i/RT)} \quad . \tag{3.41}$$

This temperature dependence makes analysis of the process more complex. For example, it has been shown that the temperature dependence of C_h for the mechanism (3.1) is given by [Döller and Förster 1962],

---

† Poisson distribution allows unlimited number of solutes in a micelle (Chapter 5).

$$C_h = \frac{k_e}{\phi N_a} \cdot e^{+E_a/RT} + \frac{\phi' N_d k_e}{\phi N_a k'_e} \cdot e^{-(E_d - E_a)/RT} , \qquad (3.42)$$

where E_a and E_d are the activation energies for association and dissociation, and N_a and N_d are the associated Arrhenius factors. A full treatment with this type of equation has been made in a few cases [Selinger 1966]. However, it has now become common to simplify them by means of limiting conditions.

For this purpose, it is necessary to define two sets of experimental conditions, which are distinguished by the relative magnitude of the dissociative and deactivating rate constants of the excimer.

Case I: α Condition

The α condition is defined by the condition

$$k_d \gg \Sigma k' , \qquad (3.43)$$

where

$$\Sigma k' = k'_e + k'_q + \ldots$$

= sum of the rate constants of all processes which deactivate the excimer.

That is, in the α condition, dissociation of the excimer predominates and the equilibrium is not perturbed by deactivations of the excited species. If the α condition is applied to equation (3.10)

$$C_h = \frac{k_e + k_q}{k'_e + k'_q} \cdot \frac{k_d}{k_a} . \qquad (3.44)$$

Here C_h is no longer dependent on k_a alone, but upon the ratio of

(k_d/k_a). C_h is then determined by the excimer dissociation equilibrium and is independent of the viscosity of the solvent.

For the α condition ϕ'/ϕ becomes (from equation 3.30)

$$\frac{\phi'}{\phi} = [A] \cdot \frac{k'_e}{k_e} \cdot \frac{k_a}{k_d} . \qquad (3.45)$$

When a small amount of quencher is added, which quenches the fluorescence of both species (e.g. oxygen), $\Sigma k'$ becomes

$$\Sigma k' = k'_e + k'_q + k_o .$$

The presence of an additional deactivation process (k_o) does not affect the defined condition, because k_d is already larger than the sum of all the deactivation rate constants. Thus, for the α condition ϕ'/ϕ will not change on the addition of a quencher. In this region, the temperature dependence of the fluorescence ratio gives ΔH^*, the enthalpy of the formation of an excimer [Selinger 1966]. Under the α condition

$$\frac{\phi'}{\phi} = [A] \frac{k'_e}{k_e} \cdot \frac{N_a}{N_d} \cdot e^{-\Delta H^*/RT} , \qquad (3.46)$$

where

$$\Delta H^* = E^*_d - E^*_a .$$

A plot of $ln(\phi'/\phi)$ versus 1/T yields a straight line of gradient $-\Delta H^*/R$ and intercept $ln[A]\ k'_e/k_e \cdot N_a/N_d$. Under the α condition

$$ln \frac{\phi'}{\phi} = ln \frac{k'_e}{k_e} [A] + \frac{\Delta S^*}{R} - \frac{\Delta H^*}{RT} . \qquad (3.47)$$

Evaluation of k_e and k'_e enables calculation of ΔH^* and ΔS^*. Stevens and Ban [1964] have used this method to determine the enthalpies and entropies of photoassociation of naphthalene derivatives. It is worth noting that the enthalpy of formation, ΔH^*, can only be obtained

accurately and easily for a system in which the excited state reaction is unperturbed by the deactivation process, i.e. α condition [McDonald and Selinger 1971a].

Case II: β Condition

The β condition is defined by the condition

$$k_d \ll \Sigma k' \ . \tag{3.48}$$

That is, once an excimer is formed it deactivates rather than dissociates. For the β condition equation (3.10) reduces to

$$C_h = \frac{k_e + k_q}{k_a} \tag{3.49}$$

and equation (3.30) becomes

$$\frac{\phi'}{\phi} = [A] \frac{k'_e}{k_e} \cdot \frac{k_a}{k'_e + k'_q} \ . \tag{3.50}$$

Equation (3.49) means that if the mean decay time, $(1/(k_e + k_q))$, of the initially excited species is known, then the value of C_h gives the bimolecular rate constant of association. It is also useful to express equation (3.49) as

$$k_a = \frac{1}{\tau \cdot C_h} \ , \tag{3.51}$$

where

$$\tau = \frac{1}{k_e + k_q}$$

= lifetime of initially excited species in the absence of a quencher.

This value of k_a can be compared with the value calculated from a diffusion equation.

When a small amount of quencher is added, the rate constant for the quenching process, k_o, causes ϕ'/ϕ to decrease because equation (3.50) becomes

$$\frac{\phi'}{\phi} = [A] \frac{k'_e}{k_e} \cdot \frac{k_a}{k'_e + k'_q + k_d + k_o} . \qquad (3.52)$$

The tests and requirements for these two limiting cases, the α and β conditions, are described elsewhere [Cohen and Selinger 1969; McDonald and Selinger 1971a]. In this study, the tests of these two limiting conditions will be: (1) the effect of a quencher (e.g. oxygen) on ϕ'/ϕ, and (2) the nature of the decay of the monomer and the excimer.

(1) For the α condition ϕ'/ϕ is not affected by the addition of a quencher. However, for the β condition ϕ'/ϕ decreases with the concentration of a quencher.

(2) For the α condition the lifetime of the monomer and that of the excimer are almost identical. The only difference will be the time delay in the build-up of the excimer. The decay time is the average of the lifetime for pure monomer and pure excimer, weighted by the relative time the system is present as one or the other species. However, for the β condition the monomer lifetime is different from that of the excimer.

The tests of the limiting conditions have been applied to the pyrene, 2-methylnaphthalene and 1-cyanonaphthalene excimer processes. These are illustrated in the subsequent figures (Figures 3.2 - 3.4).

The effect of an added quencher on the ratio ϕ'/ϕ is used in Chapter 5 to investigate the nature of the solute-micelle-solvent system. In homogeneous solutions ϕ'/ϕ cannot be increased by the addition of a quencher (see equation 3.52). However, the ratio ϕ'/ϕ increases on the

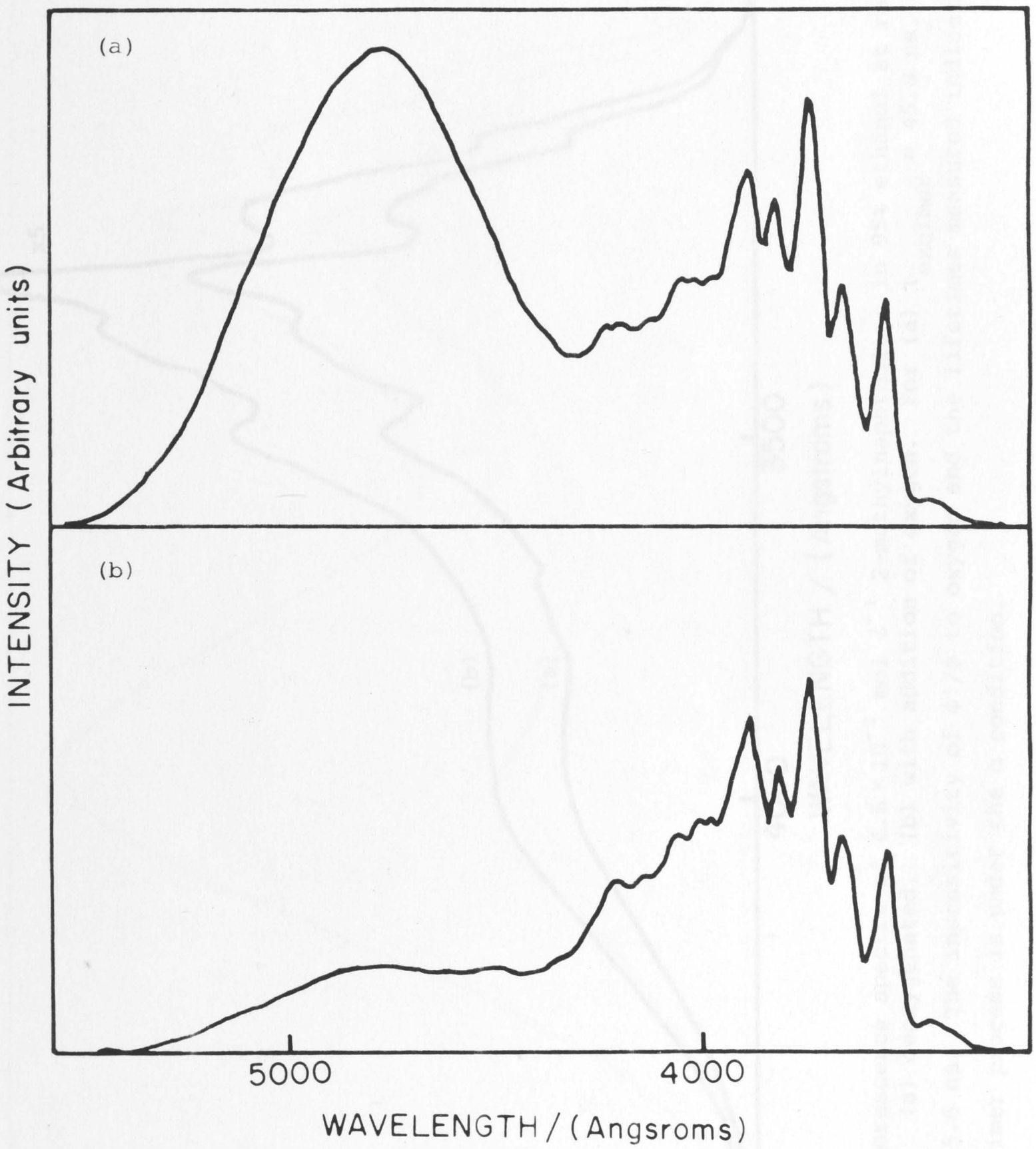

Figure 3.2. Fluorescence spectra of 10^{-3} mol l^{-1} pyrene in cyclohexane at room temperature.

(a) deoxygenated; (b) with addition of oxygen.

The fluorescence lifetimes of the excimer and the monomer are 123 (ns) and 112 (ns) respectively. The difference in the lifetimes and the decrease in the ratio ϕ'/ϕ with the addition of oxygen indicate that the pyrene excimer process is occurring under the β condition.

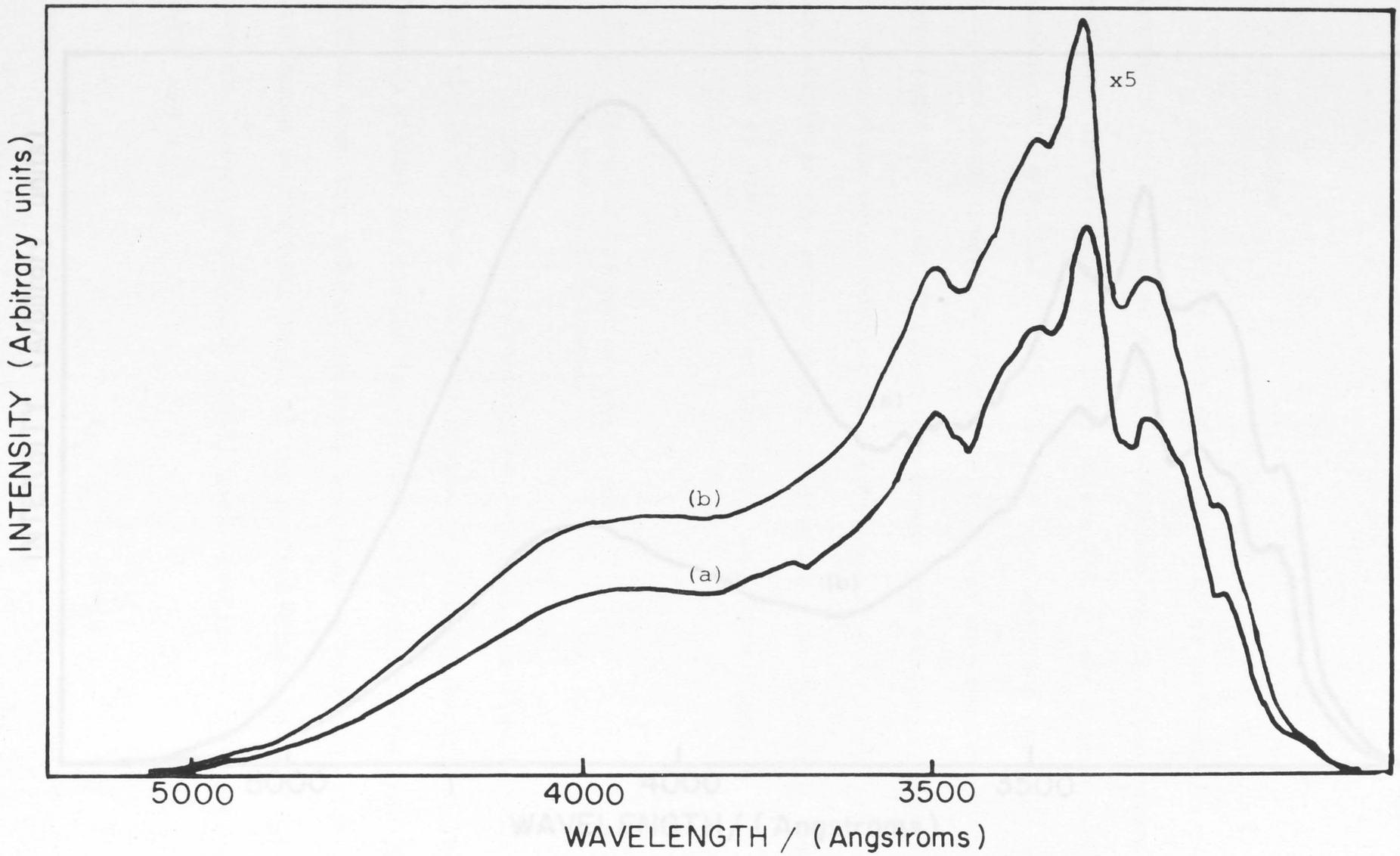

Figure 3.3. Fluorescence spectra of 4.6×10^{-1} mol ℓ^{-1} 2-methylnaphthalene in 95% ethanol at room temperature: (a) deoxygenated, (b) with addition of oxygen. For (a) $\tau_{excimer}$ = 45.8 ns, $\tau_{monomer}$ = 45.6 ns. The insensitivity of ϕ'/ϕ to oxygen and the lifetimes measured indicate that the excimer process is under the α condition.

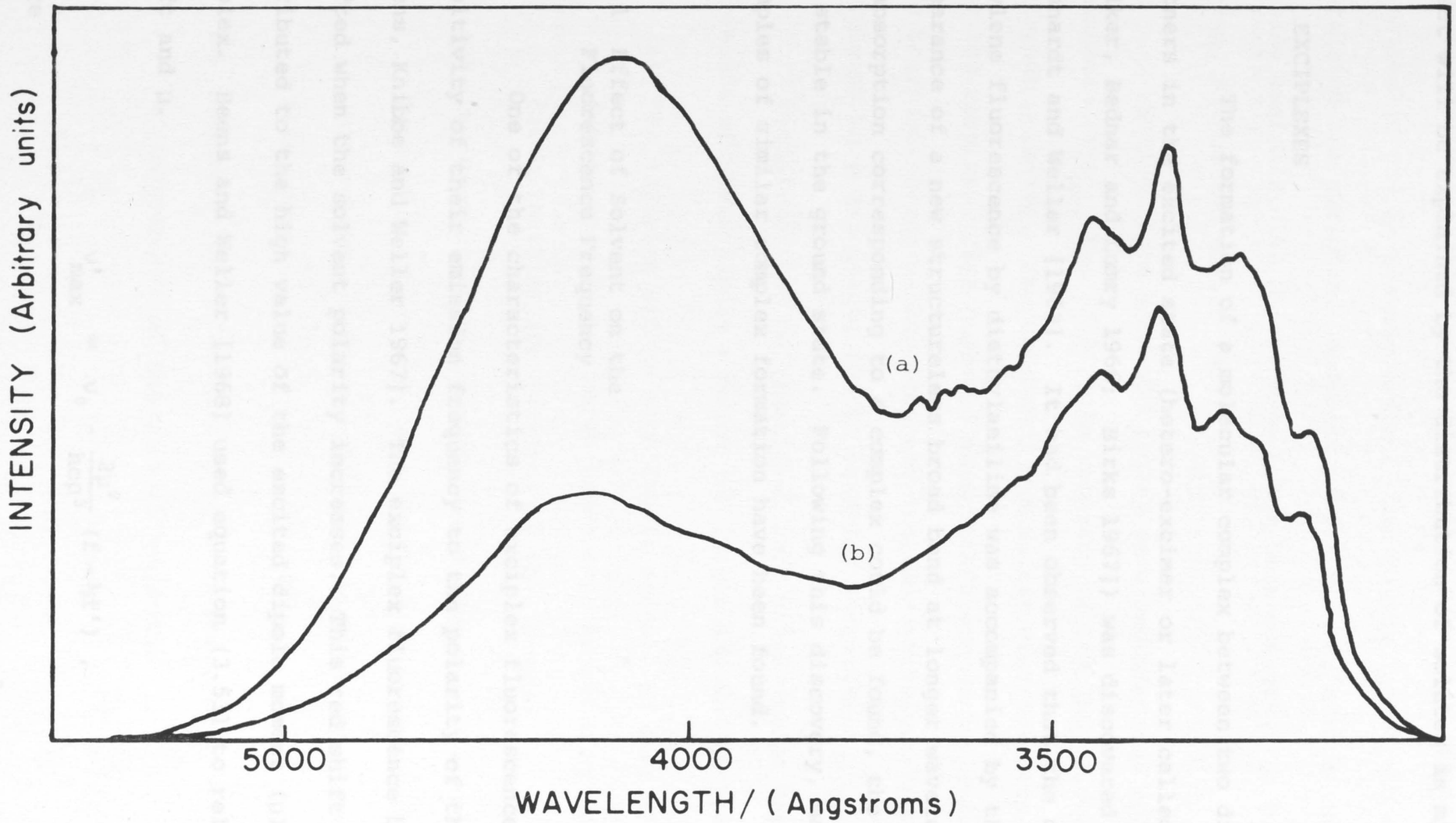

Figure 3.4. Fluorescence spectra of 3.12×10^{-2} mol ℓ^{-1} 1-cyanonaphthalene in cyclohexane at room temperature: (a) deoxygenated, (b) with addition of oxygen. For (a) $\tau_{excimer}$ = 10.5 ns, $\tau_{monomer}$ = 4.9 ns. The difference in the lifetimes and the decrease in ϕ'/ϕ with the addition of oxygen show that the system is under the β condition.

addition of a quencher to a micellar solution of pyrene. This anomalous effect will be explained by the distribution of solutes in micelles.

3.2 EXCIPLEXES

The formation of a molecular complex between two different partners in the excited state (hetero-excimer or later called exciplex [Walker, Bednar and Lumry 1966; Birks 1967]) was discovered by Leonhardt and Weller [1963]. It had been observed that the quenching of perylene fluorescence by diethylaniline was accompanied by the appearance of a new structureless broad band at longer wavelengths. As no absorption corresponding to a complex could be found, the complex is not stable in the ground state. Following this discovery, many other examples of similar complex formation have been found.

3.2.1 Effect of Solvent on the Fluorescence Frequency

One of the characteristics of exciplex fluorescence is the sensitivity of their emission frequency to the polarity of the solvent [Beens, Knibbe and Weller 1967]. The exciplex fluorescence band is red shifted when the solvent polarity increases. This red shift is attributed to the high value of the excited dipole moment (μ) of the complex. Beens and Weller [1968] used equation (3.53) to relate the red shift and μ.

$$\nu'_{max} = \nu_0 - \frac{2\mu^2}{hc\rho^3}\,(f - \tfrac{1}{2}f') \,, \qquad (3.53)$$

where

$$f = \frac{\varepsilon - 1}{2\varepsilon + 1} \qquad \text{and} \qquad f' = \frac{n^2 - n}{2n^2 + 1} \,.$$

Although plots of ν'_{max} versus $(f - \frac{1}{2}f')$ exhibit some scatter due to specific solvent-solute interactions, they enable the dipole moment to be estimated for an assumed value of the radius (ρ) of the cavity containing the exciplex. Assuming $\rho = 5$ Å for the anthracene-diethylanaline exciplex, its dipole moment has been estimated to be > 10 Debye [Beens, Knibbe and Weller 1967].

Selinger and McDonald [1972] have measured the polarity dependence of ν'_{max} and of ϕ'/ϕ in solvents of similar viscosity but different polarity. The extent of charge transfer has been estimated from the results. They observed that anthracene-diethylaniline, 2-methoxynaphthalene-naphthalene and 1-cyanonaphthalene-naphthalene exciplexes have decreasing charge transfer character.

Exciplexes can be classified into three groups depending upon the values of their dipole moments (μ) [Beens and Weller 1968].

(1) The exciplex with a high dipole moment, μ, owes its stability almost totally to charge transfer. Aromatic hydrocarbons-diethylaniline are examples of this group.

(2) The exciplex with a small dipole moment, μ (but $\mu \neq 0$). This type of exciplex will be stabilised partly by resonance interaction. 1-Cyanonaphthalene-naphthalene is an example of this group.

(3) Excimers can be treated as an exciplex with $\mu = 0$. Here ν'_{max} is independent of the solvent polarity.

3.2.2 Effect of Solvent on the Quantum Yield

The intensity of emission from the exciplex decreases with increasing solvent polarity. The effect is stronger for exciplexes having almost pure charge transfer character [Knibbe 1969]. The fluorescence lifetime of the exciplex also decreases with increasing polarity of the solvent. For the anthracene-diethylaniline exciplex, the exciplex intensity and the decay time have been found to decrease by a factor of 35 and 3.5 respectively when the dielectric constant of the solvent changes from 2 to 12 [Knibbe, Röllig, Schäfer and Weller 1967]. In similar studies on the dimethylaniline-pyrene exciplex, Mataga, Okada and Yamamoto [1967] have reported change factors of 44 and 2.8 respectively. Mataga *et al.* explained these observations on the basis of the complex-solvent interaction which led to the conclusion that the radiative rate constant decreases with increasing solvent polarity. However, Knibbe *et al.* explained the effect on the basis of formation of a solvated ion pair between the solvent and each of the components. The following kinetic scheme has been suggested for the latter interpretation of exciplex formation in polar solvents [Selinger and McDonald 1972].

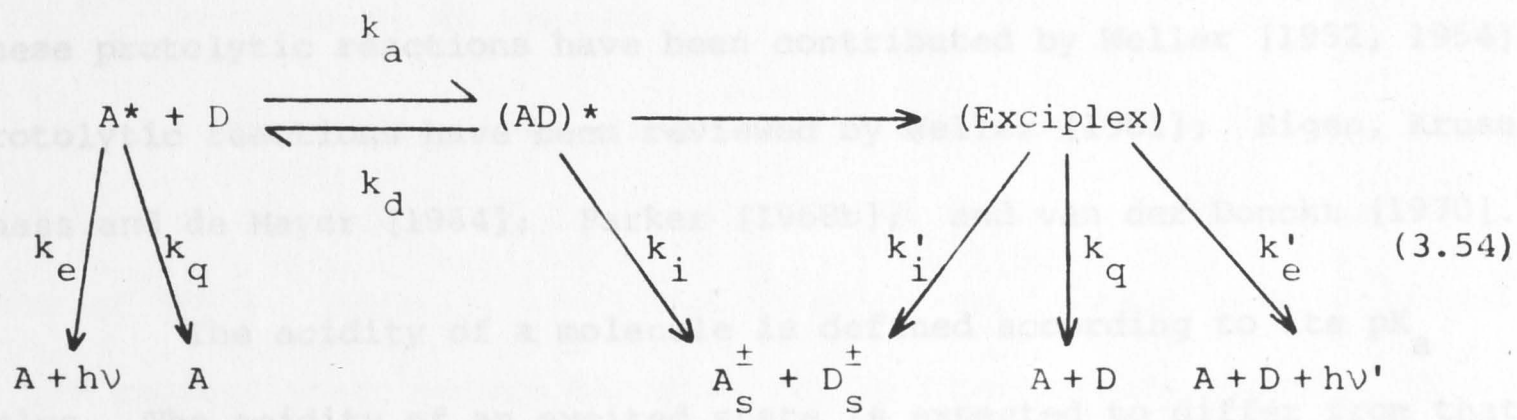

(3.54)

where k_i and k_i' are polarity dependent rate constants for the formation of solvated ions. Although the nature of the quench complex is not

specified, it has been assumed that (AD)* deactivates directly prior to exciplex formation. According to this kinetic scheme an increase in k_i' reduces both the exciplex lifetime and the emission intensity whereas an increase in k_i reduces only the emission intensity of the exciplex.

As the emission frequency of an excimer is insensitive to the polarity of the solvent it is not a good fluorescent probe to use for estimating the polarity of the interior of micelles. However, exciplex emission is sensitive to solvent polarity and the red shift of the emission maximum band of an exciplex is used to investigate the polarity of the interior of micelles in Section 5.2.

3.3 PROTOLYTIC REACTIONS

The pH dependence of the fluorescence spectrum of 1-naphthalamine-9-sulphonate was discovered by Weber [1931]. Nearly twenty years later, the effect was interpreted by Förster who also reported the excited state dissociation of hydroxy- and amino-pyrene sulphonates [Förster 1950a]. Similar results have been obtained with naphthalene derivatives [Förster 1950b]. Following these experimental observations, a detailed study and a full derivation of the kinetics of these protolytic reactions have been contributed by Weller [1952, 1954]. Protolytic reactions have been reviewed by Weller [1961]; Eigen, Kruse, Maass and de Mayer [1964]; Parker [1968b]; and van der Donckt [1970].

The acidity of a molecule is defined according to its pK_a value. The acidity of an excited state is expected to differ from that of the ground state. The ground state pK_a value can be obtained from the pH dependence of the absorption spectra [Jaffé and Orchin 1962]. The acidity of the excited state pK_a^* can be obtained directly, if

equilibrium is attained within the lifetime of the excited molecule, by measuring the fluorescence intensities as a function of pH. Förster [1950a] proposed a method for determining the pK_a^* using the following equation, which assumes that the entropy changes are the same in the ground and excited singlet states:

$$pK_a^* = pK_a - \frac{0.625}{T} (\Delta\bar{\nu}) \quad . \qquad (3.55)$$

$\Delta\bar{\nu}$ (cm^{-1}) can be obtained from the difference in the absorption maxima (or the fluorescence maxima) of the acidic and basic forms. This method enables pK_a^* to be calculated from the absorption spectra alone. pK_a^* can also be obtained from the rate constants of the proton transfer reaction in the excited state from fluorescent measurement [Weller 1952].

According to their pK_a and pK_a^* values, aromatic acids can be classified in two groups [Weller 1961].

(1) Aromatic amines and phenols have $pK_a^* < pK_a$. That is, they are much stronger acids in their excited state than in their ground states. Examples are 2-naphthylamine and 2-naphthol.

(2) Aromatic carboxylic acids and aromatic ketones have $pK_a^* > pK_a$. They become much stronger bases in the excited states. Acridine is an example.

Furthermore, there are two different types of reactions depending on the nature of the equilibria in their excited states [Förster 1960]. Firstly, reactions in which equilibrium is established in the excited state before deactivation by fluorescence occurs. This is indicated by the rapid change over from the basic to the acidic spectrum with changing pH values. 2-Naphthylamine is an example. Secondly, reactions whose rates are generally not sufficiently rapid to

establish equilibrium before radiative and radiationless depopulation of the excited state occurs. This is indicated by the fact that the fluorescence of both forms are present over a wide range of pH values. 2-Naphthol is an example.

3.3.1 The Equilibrium of 2-Naphthol*-Water Reaction

The fluorescence spectra of 2-naphthol in water as a function of pH is shown in Figure 3.5. In a strong acid solution only naphthol fluorescence is observed. Only naphtholate ion fluorescence at longer wavelengths is detected for a strong basic solution. From the corrected fluorescence spectra of 2-naphthol at different values of pH, a plot of ϕ/ϕ_0 against pH or ϕ'/ϕ_0' against pH can be obtained. ϕ_0 and ϕ_0' are the fluorescence quantum yield of naphthol in acidic and basic solutions respectively; ϕ and ϕ' are the corresponding values at a certain pH. For an accurate determination of the quantum yield ratios, the mutual overlap in the fluorescence spectrum due to the two species must be taken into account as described for pyrene in Section 2.1.2.

The plots of ϕ/ϕ_0 and ϕ'/ϕ_0' against pH are shown in Figure 3.6. At first ϕ/ϕ_0 decreases as the pH value increases. However, ϕ/ϕ_0 becomes constant for the region ($\sim$ pH 3 - 7) and it decreases again as the pH value further increases. On the other hand, ϕ'/ϕ_0' increases with the increase in pH values except for the region between pH 3 - 7. These experimental observations can be explained by the acid-base reaction of a molecule in water where the latter is a proton acceptor. At 25 °C, the following values are obtained for the flat region of the curves [Weller 1952]:

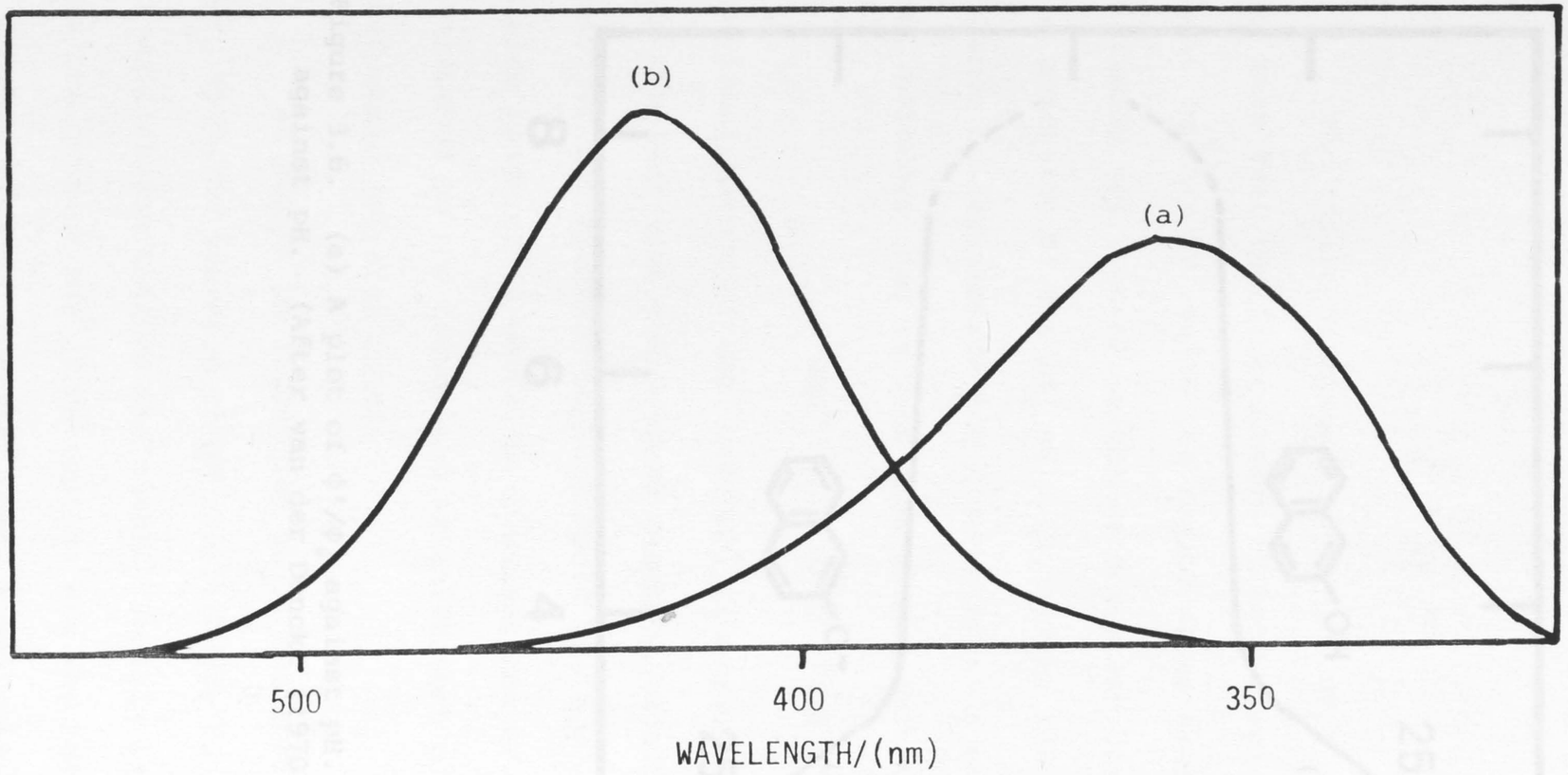

Figure 3.5. Fluorescence spectra of 2-naphthol in water. Excitation at 316 nm. (a) acidic, and (b) basic.

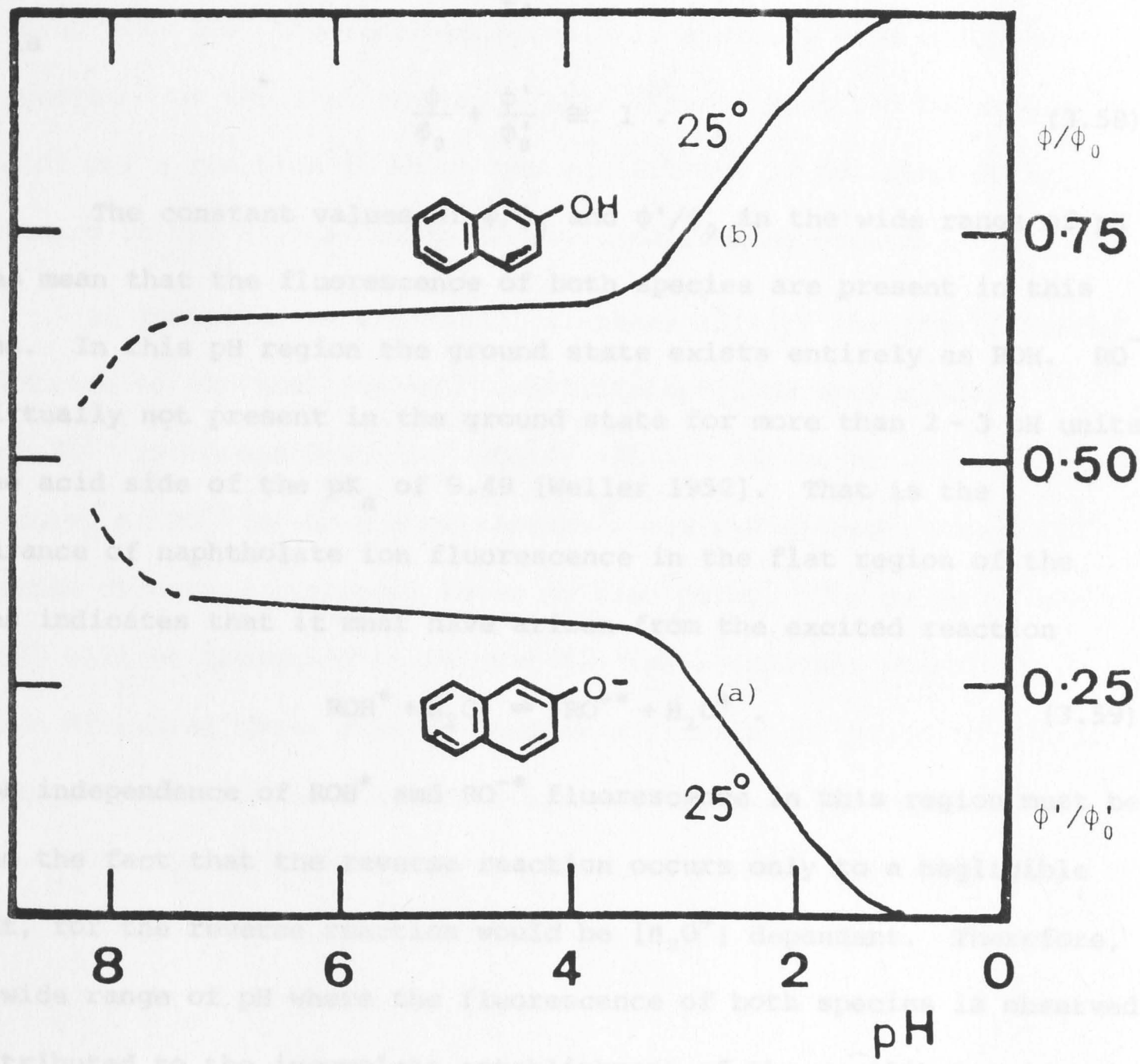

Figure 3.6. (a) A plot of ϕ'/ϕ_0' against pH. (b) a plot of ϕ/ϕ_0 against pH. (After van der Donckt [1970].)

$$\frac{\phi}{\phi_0} = 0.73 \qquad (3.56)$$

$$\frac{\phi'}{\phi_0'} = 0.28 \ . \qquad (3.57)$$

That is

$$\frac{\phi}{\phi_0} + \frac{\phi'}{\phi_0'} \cong 1 \ . \qquad (3.58)$$

The constant values of ϕ/ϕ_0 and ϕ'/ϕ_0 in the wide range of pH values mean that the fluorescence of both species are present in this region. In this pH region the ground state exists entirely as ROH. RO^- is virtually not present in the ground state for more than 2 - 3 pH units to the acid side of the pK_a of 9.49 [Weller 1952]. That is the appearance of naphtholate ion fluorescence in the flat region of the curves indicates that it must have arisen from the excited reaction

$$ROH^* + H_2O \rightleftharpoons RO^{-*} + H_3O^+ \ . \qquad (3.59)$$

The pH independence of ROH^* and RO^{-*} fluorescence in this region must be due to the fact that the reverse reaction occurs only to a negligible extent, for the reverse reaction would be $[H_3O^+]$ dependent. Therefore, this wide range of pH where the fluorescence of both species is observed is attributed to the incomplete establishment of the equilibrium in the excited state [Förster 1960].

At higher pH (above the pK_a), the rise in ϕ'/ϕ_0' and the fall of ϕ/ϕ_0 with the increase of pH are both due to the shift in the ground state equilibrium towards the right. In this region the decrease of ROH causes the drop of ROH^* fluorescence and the increase of RO^- causes the RO^{-*} fluorescence to increase. Thus ϕ'/ϕ_0' increases and there is virtually only RO^- present in both the ground state and the excited state in the strong basic solutions.

In the region beyond the flat curve, the reverse reaction becomes more and more significant due to the increase in $[H_3O^+]$. This marked increase in $[H_3O^+]$ causes the rise in ϕ/ϕ_0 and the drop in ϕ'/ϕ'_0. Therefore, only ROH^* fluorescence appears in a strong acid solution. The appearance of the flat region in this type of plot can be used as an indicator for a reaction in which the equilibrium is not completely established in the excited state before fluorescence occurs.

As indicated in the reaction scheme (3.59), the time resolved fluorescence of the ROH^* and RO^{-*} are different from each other. Because RO^{-*} is formed from ROH^*, there will be a time delay before the decay curve of RO^{-*} fluorescence reaches a maximum whereas, since ROH^* is excited directly, its decay shows no time delay. The decay of ROH^* and RO^{-*} will be presented in Chapter 5. The 2-naphthol protolytic reaction discussed above will be used as a fluorescent probe to locate the charged particles in a micellar-aqueous-system. The experiment involves the selective fluorescence quenching of ROH^* and RO^{-*} using both water soluble and water insoluble quenchers. The full treatment will be given in Section 5.4.4.

CHAPTER 4

MICELLE FORMATION IN AQUEOUS SOLUTION

Soap solutions were first investigated by McBain and co-workers in the 1900's and the term "ionic micelle" was suggested for an aggregate of soap molecules by McBain [1913]. Hartley [1936], after working on an alkyl quaternary ammonium salt, interpreted micelle formation in aqueous solution as being a hydrophobic effect and postulated the existence of the "spherical micelle". Since the 1940's these early works on ionic micelles have been followed with the study of micelle formation by nonionic surfactants.

Intensive studies on micelle formation in aqueous and non-aqueous solutions have led to a fairly detailed understanding of the micelle. In many systems, the micelle appears to be a compact spheroidal particle 12 - 30 Å in radius in which the hydrocarbon tail is inside, remote from the aqueous phase and the hydrophilic groups are at the surface. Micelles may be considered as structures capable of both rapid breakdown and rapid formation. The breakdown time of the micelles of cetyltrimethylammonium bromide is less than 1 ms [Heckman 1958]. Jaycock and Ottewill [1964] reported that the breakdown of sodium dodecyl sulphate (SDS) and dodecyl pyridinium iodide is also fast, the half-life being the order of 10 ms.

Besides the commercial importance of surfactants, the understanding of micelle formation is extremely important, because micelle formation is an example of the hydrophobic effect which is of foremost importance in biological macromolecules. Therefore, the micelles themselves, which offer the advantage of simple structure and surface composition, can be utilised as models for studying biological systems. In this thesis micelle formation in aqueous solution has been studied using the fluorescent probe technique. Therefore, in this chapter the study of some relevant physical properties of micellar systems and some factors which influence them is reported.

4.1 IONIC MICELLES

In the development of some fluorescent probes to be applied to micellar aqueous systems, ionic micelles will be investigated in Chapter 5. Anionic micelles formed by SDS will be the focus of the study. The distribution of solutes in the micelles and location of the solute in the micellar aqueous system will be investigated. For these reasons the structure of ionic micelles is presented in this section.

An ionic surfactant molecule has a hydrocarbon chain as the hydrophobic part, and a water soluble polar head group. For example, the SDS molecule can be presented as follows:

$$\underbrace{CH_3CH_2CH_2CH_2CH_2CH_2CH_2CH_2CH_2CH_2CH_2CH_2}_{\text{hydrophobic region}}\ \underbrace{SO_4^-Na^+}_{\substack{\text{hydrophilic}\\ \text{region}}}$$

A schematic representation of the regions of a spherical ionic micelle is shown in Figure 4.1. An ionic micelle has three different regions,

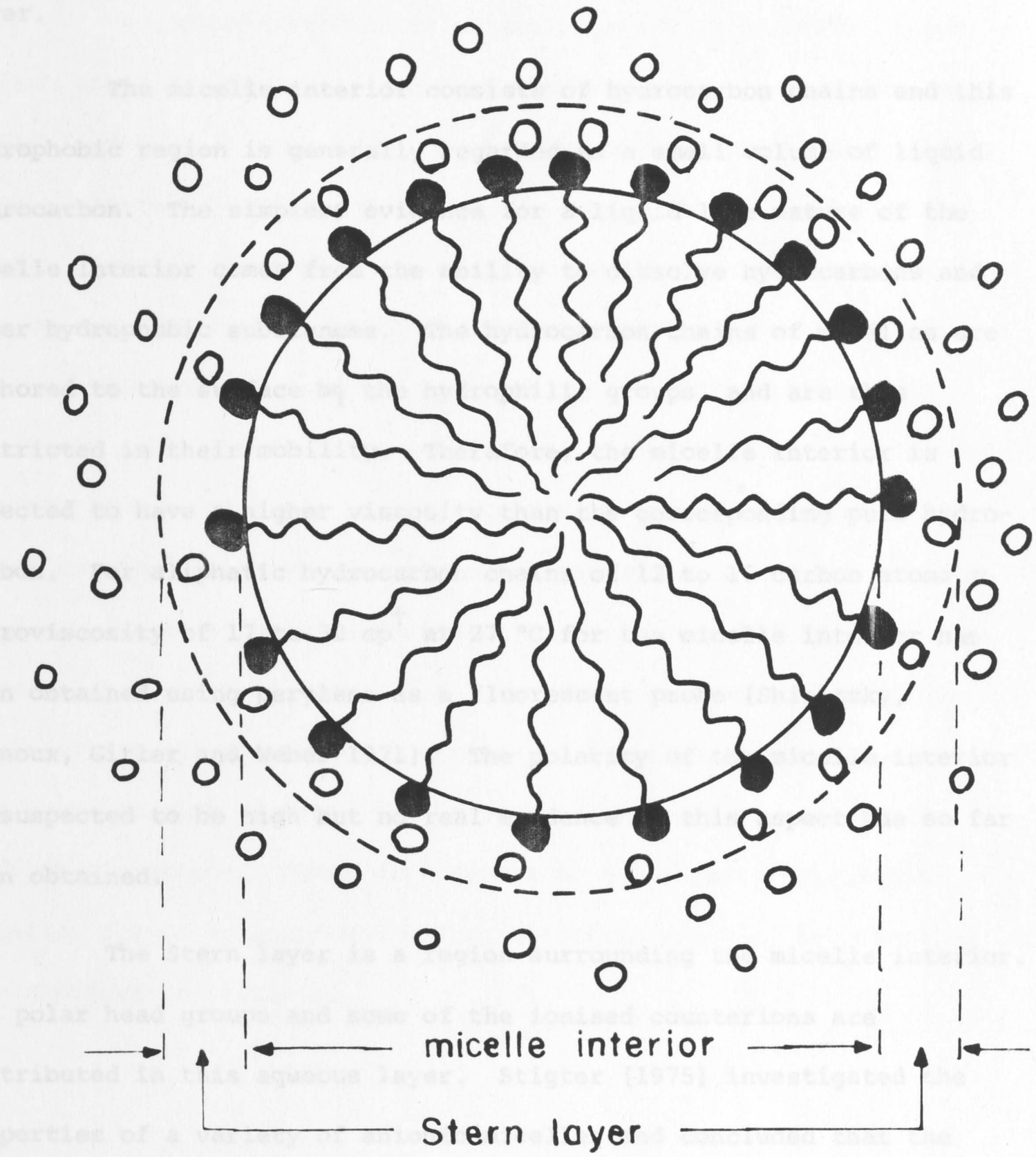

Figure 4.1. A schematic representation of the region of a spherical ionic micelle. (●) are the polar head groups, (○) are the counterions and (~~~~) are the hydrocarbon chains. The Gouy-Chapman layer (not indicated) is a region outside the Stern layer. (After Fendler and Fendler [1970].)

namely the micelle interior (core), the Stern layer and the Gouy-Chapman layer.

The micelle interior consists of hydrocarbon chains and this hydrophobic region is generally regarded as a small volume of liquid hydrocarbon. The simplest evidence for a liquid-like nature of the micelle interior comes from the ability to dissolve hydrocarbons and other hydrophobic substances. The hydrocarbon chains of micelles are anchored to the surface by the hydrophilic groups, and are thus restricted in their mobility. Therefore, the micelle interior is expected to have a higher viscosity than the corresponding pure hydrocarbon. For aliphatic hydrocarbon chains of 12 to 16 carbon atoms a microviscosity of 17 to 32 cp[†] at 27 °C for the micelle interior has been obtained using perylene as a fluorescent probe [Shinitzky, Dianoux, Gitler and Weber 1971]. The polarity of the micelle interior is suspected to be high but no real evidence on this aspect has so far been obtained.

The Stern layer is a region surrounding the micelle interior. The polar head groups and some of the ionised counterions are distributed in this aqueous layer. Stigter [1975] investigated the properties of a variety of anionic micelles and concluded that the thickness of the Stern layer for sodium alkyl sulphates is 4.6 Å. The rest of the counterions are distributed outside the shear surface. The diffuse atmosphere where these counterions are distributed is known as the Gouy-Chapman layer.

[†] These values are to be compared with viscosities of 3.0 cp for liquid n-hexadecane at a comparable temperature, and of 13.4 cp for n-hexadecyl alcohol at 50 °C (about twice this value is to be expected at 25 °C) [Tanford 1973].

4.2 NONIONIC MICELLES

A nonionic surfactant molecule generally consists of a hydrocarbon chain attached to a chain of ethylene oxide or propylene oxide units (hydrophilic region). For example, polyoxyethene alcohols have a general formula: $RO(CH_2CH_2O)_nC_2H_4OH$; where $(n+1)$ is the average number of moles of ethylene oxide added to one mole of a given alcohol. The solubility of these nonionic surfactants in water is probably due to the hydration of ether oxygen atoms in the hydrophilic region [Ferguson 1955]. Thus the solubility of nonionic surfactants depends on the ethylene oxide chain length. Depending on the hydrophobic group, at least four to six ethylene oxide units per molecule are required to produce a water soluble surfactant. Solubility charts for some ICI products are given in Figure 4.2. The most remarkable observation with nonionic surfactants is the formation of micelles at about one-hundredth the concentration required for ionic surfactants with comparable hydrophobic groups. Other differences in the physical properties of micelles formed by ionic and nonionic surfactants will be presented in the appropriate sections.

4.2.1 Cloud Point

When the temperature of a nonionic surfactant solution is raised the disruption of hydrogen bonding causes a nonionic surfactant to become less soluble in water. In practice, there is a narrow, well defined temperature over which the solution of the nonionic surfactant becomes turbid. This temperature is called the "cloud point" [Maclay 1956]. A surfactant molecule with a longer ethylene oxide chain and the same hydrophobic length can exist in solution to a higher temperature

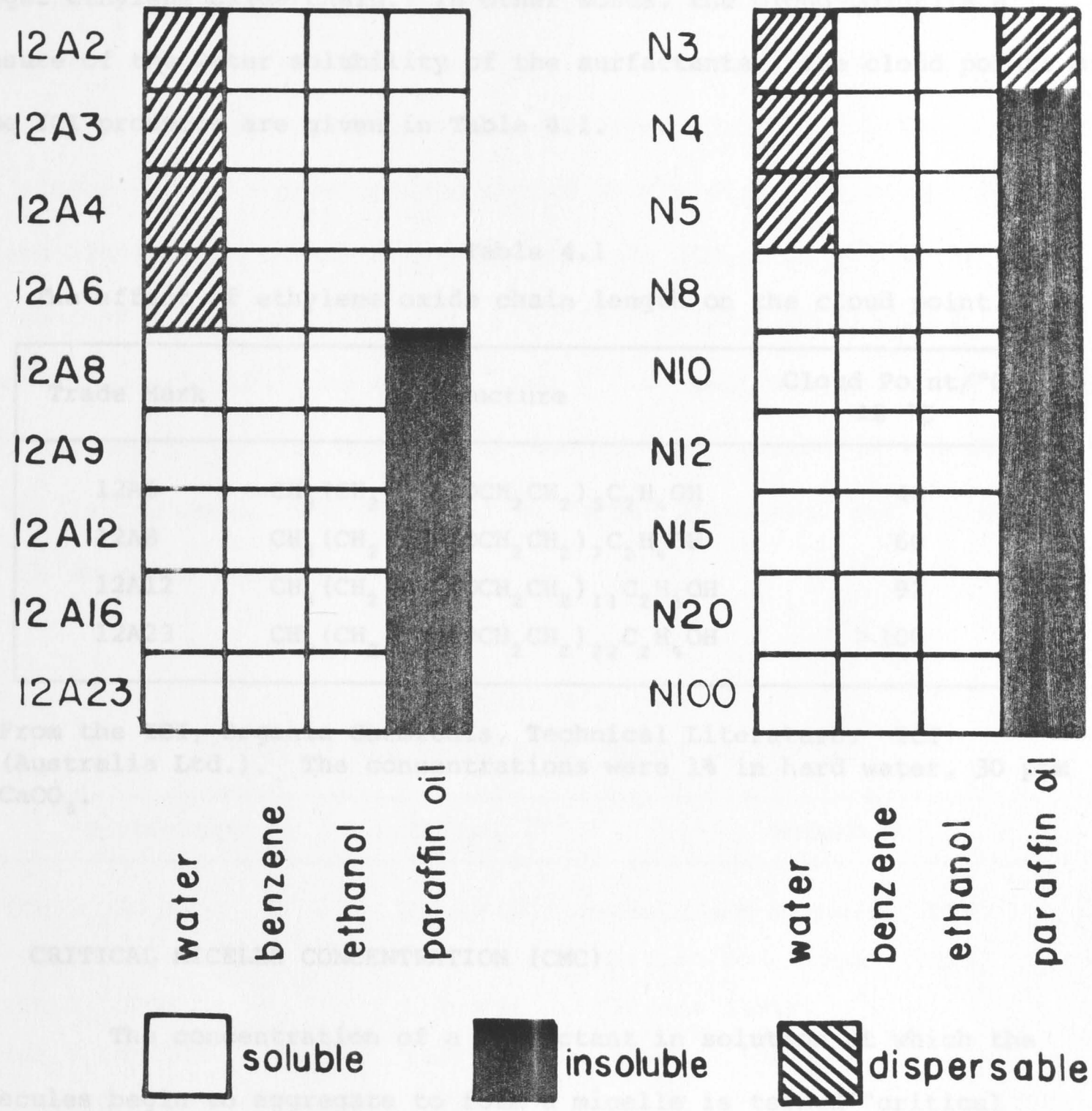

Figure 4.2. Solubility charts for Teric 12A series and Teric N series of ICI (Australia Ltd.) products. 12A and N stand for lauryl alcohol and nonyl phenol respectively. The numbers on the right represent the number of ethylene oxide per molecule (for example, 12A8 is lauryl alcohol with 8 ethylene oxide chains).

because of the greater hydrogen bonding between water molecules and the longer ethylene oxide chain. In other words, the cloud point is a measure of the water solubility of the surfactants. The cloud points of some ICI products are given in Table 4.1.

Table 4.1

The effect of ethylene oxide chain length on the cloud point.†

Trade Mark	Structure	Cloud Point/°C ±2 °C
12A6	$CH_3(CH_2)_{11}O(OCH_2CH_2)_5C_2H_4OH$	40
12A8	$CH_3(CH_2)_{11}O(OCH_2CH_2)_7C_2H_4OH$	60
12A12	$CH_3(CH_2)_{11}O(OCH_2CH_2)_{11}C_2H_4OH$	92
12A23	$CH_3(CH_2)_{11}O(OCH_2CH_2)_{22}C_2H_4OH$	> 100

† From the ICI, Organic Chemicals, Technical Literature. ICI (Australia Ltd.). The concentrations were 1% in hard water, 30 ppm $CaCO_3$.

4.3 CRITICAL MICELLE CONCENTRATION (CMC)

The concentration of a surfactant in solution at which the molecules begin to aggregate to form a micelle is termed "critical micelle concentration" (CMC). Above the CMC a further increase in the surfactant concentration just increases the number of micelles, not the number of molecules in a micelle. In practice, the CMC is determined from the change in slope obtained when an appropriate physical property that distinguishes between micellar surfactant and free surfactant monomer is plotted against total surfactant concentration. Therefore, the determination of CMC may be carried out by a variety of methods. These have been described previously in some detail [McBain and Hutchinson 1955; Shinoda 1963].

The CMC of surfactant micelles depends on the nature and the structure of the surfactant molecules. The longer the hydrocarbon chain length the stronger the hydrophobicity and thus the lower the CMC. The position of the head group in the hydrocarbon chain also affects the CMC. The closer the head group to the centre of the chain the higher the CMC [Evans 1956]. The CMC of potassium stearate ($CH_3(CH_2)_{16}COOK$) at 55 °C and that of potassium oleate ($CH_3(CH_2)_7CH = CH(CH_2)_7COOK$) at 50 °C are found to be 4.5×10^{-4} and 12×10^{-4} mol l^{-1} respectively [Klevens 1953]. The increase in CMC has been attributed to the presence of a double bond in the latter case. The effect of different polar head groups on the CMC is shown in Table 4.2.

Table 4.2

Effect of the polar head groups on the CMC.

Surfactant	CMC/mol l^{-1}	Reference
$CH_3(CH_2)_{11}SO_4Na$	8.10×10^{-3}	Mysels and Princen [1959]
$CH_3(CH_2)_{11}SO_3Na$	1.00×10^{-2}	Berrnet and Zisman [1959]
$CH_3(CH_2)_{11}COOK$	1.25×10^{-2}	Klevens [1948]
$CH_3(CH_2)_9CH(COOK)_2$	1.30×10^{-1}	Shinoda [1955]
$CH_3(CH_2)_8C_6H_4(OCH_2CH_2)_{10}OH$	7.50×10^{-5}	Schick, Atlas and Eirich [1962]
$CH_3(CH_2)_8C_6H_4(OCH_2CH_2)_{20}OH$	1.45×10^{-4}	"
$CH_3(CH_2)_8C_6H_4(OCH_2CH_2)_{50}OH$	2.80×10^{-4}	"

For anionic micelles the CMC is affected by the nature of the head groups. For example, the CMC increases as the head groups change from sulphate to sulphonate to carboxylate. A decrease in the number of head groups also lowers the CMC. The effect of the head groups on the CMC is due to the electrostatic repulsion between these charged ions. The effect of the nature of the counterions, whose charge is opposite to

that of the polar head groups, on the CMC has been studied. The CMC of dodecyltrimethyl ammonium chloride is 0.062 while that of the corresponding bromide is 0.016 mol l^{-1} [Wright, Abbott, Sivertz and Tartar 1939]. More recently, the effect of different counterions on the CMC of lauryl sulphates has been reported to be fairly large [Mukerjee 1967]. The CMC of lauryl sulphates with different counterions are given in Table 4.3.

Table 4.3

Variation of the CMC of lauryl sulphates with different counterions.†

Counterions of Lauryl Sulphate	CMC/10^{-3} mol l^{-1}
Li^+	8.92
Na^+	8.32
K^+	7.17 (32 °C)
Cs^+	6.09
$(CH_3)_4N^+$	5.52
$(C_2H_5)_4N^+$	3.85

†From Mukerjee [1967]. The solvent was water (25 °C).

For nonionic micelles, where there is no charged head group, the CMC are much lower than those of ionic micelles. For a series of compounds with the same hydrophobic group, an increase in the number of ethylene oxide units is accompanied by an increase in the CMC (Table 4.2). Thus the CMC values of nonionic micelles depend on the length of both hydrophobic and hydrophilic regions of the surfactant molecules.

Besides the effects of the nature and the structure of surfactant molecules on the CMC, there are other factors which influence the CMC. It can be expected that the addition of any foreign compounds,

which affect the nature and the environment of the surfactant molecules, might change the CMC. The addition of an electrolyte, which reduces the repulsion between the polar head groups, lowers the CMC. The CMC of cetylpyridinium chloride, 1.2×10^{-4} mol l^{-1}, is lowered to 0.41×10^{-4} mol l^{-1} by the addition of 0.730 mol l^{-1} of NaCl [Anacker 1958]. The CMC is temperature dependent and SDS has a minimum for its CMC at 25 °C [Goddard and Benson 1957]. For nonionic micelles the CMC decreases monotonically with decreasing temperature. The increase in the CMC of anionic micelles with an increase in temperature may be due to thermal agitation which prevents association of the monomer surfactant molecules. The decrease in the CMC with a decrease in temperature is thought to be due to the dominance of a process which dehydrates surfactant molecules over the effect of thermal agitation. At higher temperatures the monomers become hydrophobic and thus the CMC is lowered.

The CMC is really a measure of the maximum solubility of a surfactant in water. At concentrations higher than the CMC, no further surfactant will dissolve so it stays in a separate phase, and because of the nature of the surfactant it forms micelles. The lower CMC values of nonionic surfactants indicate that the nonionic surfactants are less soluble in water than ionic surfactants.

4.4 SIZE AND SHAPE

The size and shape of a micelle can be determined by a variety of experimental methods. These have been reviewed by Anacker [1970]. Several different configurations have been postulated for the micelle, ranging from a sphere [Hartly 1936] through oblate and prolate ellipsoids to a large cylinder. The fluorescent probe technique,

discussed further in Chapter 5, has been used to determine the size of the micelles. However, the shape of the micelle cannot be predicted using the fluorescent probe, because the probe is not sensitive to this variable. As the technique will be applied to anionic and nonionic micelles, factors which influence the size and shape of both types of micelle are discussed here.

The micelle size depends on the nature and the structure of the surfactant molecules. An increase in the hydrocarbon chain length causes an increase in the micelle size. For example, sodium decyl sulphate ($CH_3(CH_2)_9SO_4^-Na^+$) has an aggregation number of 50 at 25 °C whereas SDS ($CH_3(CH_2)_{11}SO_4^-Na^+$) has the value 62 at the same temperature [Fendler and Fendler 1970]. For all types of surfactants the micelle size increases with the hydrocarbon chain length, but the magnitude of the effect may be quite different for different types of surfactant. The aggregation numbers of n-alkyl hexaoxyethylene glycol mono ether are 73 and 3100 at 25 °C for n = 10 and n = 14 respectively [Balmbra, Clunie, Corkill and Goodman 1964]. The dependence of the micelle size on the polar head group structure has been studied with light scattering techniques [Geer, Eyler and Anacker 1971]. The aggregation numbers of substituted ammonium salts, each having the decyl hydrocarbon chain are given in Table 4.4. The aggregation number is influenced by the substitution of CH_3 groups for H atoms on the polar head. The increase in the ionic strength decreases the repulsion between the ionic head groups and so the micelles become bigger. For example, when the head group is $-NH_3^+$ the effective ionic strength in the vicinity of the head group is larger than when the head group is $-N(CH_3)_3^+$ because the counterions can approach the $-NH_3^+$ group more closely. It can also be seen from Table 4.4 that a change in counterions from Br^- to Cl^- causes

Table 4.4

Micelle sizes for decylammonium salt.†

Surfactant	Structure	Aggregation Number
Decyltrimethylammonium bromide	$C_{10}H_{21}N(CH_3)_3^+Br^-$	48
Decyldimethylammonium bromide	$C_{10}H_{21}NH(CH_3)_2^+Br^-$	69
Decylmethylammonium bromide	$C_{10}H_{21}NH_2(CH_3)^+Br^-$	670
Decylammonium bromide	$C_{10}H_{21}NH_3^+Br^-$	1100
Decylammonium chloride	$C_{10}H_{21}NH_3^+Cl^-$	78

† From Geer *et al.* [1971]. The solvent was 0.5 mol l^{-1} NaBr at 25 °C except for decylammonium chloride which was 0.1 mol l^{-1} NaCl at 30 °C.

a very large change in the aggregation number. For nonionic surfactants an increase in the polyoxyethylene chain length appears to be associated with a decrease in the aggregation number. For example, the nonylphenol with 10 ethylene oxide units in the chain has 276 molecules in a micelle whereas the nonylphenol with 30 ethylene oxide units in the chain has only 55 molecules per micelle [Schick, Atlas and Eirich 1962].

One way of reducing the repulsion between the charged polar groups is to increase the electrolyte concentration in the aqueous phase. Thus, an addition of electrolyte makes the micelle size bigger. Anacker [1958] reported that the micelle sizes of cetylpyridinium chloride in water and 0.73 mol l^{-1} NaCl aqueous solutions were 95 and 137 respectively. The effect of added electrolyte on the size of non-ionic micelles is much less straightforward. The size of micelles formed by most nonionics is relatively unaffected by added electrolyte, as one would expect. However, nonionics containing both very few ethylene oxide units (8) and very many (100) give divergent results. In the former case the aggregation number of lauryl alcohol 8 ethylene

oxide increases on the addition of electrolyte, and the magnitude of the increase depends on the nature of the electrolyte: 0.50 mol l^{-1} $CaCl_2$ causes an increase from 123 to 149, but 0.50 mol l^{-1} Na_2SO_4 causes an increase to 856. In the case of octadecanol 100 ethylene oxide the addition of electrolyte causes a marked decrease in aggregation number. Despite some attempt to attribute these results to a change in the structure of water caused by the electrolyte [Schick 1962], they remain largely unexplained.

The presence of octane, decane, cyclohexane or benzene increases the micelle size of hexadecyltrimethylammonium bromide micelles [Hyde and Robb 1964]. A similar effect has been observed for n-decane and n-decanol in methoxy-polyoxyethylene decyl ether [Nakagawa, Kuriyame and Inoue 1960].

The temperature dependence of the size of the ionic micelle has been studied by light scattering methods [Kuriyama 1962]. The sizes of SDS micelles in 0.1 mol l^{-1} NaCl at different temperatures are given in Table 4.5. The results indicate that the aggregation number decreases as the temperature is increased.

Table 4.5

Micelle sizes of SDS at various temperatures.†

Temperature	Aggregation Number
17.0	106
20.0	101
30.0	88
50.2	78
69.8	68

† From Kuriyama [1962]. The solvent was 0.1 mol l^{-1} NaCl aqueous solution.

In nonionic surfactants, the hydrophilic group will exert a strong attraction for water molecules and the resulting hydrogen bonding with the ethylene oxide chain is one of the contributing factors in forming a micelle. Hydrogen bonding is an exothermic process, and so as the temperature rises, the extent of hydrogen bonding decreases and bigger micelles become energetically favourable. Therefore, in contrast to ionic micelles, nonionic micelles increase rapidly in size with an increase in temperature [Maclay 1956; Kuriyama 1962; Balmbra, Clunie, Corkill and Goodman 1962, 1964; and Elworthy and McDonald 1965]. Kuriyama [1962] studied the temperature dependence of micelle formation by methoxy-polyoxyethylene decyl ether ($C_{10}H_{21}(OCH_2CH_2)_{12}OCH_3$). The results of his light scattering experiments, which indicate an increase in micelle size with temperature, are given in Table 4.6.

Table 4.6

Micelle sizes of methoxy-polyoxyethylene decyl ether at various temperatures.†

Temperature °C	Aggregation Number
9.7	47
29.0	53
50.7	65
58.5	73
69.7	101
73.4	131
75.0	165

† From Kuriyama [1962]. The solvent was water.

The effect of temperature on the micelle size of n-dodecyl hexaoxyethylene glycol mono ether ($CH_3(CH_2)_{11}(OCH_2CH_2)_6OH$) has been studied by

Balmbra *et al.* [1962], and the increase in the micelle size with temperature was found to be exponential. From these experimental observations the magnitude of the effect of temperature on nonionic micelles seems to be quite different. The smaller micelles may have a spherical shape, however the increase in size seems to be accompanied by a distortion of the micelle shape. Elworthy and McDonald [1965] have studied the hexadecyl series with 7, 8 and 9 ethylene oxide chain units. Distinct temperature regions where the size increases slightly and where the size increases rapidly have been observed. The threshold temperatures for hexadecyl with 7, 8 and 9 ethylene oxide units have been reported to be 22°, 36.3° and 47.9 °C. Below the threshold temperature the spherical model fits the experimental results, but above the threshold temperature the micelles become asymmetric and the oblate ellipsoidal model fits the result best [Elworthy *et al.*].

In Chapter 5 the effect of the addition of electrolyte on the micelle size of SDS and the effect of temperature and ethylene oxide chain length on the micelle size of some nonionic surfactants will be investigated using the fluorescent probe technique.

4.5 SOLUTES IN MICELLES

In the fluorescent probe technique the exact location of the probe in the micellar aqueous system becomes important. We have developed a technique, based on the selective quenching of fluorescence, which has enabled us to locate the neutral and the charged species in the micelle-aqueous two-phase system. This will be described in Section 5.3.2.

When an aromatic hydrocarbon with very low solubility in water is added to a surfactant solution which forms micelles, the solute solubility is markedly greater than in pure water. For example, the solubility of pyrene in 0.1 mol l^{-1} SDS anionic surfactant solution is about a thousand times greater than that of pyrene in pure water. However, the actual location of the solute, solubilised by micelles, depends on the nature of both the solute and the surfactant. A solute can be located in three different positions in an anionic micelle. Non-polar molecules are dissolved in the micelle interior. Polar molecules consisting of a hydrocarbon chain and a weakly hydrophilic group, such as long chain alcohols or amines, are incorporated into the micelle with the hydrocarbon tail in the micelle interior and the hydrophilic heads pointing towards the polar head groups of the micelles. Solute with very low solubility in both water and in a hydrocarbon may be solubilised in micelles by their adsorption onto the surface of the micelles. McBain and McHan [1948] found that dimethylphthalate adsorbed onto the exterior polar groups of the micelles. For nonionic micelles, apart from the above three possibilities, there is another possible region where a solute can be situated. Since in nonionic micelles hydrogen bonded polyoxyethylene chains form a hydrophilic region, it is possible for a solute to be incorporated in this region, depending of course on the strength of the affinity of the solute for the polyoxy-ethylene group. These possible locations of a solute in a micelle are all illustrated in Figure 4.3.

For a solute which is reasonably soluble in both water and in a hydrocarbon, the distribution of the solute between the aqueous and surfactant phases depends on the concentration of surfactant molecules. Hautala, Schore and Turro [1973] obtained the distribution of

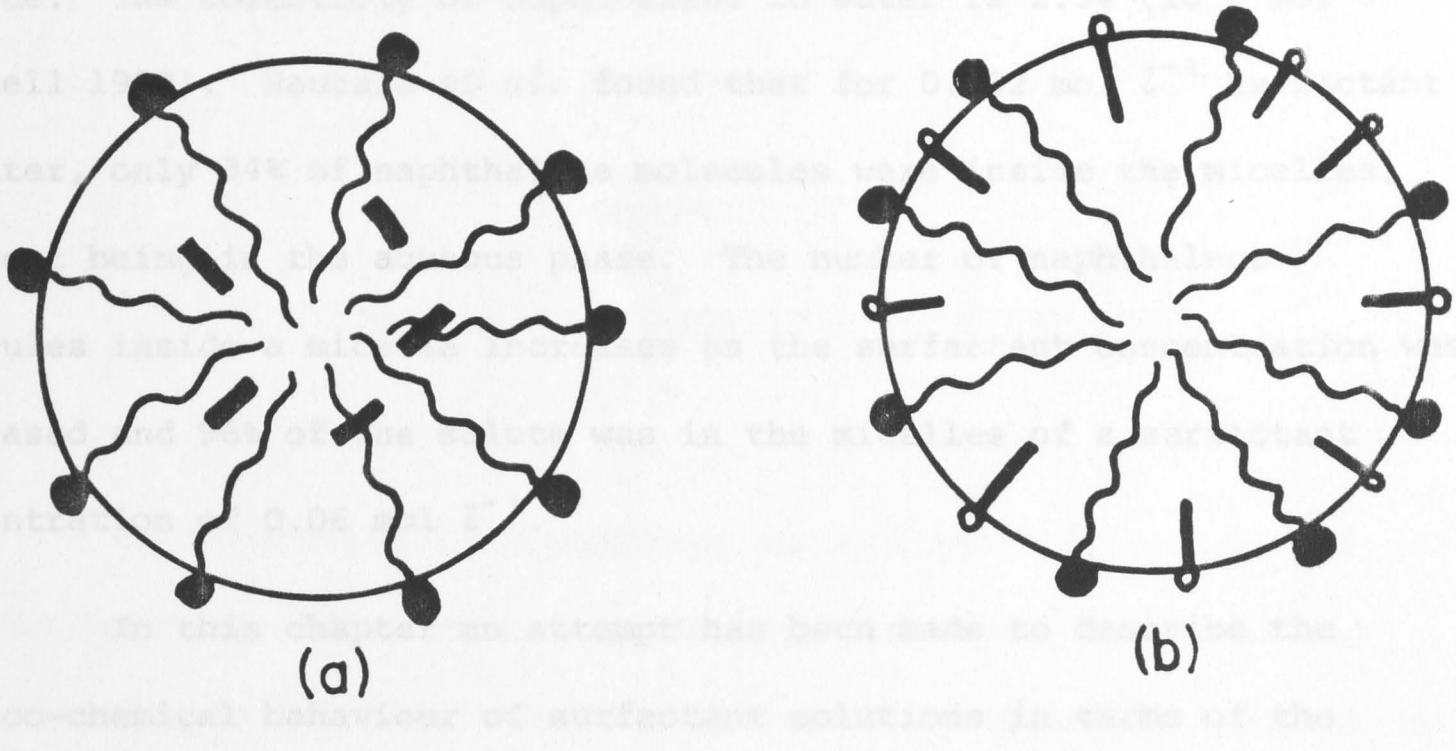

Figure 4.3. Location of (a) nonpolar solutes (▬) and (b) polar solutes (o▬) in ionic micelles; (c) solutes (▬) in nonionic micelles. (∿∿) are polyoxyethylene chains. (After Nakagawa and Shinoda [1963].)

naphthalene molecules in water containing hexadecyltrimethylammonium bromide. The solubility of naphthalene in water is 2.34×10^{-4} mol l^{-1} [Seidell 1952]. Hautala *et al.* found that for 0.002 mol l^{-1} surfactant in water, only 34% of naphthalene molecules were inside the micelles, the rest being in the aqueous phase. The number of naphthalene molecules inside a micelle increases as the surfactant concentration was increased and 96% of the solute was in the micelles of a surfactant concentration of 0.06 mol l^{-1}.

In this chapter an attempt has been made to describe the physico-chemical behaviour of surfactant solutions in terms of the structure of the micelles and the nature of the solvent. However, although there is no shortage of experimental data, there is as yet no good general theoretical explanation for much of it. Although there have been some advances in the last few years, the quotation below from Anacker [1970] is still largely true:

> "In spite of the great amount of research that has been carried out in the field of surfactants, there remains much to be learned about the micellization process. We would like to know, for example, the details of monomer-micelle equilibria, the extent of dimerization and other forms of pre-cmc association, something about the kinetics of micelle formation, micelle size distribution and the factors which control it, the exact role of the solvent, the relative importance of water-hydrocarbon interfacial energy and attractive cohesive energy between hydrocarbon chains, why the aggregation number is strongly dependent upon concentration and ionic strength for some surfactants but not for others, and exactly why different counterions have different aggregating powers. Solutions to problems such as these will require the utilization of all available techniques."

CHAPTER 5

EXCITED STATE PROCESSES IN MICELLES

In fluorescence spectroscopy excited state processes such as complex formation, fluorescence quenching, protolytic reactions and isomerisation in solution have been extensively studied in the past few years. The present state of knowledge of the photophysical properties of these excited state processes can be used to study some physical properties of a solvent.

In this chapter the main interest is to examine the nature of some excited state processes in a surfactant which forms micelles in aqueous solution. The following processes have been used as fluorescent probes to explore the physical properties of micelles in aqueous solutions:

(a) complex formation (excimer and exciplex);

(b) quenching of fluorescence;

(c) protolytic reactions;

and (d) energy transfer.

The use of a fluorescent probe in studying excimer kinetics in a surfactant micelle was first attempted by Förster and Selinger [1964]. They studied excimer formation by pyrene and 2-methylnaphthalene. For seven years this technique received little attention. Then, because of the similarity between micelles and biological membranes and the analogy

between micellar and enzymatic catalysis, kinetic studies of reactions in micelles became increasingly important in biochemical research. It has also become a technique of interest to preparative organic chemists because of the unusual syntheses that can be carried out in micelles [Fendler and Fendler 1970]. Because of the extensive use of surfactants in modern industries, the understanding of micellar systems has become more and more important.

From a spectroscopic point of view, surfactant solutions are suitable solvents; many are transparent down to 250 nm. They have good solubilising properties and most of them do not fluoresce. However, a more detailed understanding of a solvent of this type is still necessary. As a result, there has been much recent study using the fluorescent probe technique [Almgren 1972; Gratzel and Thomas 1972; Hauser and Klein 1972, 1973; Hautala and Turro 1972; Hautala, Turro and Schore 1973; Dorrance and Hunter 1972, 1974; Kenney-Wallace and Flint 1975; Klein and Hauser 1975; Geiger and Turro 1975].

5.1 EXCIMER FORMATION IN SURFACTANT MICELLES

The kinetic scheme for the formation of fluorescing excited dimers of aromatic compounds (later called excimers) was developed by Förster and co-workers in the 1950's. It was found that these rate parameters were fast enough to compete with fluorescence and radiationless processes ($\sim 10^7$ sec^{-1}). By the early 1960's, a sufficient variety of compounds and solvents had been examined to establish a clear pattern. The excimer system is an ideal one with which to study surfactant micelles because although these micelles are in dynamic equilibrium with individually dissolved surfactant molecules, indications are that this

equilibrium involves processes occurring at many orders of magnitude lower rate than the rates of excimer formation. The micellar solution offers an instantaneous microsolvent system in which the individual micelles are isolated completely from each other as far as the fluorescent system is concerned.

The experiments of Förster and Selinger [1964] showed two things. The monomer-excimer steady state is not affected by diluting the surfactant system with water because this does not influence the number of micelles (except at concentrations near the critical micelle concentration (CMC) but merely moves the micelles further apart). This result established the essentially intramicellar nature of the excimer kinetic process, which is consistent with the time scale of excimer formation being of the order of the lifetime of the excited singlet state of the monomer — about one-tenth of a microsecond. Secondly, when the average number of molecules per micelle was of the order of unity or less (as was the case for pyrene), the excimer steady state was influenced by the statistical distribution of micellar occupation. It takes two pyrene molecules to form an excimer rather than the bulk concentration of pyrene in solution. Excimer formation in "homogeneous" normal organic solvent have been described elsewhere [Förster 1963; Birks, Dyson and Munro 1963; Selinger 1966; Förster 1969; and Speed and Selinger 1969].

5.1.1 Static Quenching Studies

In this section the quenching of pyrene fluorescence from micelles by an external quenching molecule or ion present in the solution has been studied. Through a comparison of the quenching of the

two types of fluorescence emanating from pyrene in solution, monomer fluorescence and excimer fluorescence, it is possible to establish that there are micelles occupied by only one pyrene molecule and from which only monomer fluorescence is observed and that there are micelles occupied by more than one pyrene molecule from which both monomer and excimer fluorescence can be observed.

The kinetics of excimer formation are well established. Although it is possible to analyse such a system fully, with the mechanism described in (3.1.1),

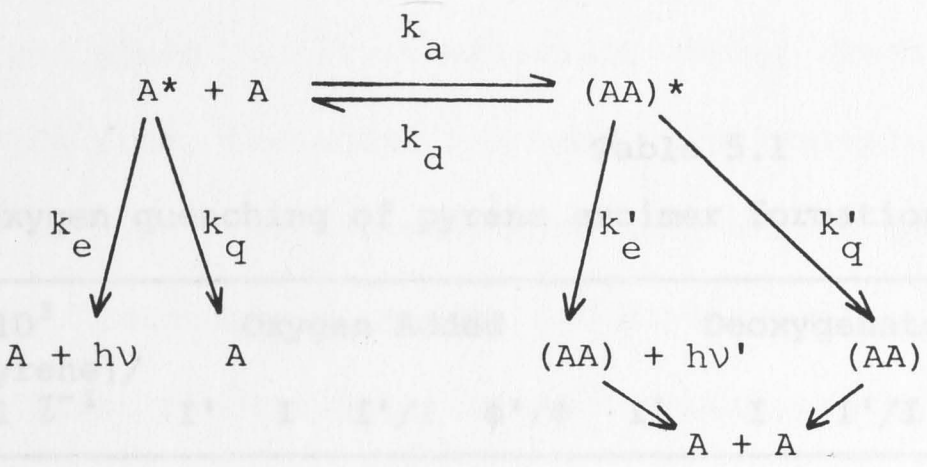

it is useful to define two sets of experimental conditions, differing in the relative magnitudes of the dissociative (k_d) and deactivating (k'_e and k'_q) rate constants of the excimer. Under quasi-equilibrium conditions

$$k_d >> k'_e + k'_q \qquad (\text{"}\alpha \text{ condition", Section 3.1.2})$$

and so the relative concentrations of excited monomer and excimer are unaffected by the addition of a quencher (as the equilibrium between the two species is maintained). Therefore, the ratio of the fluorescence intensities is unaffected by a quencher. When

$$k_d << k'_e + k'_q \qquad (\text{"}\beta \text{ condition", Section 3.1.2})$$

the addition of a quencher will decrease the ratio of excimer to monomer and thus decrease the ratio ϕ'/ϕ, the excimer:monomer emission intensities.

In these two limiting conditions, the addition of a quencher to a monomer-excimer system may cause either no change in ϕ'/ϕ or a decrease in ϕ'/ϕ. It is in this context that the results presented in Table 5.1 are interesting. When the ubiquitous quencher oxygen is added to pyrene in surfactant solutions, the ratio of excimer to monomer emission (ϕ'/ϕ) is increased, the one possibility which is excluded in homogeneous solvents. The effect is more pronounced at lower concentrations.

Table 5.1

Oxygen quenching of pyrene excimer formation in 0.1 mol l^{-1} SDS.

10^3 × [pyrene]/ mol l^{-1}	Oxygen Added				Deoxygenated				$\frac{(\phi'/\phi)_{quenched}}{(\phi'/\phi)_{unquenched}}$
	I'	I	I'/I	ϕ'/ϕ	I'	I	I'/I	ϕ'/ϕ	
1.0	52	27	1.93	1.96	145	85	1.71	1.74	1.13
0.45	34	44	0.77	0.79	100	193	0.52	0.53	1.49

One possible explanation of these results would be that the observed monomer fluorescence is a sum of fluorescence from micelles and from monomeric pyrene in aqueous solution. The addition of oxygen might quench the latter without affecting the monomer-excimer equilibrium in the micelles. The reported solubility of pyrene in water is 10^{-6} mol l^{-1} [Seidell 1952]. However, for 3.9×10^{-7} mol l^{-1} pyrene, a 100-fold increase in instrumental sensitivity was necessary to detect the fluorescence of aqueous pyrene and so the fluorescence of aqueous pyrene

did not contribute to the observed fluorescence. Furthermore, dilution of the solution with water, which would increase the relative amount of aqueous pyrene monomer compared to the micellar pyrene (monomer + excimer) did not decrease the ratio ϕ'/ϕ.

Another possible explanation is that the anomalous quenching effect is due to microcrystal formation in micelles, for pyrene has been found to crystallise from detergent solutions when the solution is diluted below the CMC. Pyrene microcrystals emit excimer type fluorescence [McDonald and Selinger 1971b], which would be insensitive to quenching by oxygen and hence result in an increase in ϕ'/ϕ. If pyrene crystals were being formed, doping with an anthracene-type compound would result in efficient energy transfer to, followed by emission from, the added compound. For example, crystals of pyrene doped with 1% 9-methylanthracene show strong guest fluorescence.† However, solutions of pyrene and 2% 9-methylanthracene show no significant fluorescence from the 9-methylanthracene. This indicates that microcrystals of pyrene were not formed under the experimental conditions.

To check that the effect is not restricted to quenching by oxygen a similar experiment using a different quencher has been carried out. The effect of adding a solution containing Mn^{2+} ions is shown in Table 5.2. Mn^{2+} is a suitable quencher for anionic micelles because its positive charge allows entry into the micelle whereas added iodide ions would be repelled and ineffective as a quencher. The opposite is true

---

† This test for microcrystal formation at low temperature has been used previously [McDonald and Selinger 1971b]; but there the doping concentration was lower because of the more efficient trapping at low temperature.

Table 5.2

Mn^{2+} quenching of pyrene excimer formation in 0.1 mol l^{-1} SDS.

$10^3 \times$ [pyrene]/mol l^{-1}	$\frac{(\phi'/\phi)_{quenched}}{(\phi'/\phi)_{unquenched}}$ for $[MnCl_2] = 2.5 \times 10^{-3}$ mol l^{-1}	$\frac{(\phi'/\phi)_{quenched}}{(\phi'/\phi)_{unquenched}}$ for $[MnCl_2] = 5.0 \times 10^{-3}$ mol l^{-1}
1.0	1.55	1.95
0.45	1.85	2.22

for cationic micelles for which iodide is a suitable quencher. It is evident that the results are analogous to those obtained with oxygen.

The results of these fluorescence quenching experiments can be explained on the basis of the distribution of pyrene molecules in the surfactant micelles.

Because the average number of molecules per micelle μ is approximately 0.6 (for 1.0×10^{-3} mol l^{-1} pyrene in 0.1 mol l^{-1} SDS assuming an aggregation number of 60 [Shinoda 1963]), most of the occupied micelles will only be singly occupied and these cannot form excimers.† The fluorescence spectra of pyrene in SDS for different concentrations of pyrene are shown in Figure 5.1. A plot of the corrected intensity ratio of excimer to monomer fluorescence as a function of bulk concentration is given in Figure 5.2. In *contrast* to homogeneous solutions, this plot is not linear, but curves upwards at higher concentrations. The individual Stern Volmer plots $1/\phi$ versus concentration, and $1/\phi'$ versus 1/concentration give different values for

---

† This explains the high apparent mean self-quenching concentration for pyrene in micelles. Förster and Selinger [1964] found that pyrene in CDBA has a half-value concentration of 2.6×10^{-2} mol l^{-1}, which is greater by a factor of 20 than that in a comparable homogeneous solution.

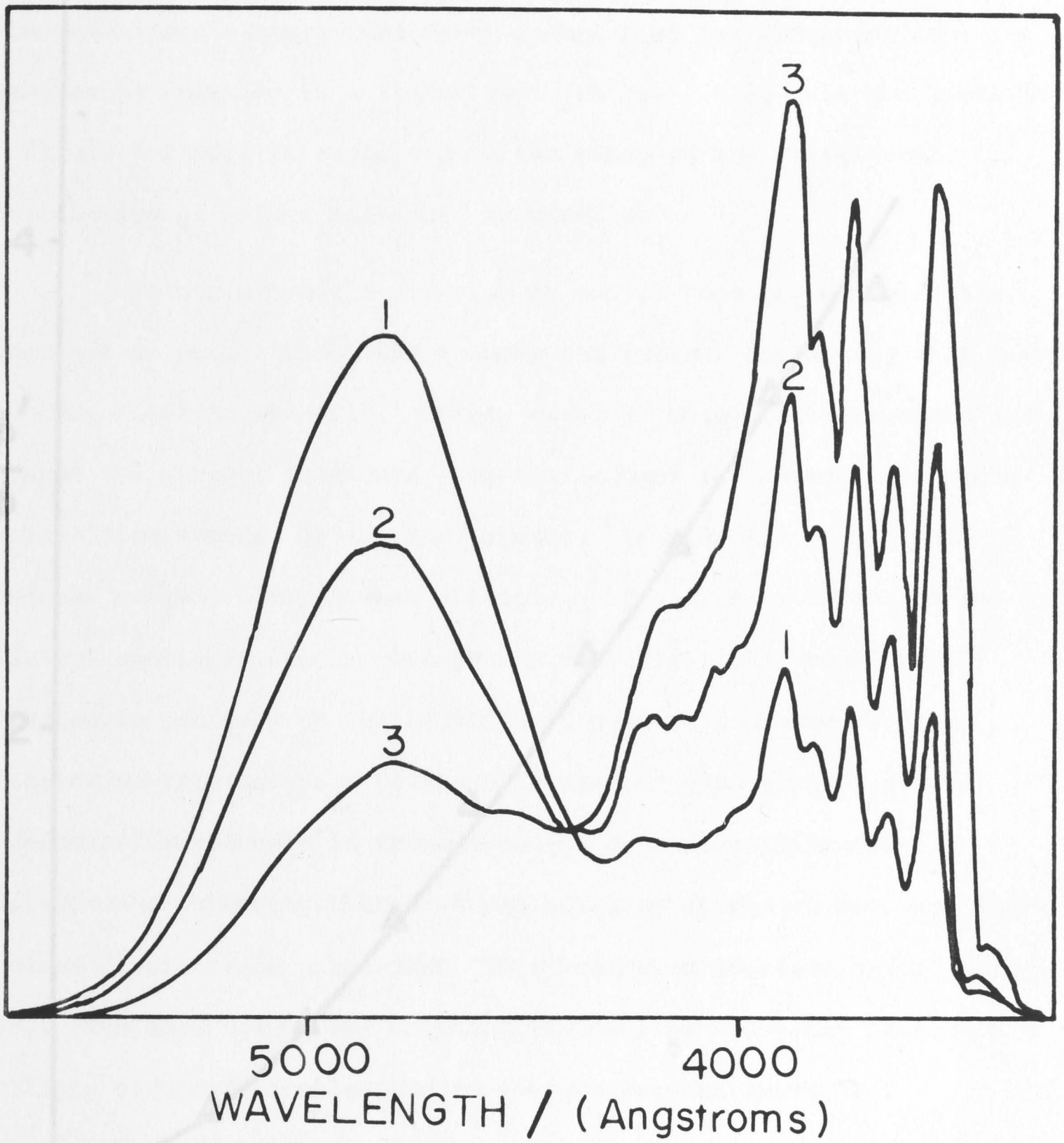

Figure 5.1. Fluorescence spectra of deoxygenated pyrene in 0.1 mol l^{-1} SDS solutions. Excitation at 337 nm.

(1) 1.42×10^{-3} mol l^{-1} pyrene;

(2) 6.80×10^{-4} mol l^{-1} pyrene;

(3) 3.15×10^{-4} mol l^{-1} pyrene.

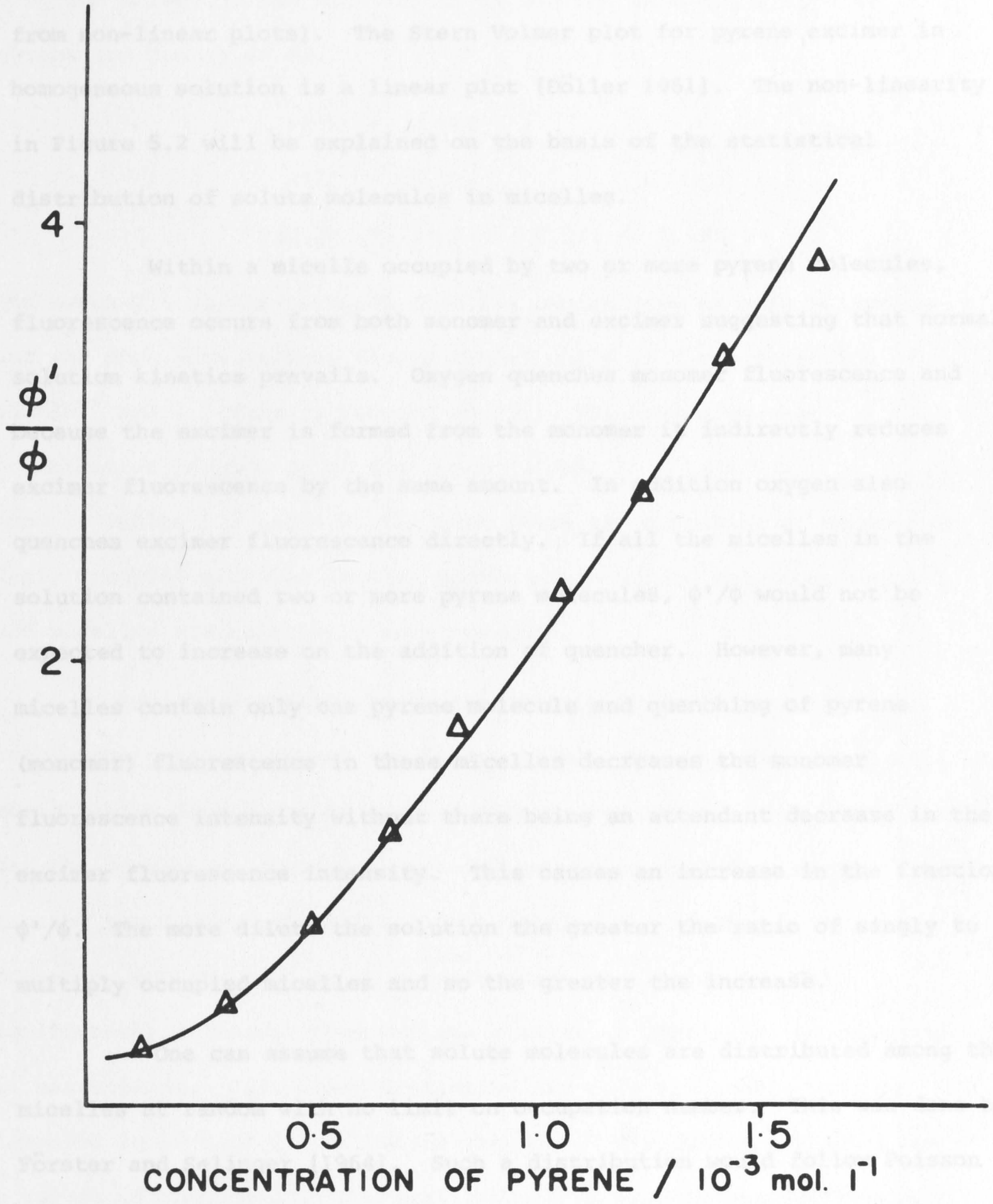

Figure 5.2. Corrected ratio of excimer/monomer fluorescence [ϕ'/ϕ] as a function of bulk concentration of pyrene in 0.1 mol l^{-1} SDS.

the mean self-quenching constants (in as far as these can be estimated from non-linear plots). The Stern Volmer plot for pyrene excimer in homogeneous solution is a linear plot [Döller 1961]. The non-linearity in Figure 5.2 will be explained on the basis of the statistical distribution of solute molecules in micelles.

Within a micelle occupied by two or more pyrene molecules, fluorescence occurs from both monomer and excimer suggesting that normal solution kinetics prevails. Oxygen quenches monomer fluorescence and because the excimer is formed from the monomer it indirectly reduces excimer fluorescence by the same amount. In addition oxygen also quenches excimer fluorescence directly. If all the micelles in the solution contained two or more pyrene molecules, ϕ'/ϕ would not be expected to increase on the addition of quencher. However, many micelles contain only one pyrene molecule and quenching of pyrene (monomer) fluorescence in these micelles decreases the monomer fluorescence intensity without there being an attendant decrease in the excimer fluorescence intensity. This causes an increase in the fraction ϕ'/ϕ. The more dilute the solution the greater the ratio of singly to multiply occupied micelles and so the greater the increase.

One can assume that solute molecules are distributed among the micelles at random with no limit on occupation number. This was done by Förster and Selinger [1964]. Such a distribution would follow Poisson statistics, viz.

$$P(x) = \mu^x e^{-\mu}/x! ,$$

where μ is the mean number of solute molecules per micelle and $P(x)$ the probability that a micelle contains x solute molecules. Thus a solution of 1.0×10^{-3} mol l^{-1} pyrene in 0.1 mol l^{-1} SDS, where the average number

of pyrene molecules per micelle, μ, is 0.6 and assuming a micelle aggregation number of 60,

$$P(0) = 0.549$$

$$P(1) = 0.329$$

$$P(\geqslant 2) = 1 - P(0) - P(1) = 0.122 .$$

This means 27% of the occupied micelles contain two or more molecules (and can thus show excimer fluorescence) while at a concentration of 4.5×10^{-4} mol ℓ^{-1} this is reduced to 13%. This explains the concentration dependence of the ratio $(\phi'/\phi)_{quenched}/(\phi'/\phi)_{unquenched}$ found in Tables 5.1 and 5.2. In both cases the quenching of monomer in singly occupied micelles is more prominent in dilute solutions where such micelles are relatively more numerous.

Excimer formation by pyrene in anionic surfactant (SDS) has been investigated by Hauser and Klein [1973]. Because they found no concentration dependence of excimer fluorescence decay, they postulated that the occupation could not exceed 2 and hence used Bose statistics to describe the distribution of solute molecules in micelles. For mean occupation numbers of less than unity these statistics are not significantly different from Poisson statistics within the accuracy of the assumptions. Just which statistics are more applicable will be discussed in Section 5.1.2.2 where the use of a solute for which μ can be larger is considered. The statistics then predict very different results.

5.1.2 Dynamic Studies

Further information on the statistical distribution of hydrocarbon among the micelles can be obtained from the fluorescence decay of

pyrene monomer and excimer in micelles. Hauser and Klein [1972, 1973] found that the decay of pyrene excimer in SDS was independent of the bulk concentration of pyrene. They fitted the decay curves for the concentration range from 10^{-4} to 1.63×10^{-3} mol l^{-1} to the general expression

$$I'(t) = c(e^{-\lambda_1 t} - e^{-\lambda_2 t})$$

where

$$\lambda_1 = 13 \times 10^6 \text{ sec}^{-1}$$

$$\lambda_2 = 44 \times 10^6 \text{ sec}^{-1}$$

and applied Boson statistics to describe the distribution of hydrocarbon molecules in micelles. If Boson statistics are assumed to describe the distribution of solutes in micelles, the occupancy cannot exceed 2. This is in conflict with the Poisson distribution suggested on the basis of the fluorescence quenching experiment described earlier. In an attempt to resolve this discrepancy, the decay of pyrene excimer and monomer have been re-examined using single photon counting decay spectroscopy. The use of different surfactants and 2-methylnaphthalene as a solute has made possible studies at higher occupancy numbers.

5.1.2.1 Solutes in micelles with low occupancy

When pyrene was used as a fluorescent probe the experimental conditions were as follows: the excitation wavelength was 337 nm with a band pass of 2 nm; monomer emission was observed at 372 nm and excimer emission at 490 nm, both with a band bass of 10 nm. The surfactant solution was 0.1 mol l^{-1} SDS.

For low pyrene concentration where micelles with more than one pyrene molecule are rare, the monomer fluorescence occurs exclusively

from singly occupied micelles and is exponential (Figure 5.3a). As the concentration is increased, micelles with two or more pyrene molecules occur and monomer fluorescence coming from these micelles contributes a shorter component to the decay curve (Figure 5.3b) which becomes more and more significant as the concentration increases (Figure 5.3c, 5.3d).

The curves can be fitted with two exponentials. The longer component τ_0 is the "true" monomer lifetime in singly occupied micelles and the shorter component τ is the monomer fluorescence decay from multiply occupied micelles. This parameter τ is a combination of the two decay parameters τ_1 and τ_2 which are associated with both monomer and excimer decay. However, the separation into three exponentials is not valid [Knight and Selinger 1971], and only where the τ_0 contribution is small could a resolution into τ_1 and τ_2 be attempted with the theoretical expression

$$I(t) = B_1 e^{-t/\tau_1} + B_2 e^{-t/\tau_2} .$$

The fitted parameters for the decay curves of Figure 5.3 are given in Table 5.3. τ_0, the lifetime of the monomer fluorescence from singly occupied micelles, remains virtually constant at 388 ns as the mean number of pyrene molecules per micelle increases from zero to one. In the table A_0 and A are the zero time amplitudes of the monomer fluorescence from singly and multiply occupied micelles respectively and $A_0\tau_0$, $A\tau$ are the corresponding fluorescence intensities. It is evident that the ratio $A_0\tau_0/A\tau$ decreases with increasing pyrene concentration (i.e. as the ratio of multiply to singly occupied micelles increases). This ratio is needed to determine the number of singly and multiply occupied micelles required for further calculations.

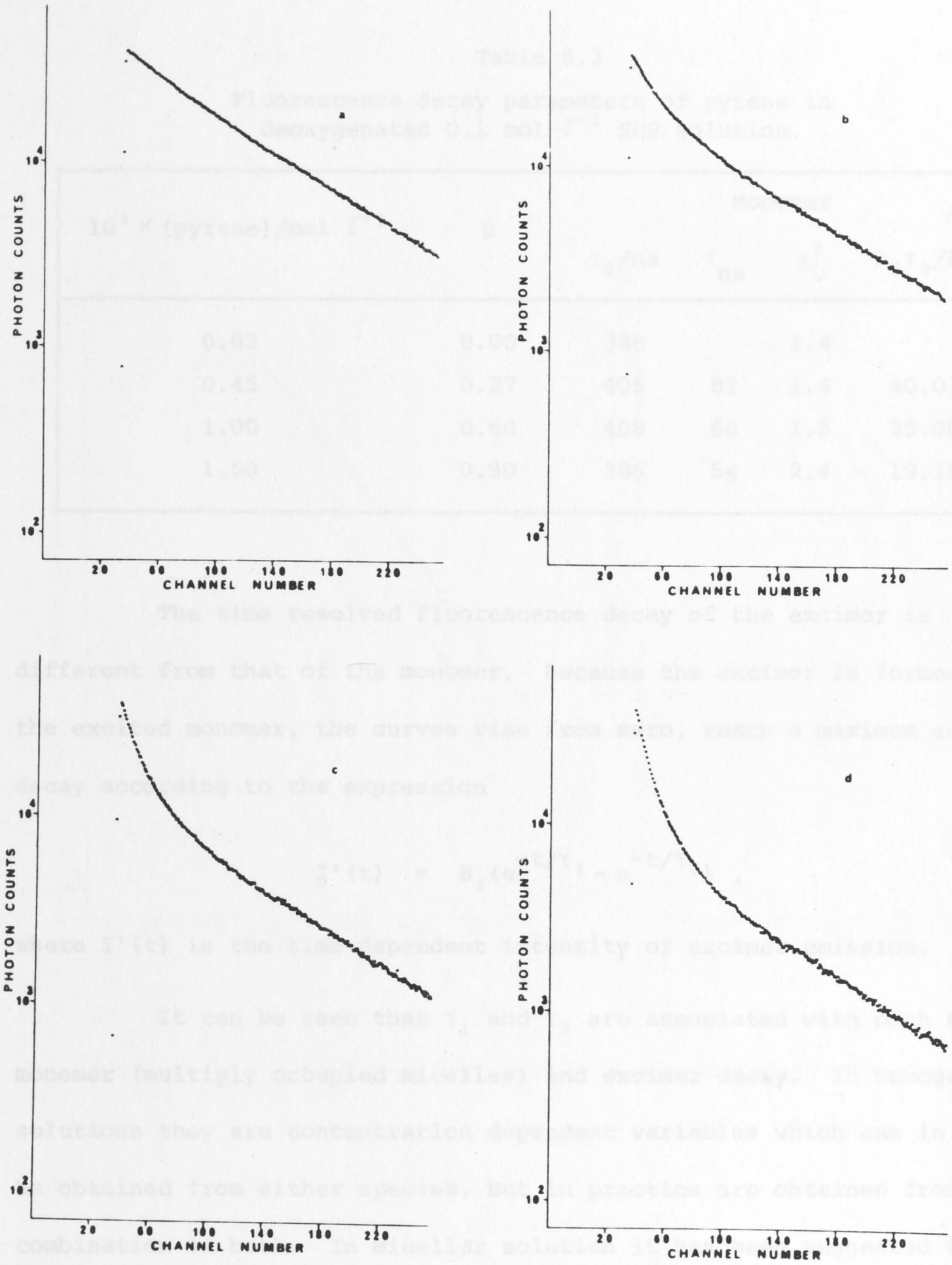

Figure 5.3. Fluorescence decay curves for pyrene monomer in 0.1 mol l^{-1} SDS.

(a) 2.0×10^{-5} mol l^{-1}; (b) 4.5×10^{-4} mol l^{-1};

(c) 1.0×10^{-3} mol l^{-1}; (d) 1.5×10^{-3} mol l^{-1}.

The time scale is 4.38 ns per channel.

Table 5.3

Fluorescence decay parameters of pyrene in deoxygenated 0.1 mol l^{-1} SDS solution.

$10^3 \times$ [pyrene]/mol l^{-1}	μ	Monomer			
		τ_0/ns	τ_{ns}	χ^2_ν	$A_0\tau_0/A\tau$
0.02	0.00	388		1.4	
0.45	0.27	405	82	1.4	40.03
1.00	0.60	408	66	1.5	25.00
1.50	0.90	386	54	2.4	19.16

The time resolved fluorescence decay of the excimer is different from that of the monomer. Because the excimer is formed from the excited monomer, the curves rise from zero, reach a maximum and then decay according to the expression

$$I'(t) = B_3(e^{-t/\tau_1} - e^{-t/\tau_2}) ,$$

where I'(t) is the time dependent intensity of excimer emission.

It can be seen that τ_1 and τ_2 are associated with both the monomer (multiply occupied micelles) and excimer decay. In homogeneous solutions they are concentration dependent variables which can in theory be obtained from either species, but in practice are obtained from a combination of both. In micellar solution it has been suggested that τ_1 and τ_2 are constants [Hauser and Klein 1973]. The decay parameters are obtained by a computer fit of the experimental decay curves (Figure 5.4) to the theoretical curve convoluted with the lamp pulse. This method of fitting has been shown to be the only statistically valid procedure [Knight and Selinger 1971] and the value of chi-square for the fits are given in the tables. Because no error was included for the lamp, the

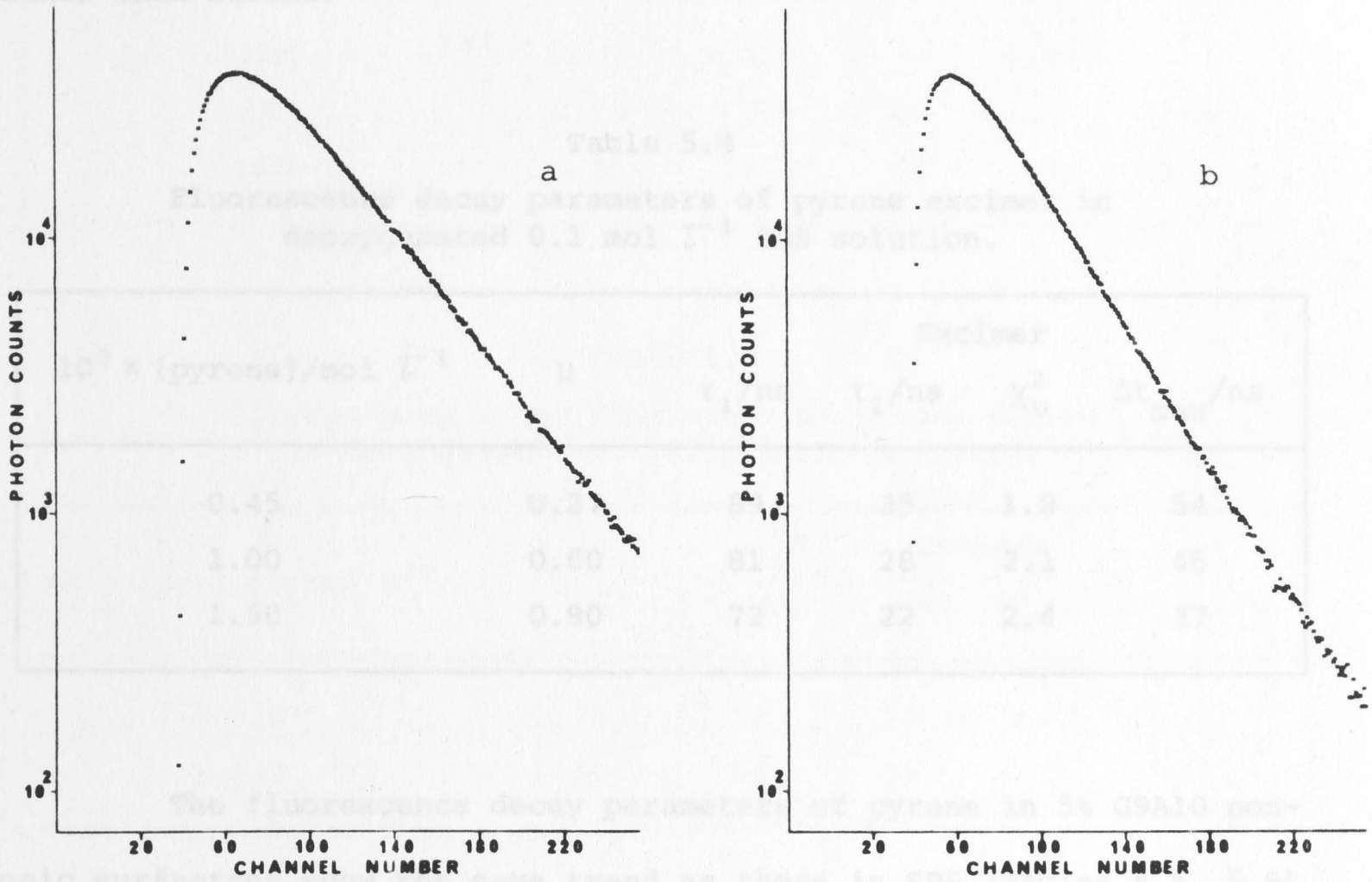

Figure 5.4. Fluorescence decay curves for pyrene excimer in 0.1 mol l^{-1} SDS:

(a) 4.5×10^{-4} mol l^{-1};

(b) 1.5×10^{-3} mol l^{-1}.

The time scale is 2.14 ns per channel.

value of chi-square (χ^2_ν) has been overestimated and the fit is in fact even better than suggested. The fitted decay parameters are found to vary with concentration (Table 5.4). It is this variation with concentration which has led us to describe micellar solutes as Poissons rather than Bosons.

Table 5.4

Fluorescence decay parameters of pyrene excimer in deoxygenated 0.1 mol l^{-1} SDS solution.

$10^3 \times$ [pyrene]/mol l^{-1}	μ	Excimer			
		τ_1/ns	τ_2/ns	χ^2_ν	Δt_{max}/ns
0.45	0.27	89	35	1.8	54
1.00	0.60	81	28	2.1	45
1.50	0.90	72	22	2.4	37

The fluorescence decay parameters of pyrene in 5% G9A10 non-ionic surfactant show the same trend as those in SDS (Tables 5.5, 5.6). Pyrene monomer fluorescence is double exponential and the ratio $A_0\tau_0/A\tau$ decreases with increase in μ. However, the pyrene monomer lifetime is shorter in G9A10 micelles than in SDS micelles. The lifetimes of pyrene monomer in different solvents are shown in Table 5.7. The parameters τ_1 and τ_2 for pyrene excimer also decrease with the concentration of solute. These experimental results provide further justification for ascribing a Poisson distribution to the distribution of solutes in polyoxyethylene alcohol type micelles.

Table 5.5

Fluorescence decay parameters of pyrene in deoxygenated 5% Teric G9A10 solution.

$10^3 \times$ [pyrene]/mol l^{-1}	μ	Monomer			
		τ_0/ns	τ/ns	χ^2_ν	$A_0\tau_0/A\tau$
0.026	0.01	329		1.4	
1.320	0.75	325	46	1.3	37.8
2.640	1.50	332	45	1.9	15.71

Table 5.6

Fluorescence decay parameters of pyrene excimer in deoxygenated 5% Teric G9A10 solution.

$10^3 \times$ [pyrene]/mol l^{-1}	μ	Excimer			
		τ_1/ns	τ_2/ns	χ^2_ν	Δt_{max}/ns
1.320	0.75	73	23	3.0	39
2.640	1.50	66	19	1.5	33

Table 5.7

Fluorescence lifetimes of pyrene monomer in different solvents.

Solvent	τ/ns
Water	207
SDS	388
Teric G9A10	329
Ethanol	290 †
Cyclohexane	450 †

† Birks [1970a].

5.1.2.2 Solutes in micelles with high occupancy

The previous section presented the use of pyrene as a fluorescent probe. The solubility of pyrene in surfactant solution is low. For example the mean occupation number of pyrene molecules in SDS is always less than one. However, because of the large enthalpy of excimer formation, fluorescence of excimer was observed. Thus, it was possible to study the statistical distribution of solute molecules amongst micelles. 2-Methylnaphthalene has a much smaller enthalpy of excimer formation but it is much more soluble, so that excimer fluorescence could again be detected in micelles. A linear plot has been obtained when the corrected intensities ratio of excimer to monomer fluorescence is plotted against the bulk concentration of 2-methyl-naphthalene (Figure 5.5). This plot is similar to the plot obtained for 2-methylnaphthalene in homogeneous solutions [Selinger 1966]. Quenching by oxygen (Table 5.8), Mn^{2+} and I^- does not affect the ratio of excimer to monomer emission intensities (ϕ'/ϕ) for two reasons.

(a) At the concentration of 2-methylnaphthalene required for excimer fluorescence (high because of the low enthalpy of formation), the number of singly occupied micelles is low and

Table 5.8

Oxygen quenching of 2-methylnaphthalene excimer fluorescence in 0.1 mol l^{-1} SDS solution.

10^2 × [2MN]/ mol l^{-1}	Oxygen Added				Deoxygenated				$\frac{(\phi'/\phi)_{quenched}}{(\phi'/\phi)_{unquenched}}$
	I'	I	I'/I	ϕ'/ϕ	I'	I	I'/I	ϕ'/ϕ	
2.0	23	50	0.46	0.37	44	95	0.46	0.37	1.00

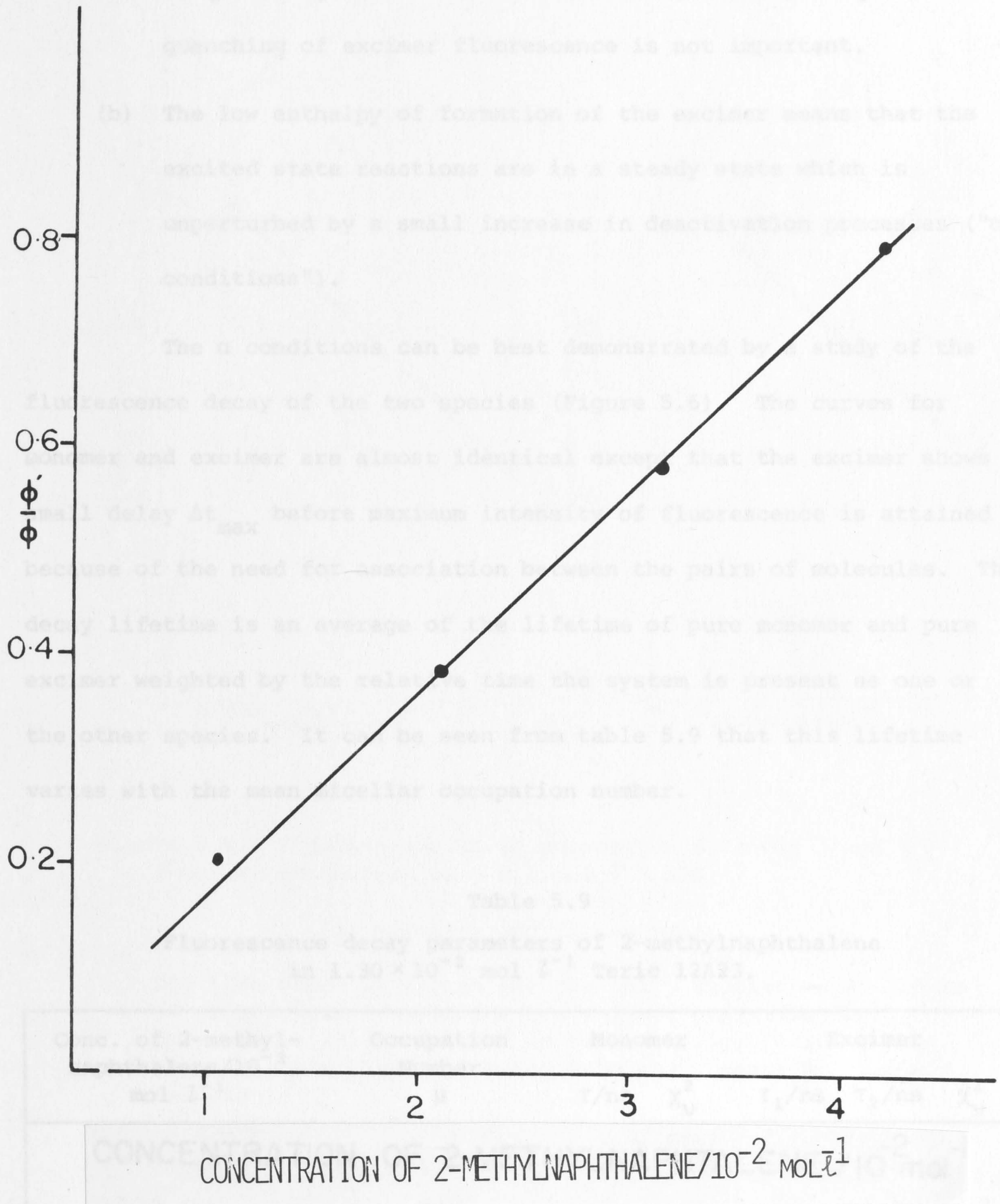

Figure 5.5. Corrected fluorescence intensity ratio of excimer to monomer (ϕ'/ϕ) as a function of bulk concentration of 2-methylnaphthalene in 0.1 mol ℓ^{-1} SDS.

so quenching of monomer fluorescence without consequential quenching of excimer fluorescence is not important.

(b) The low enthalpy of formation of the excimer means that the excited state reactions are in a steady state which is unperturbed by a small increase in deactivation processes ("α conditions").

The α conditions can be best demonstrated by a study of the fluorescence decay of the two species (Figure 5.6). The curves for monomer and excimer are almost identical except that the excimer shows a small delay Δt_{max} before maximum intensity of fluorescence is attained because of the need for association between the pairs of molecules. The decay lifetime is an average of the lifetime of pure monomer and pure excimer weighted by the relative time the system is present as one or the other species. It can be seen from table 5.9 that this lifetime varies with the mean micellar occupation number.

Table 5.9

Fluorescence decay parameters of 2-methylnaphthalene in 1.30×10^{-2} mol l^{-1} Teric 12A23.

Conc. of 2-methyl-naphthalene/10^{-3} mol l^{-1}	Occupation Number μ	Monomer		Excimer		
		τ/ns	χ^2_ν	τ_1/ns	τ_2/ns	χ^2_ν
0.48	0.9	53	1.7	no excimer		
2.43	4.5	59	1.8	57	0.99	7.3
4.88	9.0	63	2.4	64	0.67	5.0

1-Cyanonaphthalene has also been used in this study, because the mean occupancy number lies between those of pyrene and 2-methyl-naphthalene. In the case of 1-cyanonaphthalene, excimer fluorescence is

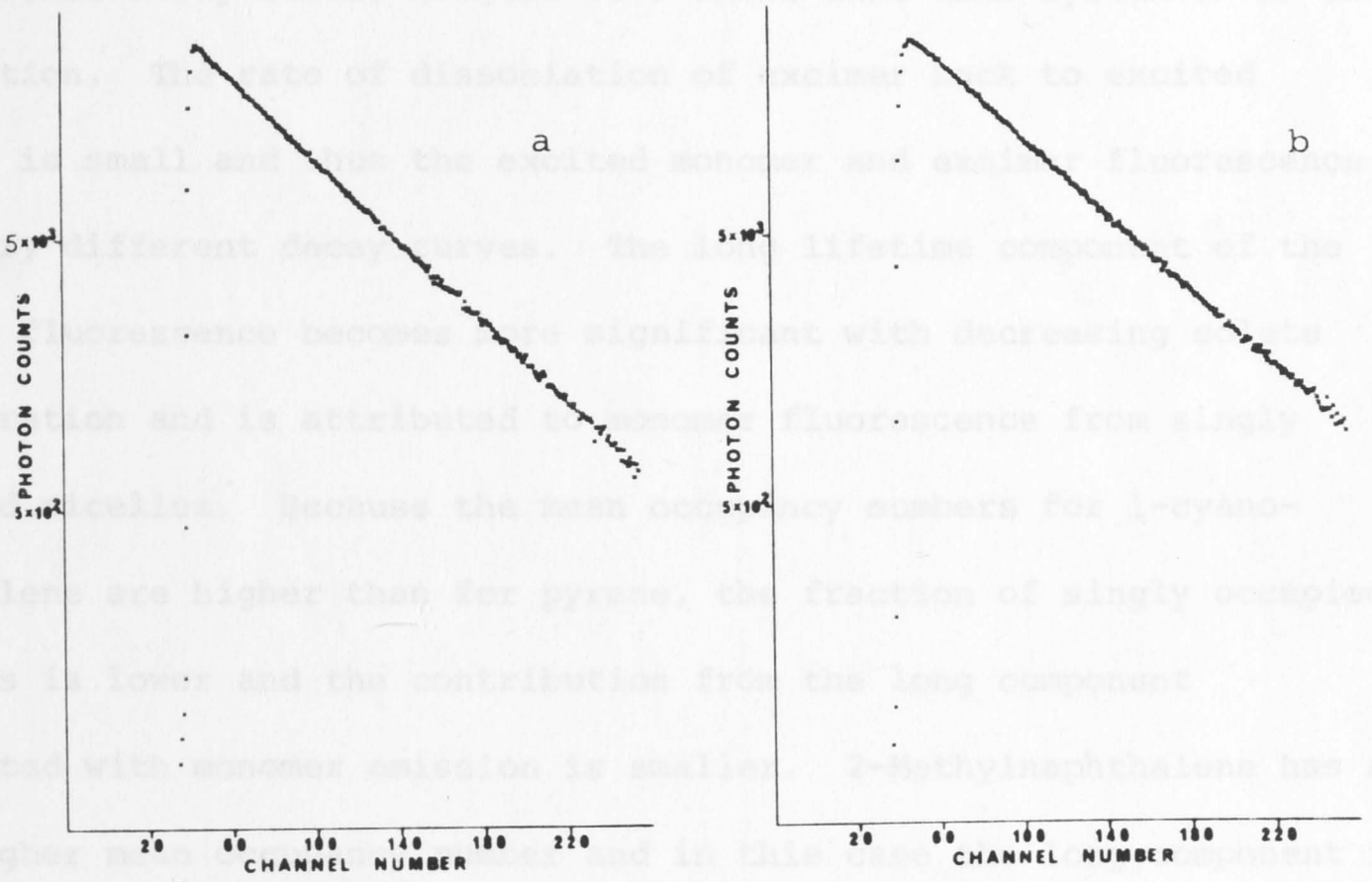

Figure 5.6. Fluorescence decay curves for 8.73×10^{-3} mol l^{-1} 2-methylnaphthalene in a 0.1 mol l^{-1} SDS.

(a) monomer, and (b) excimer.

The time scale is 1.0 ns per channel. Excitation at 316 nm (2 nm band pass). Monomer and excimer emissions were observed at 335 nm and 416 nm respectively. A 10 nm band pass was used when monitoring both the monomer and excimer emission.

observed in homogeneous solutions above a concentration of 0.002 mol l^{-1}. A mean micellar occupation number in the range 0.6 to 10 corresponds to fluorescence from mainly monomer to mainly excimer. A study of the fluorescence decay curves (Figure 5.7) shows that this system is in the β condition. The rate of dissociation of excimer back to excited monomer is small and thus the excited monomer and excimer fluorescence show very different decay curves. The long lifetime component of the monomer fluorescence becomes more significant with decreasing solute concentration and is attributed to monomer fluorescence from singly occupied micelles. Because the mean occupancy numbers for 1-cyano-naphthalene are higher than for pyrene, the fraction of singly occupied micelles is lower and the contribution from the long component associated with monomer emission is smaller. 2-Methylnaphthalene has a much higher mean occupancy number and in this case the long component is completely absent.

Thus, the series pyrene, 1-cyanonaphthalene and 2-methyl-naphthalene form excimers with decreasing enthalpy (requiring increasing concentration for their formation) with a consequent quasi-equilibrium excited state reaction in the latter case. With pyrene the statistical argument predominates. In the case where the average occupancy, μ, is large, as with 2-methylnaphthalene, we are virtually dealing with a dispersed lipophilic "normal" solution. For large μ a Poisson distribution leads to a nonlinear micelle occupancy probability for $P(\geqslant 2)/P(1)$ versus μ, presented in Figure 5.8. The analogous plot for a Boson distribution where μ cannot exceed 2 is shown in Figure 5.9. Although Poisson and Boson statistics predict very similar distributions for small values of μ they predict very different distributions for large values of μ. The experimental results for

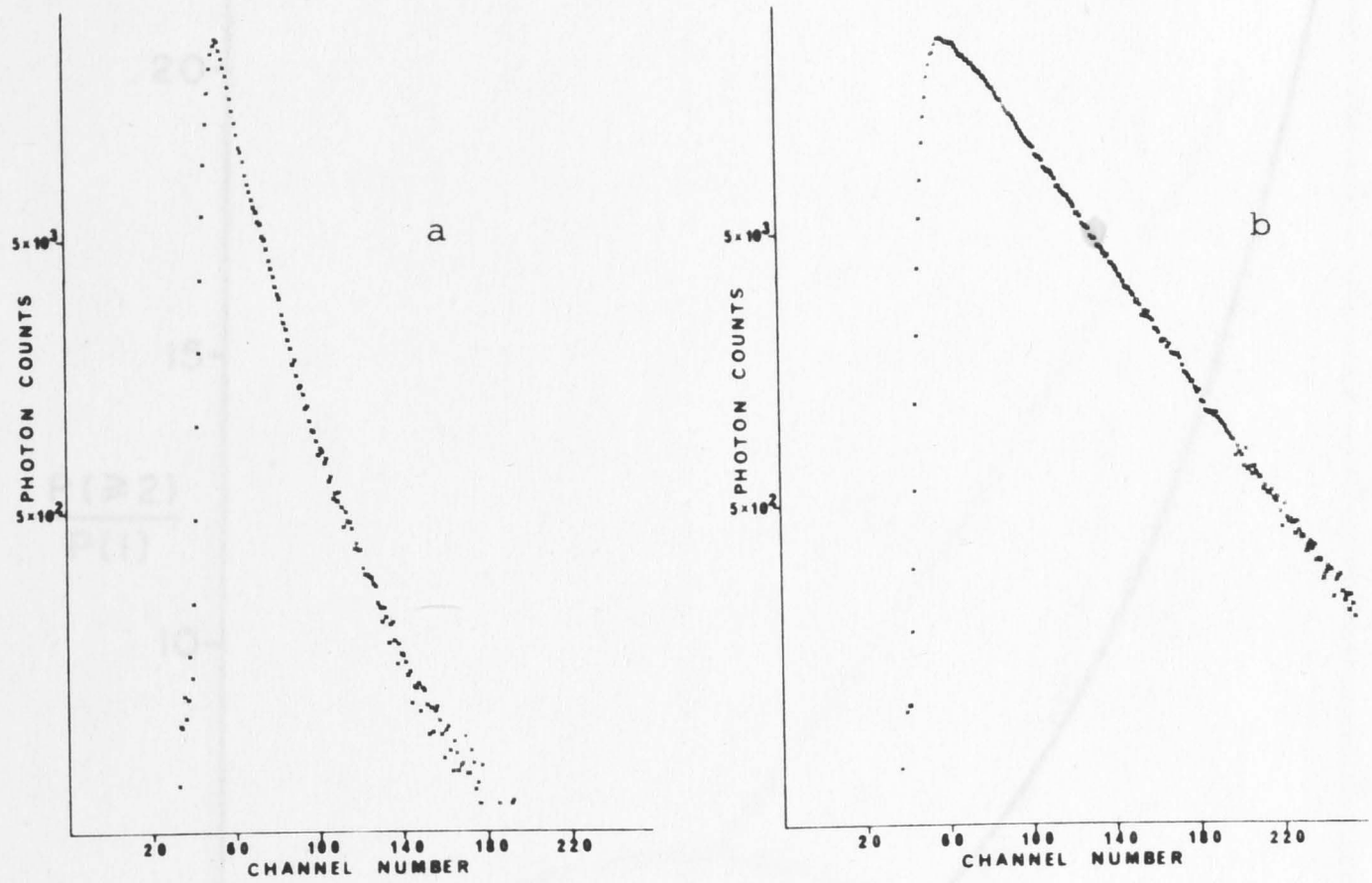

Figure 5.7. Fluorescence decay curves for 3.0×10^{-3} mol l^{-1} 1-cyanonaphthalene in 1.3×10^{-2} mol l^{-1} Teric 12A23.

(a) monomer, and (b) excimer.

The time scale is 0.41 ns per channel. Excitation at 316 nm (2 nm band pass). Monomer and excimer emissions were observed at 343 nm and 442 nm respectively. A 10 nm band pass was used both for monomer and excimer emission.

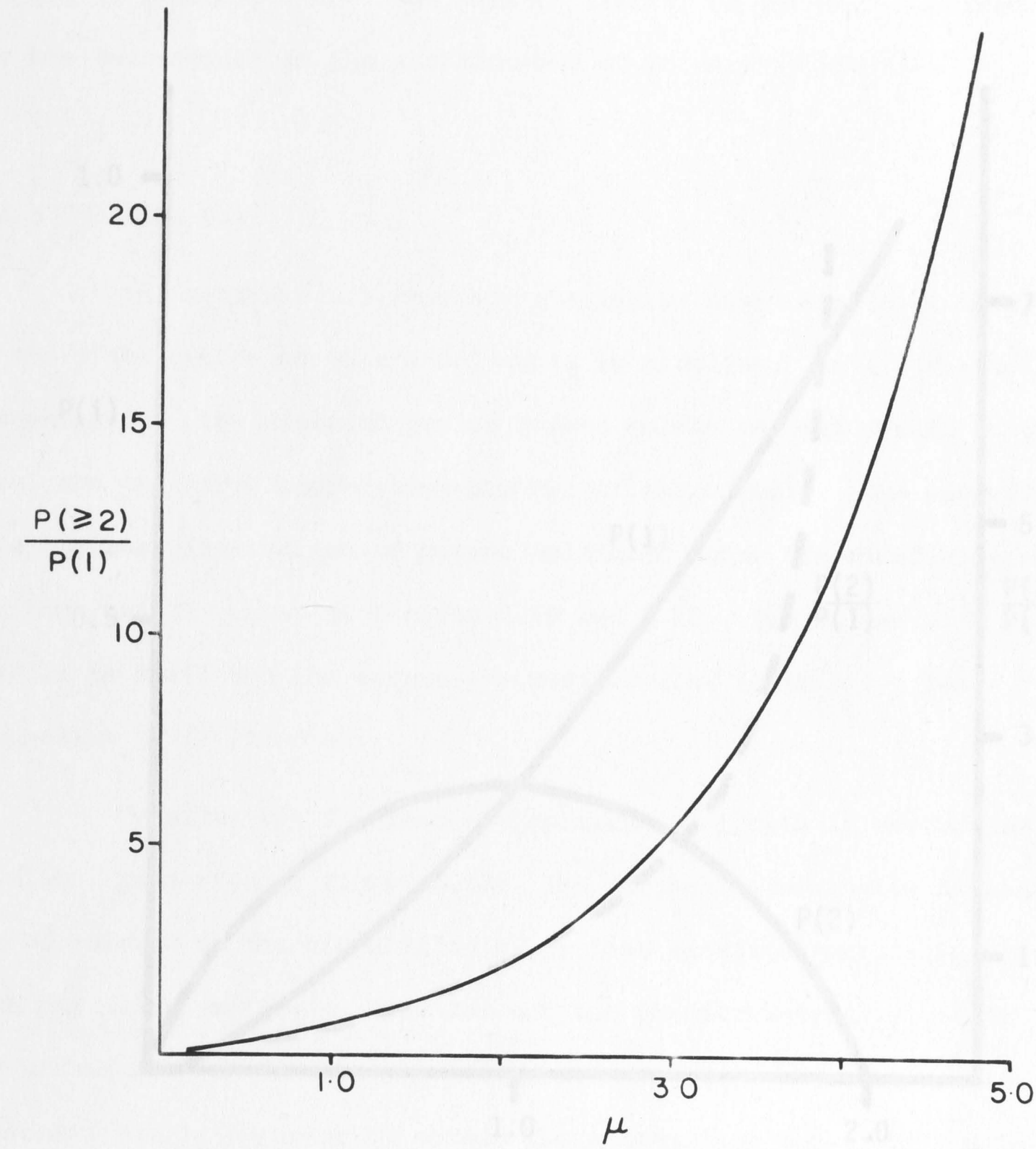

Figure 5.8. Plot of P ($\geq$ 2)/P(1) against μ for a Poisson distribution.

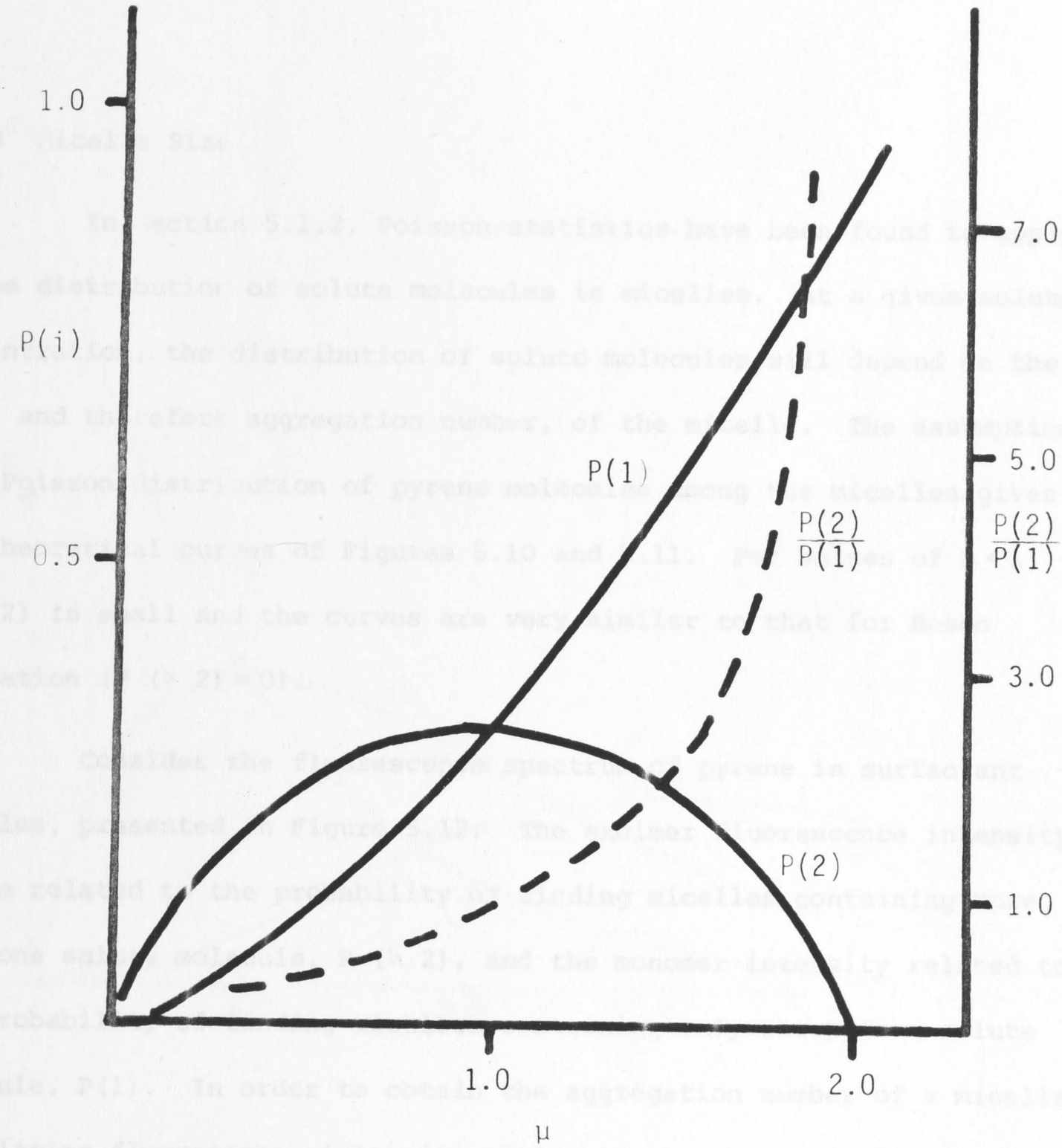

Figure 5.9. Boson distribution curves.

2-methy naphthalene have verified that a micelle can contain more than two sol ıte molecules, and thus Poisson statistics are more applicable for the description of the distribution of solutes in micelles.

5.1.3 Micelle Size

In Section 5.1.2, Poisson statistics have been found to apply to the distributior of solute molecules in micelles. At a given solute concentration, the distribution of solute molecules will depend on the size, and therefore aggregation number, of the micelle. The assumption of a Poisson distribution of pyrene molecules among the micelles gives the theoretical curves of Figures 5.10 and 5.11. For values of $\mu < 1$, P (> 2) is small and the curves are very similar to that for Boson occupation (P (> 2) = 0).

Consider the fluorescence spectrum of pyrene in surfactant micelles, presented in Figure 5.12. The excimer fluorescence intensity can be related to the probability of finding micelles containing more than one solute molecule, P (> 2), and the monomer intensity related to the probability of finding micelles containing only one pyrene solute molecule, P(1). In order to obtain the aggregation number of a micelle by relating fluorescence intensity ratios to the theoretical $P (\geqslant 2)/P(1)$ ratio, two important adjustments must be made.

(1) Micelles which are multiply occupied have that multiple of the absorbance. The probability distribution is for micelle numbers: for example, separate beakers of singly and doubly occupied micelles containing equal numbers of micelles would differ by a factor of two in their absorbance. Thus the ratio of excimer fluorescence to monomer fluorescence from singly

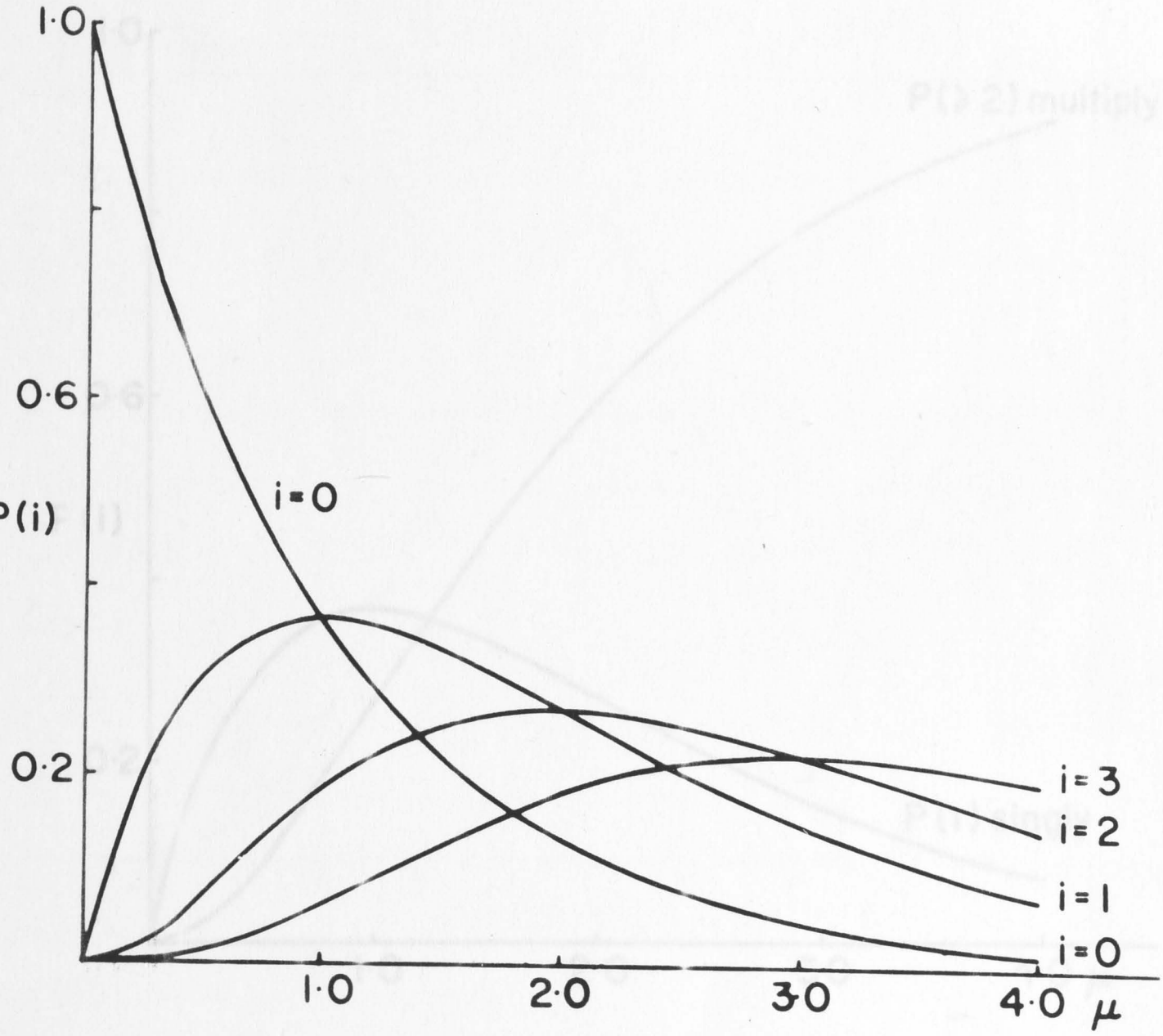

Figure 5.10. Poisson distribution curves for P(i); i = 0,3.

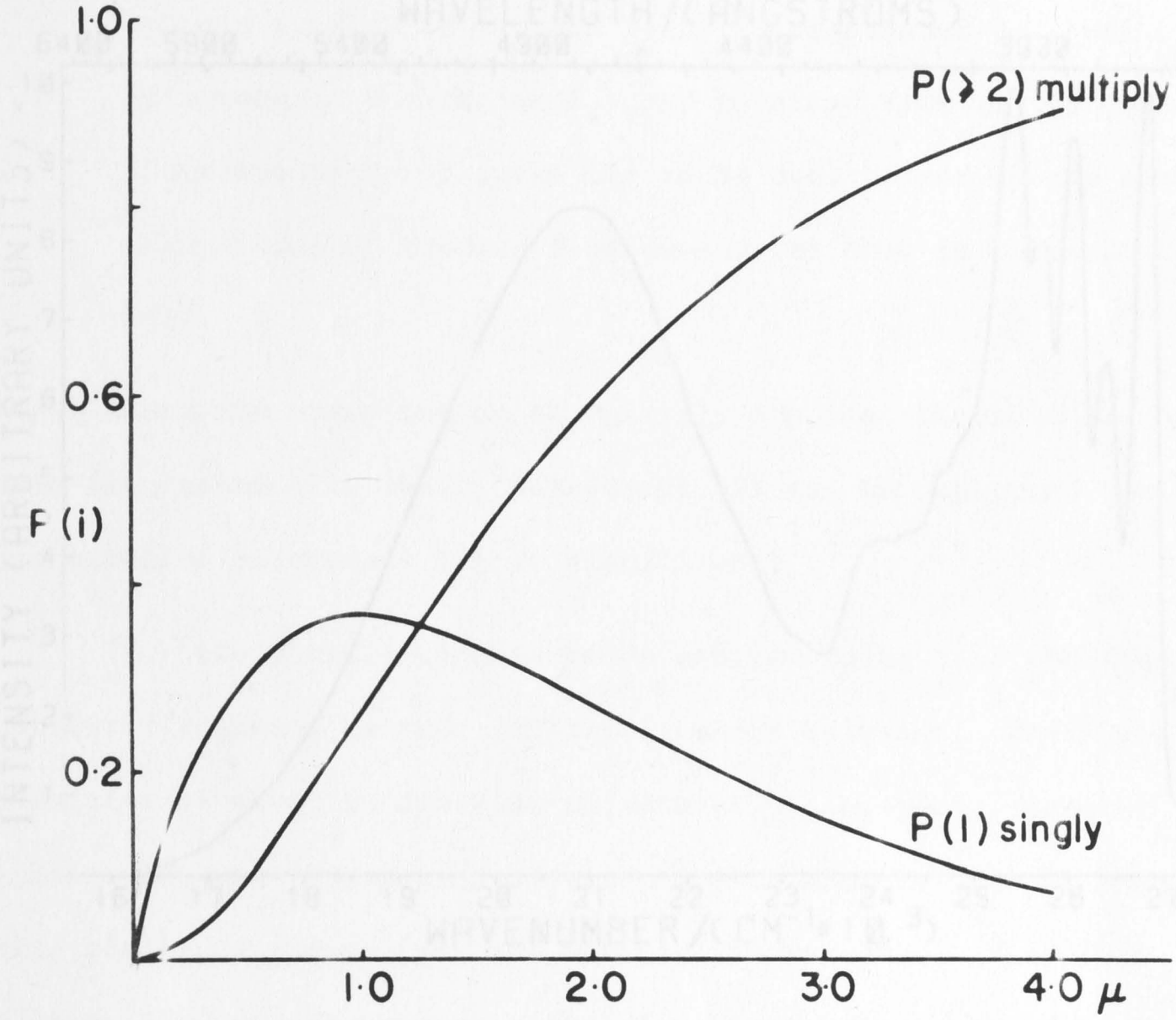

Figure 5.11. Plots of P (⩾ 2) and P(1) against μ. P (⩾ 2) corresponds to multiply occupied micelles and P(1) corresponds to singly occupied micelles.

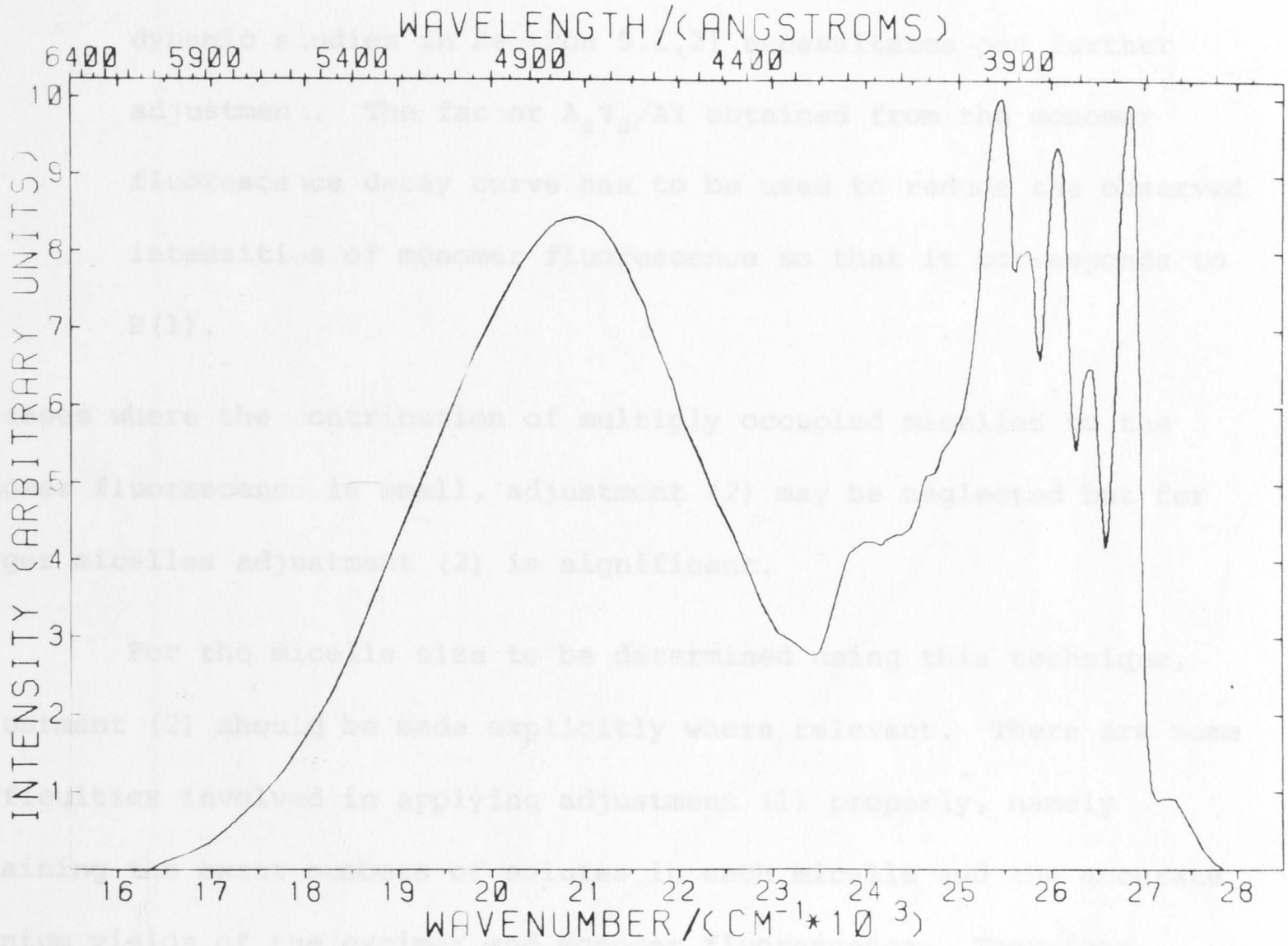

Figure 5.12. Corrected fluorescence spectrum of pyrene in SDS. Excimer emission corresponds to P ($\geqslant 2$) and monomer emission corresponds to P(1). Excitation at 337 nm.

occupied micelles would be expected to be proportional to

$$[2 \times P(2) + 3 \times P(3) + 4 \times P(4) + \ldots]/P(1) \ .$$

(2) On the other hand, the fact that a certain amount of monomer fluorescence comes from multiply occupied micelles (see dynamic studies in Section 5.1.2) necessitates one further adjustment. The factor $A_0\tau_0/A\tau$ obtained from the monomer fluorescence decay curve has to be used to reduce the observed intensities of monomer fluorescence so that it corresponds to P(1).

In cases where the contribution of multiply occupied micelles to the monomer fluorescence is small, adjustment (2) may be neglected but for larger micelles adjustment (2) is significant.

For the micelle size to be determined using this technique, adjustment (2) should be made explicitly where relevant. There are some difficulties involved in applying adjustment (1) properly, namely obtaining the exact numbers of solutes in each micelle and the accurate quantum yields of the excimer and monomer fluorescence. Therefore adjustment (1), at the present state of understanding, should be made by using a general plot $f \times (P\ (\geqslant 2)/P(1))$ versus μ. By taking the ratio of excimer to monomer fluorescence quantum yields to be 1.5[†] and setting the factor f equal to 2.5, the aggregation number of SDS obtained was in agreement with the literature value. These assumptions and the plot of $2.5 \times (P\ (\geqslant 2)/P(1))$ versus μ (Figure 5.13) will be used to study the effect of electrolyte and temperature on the size of ionic and nonionic micelles respectively.

[†] The ratio of the quantum yields of excimer to monomer in n-hexadecane and paraffin oil are given as 1.31 and 1.92 respectively [Seidel 1963].

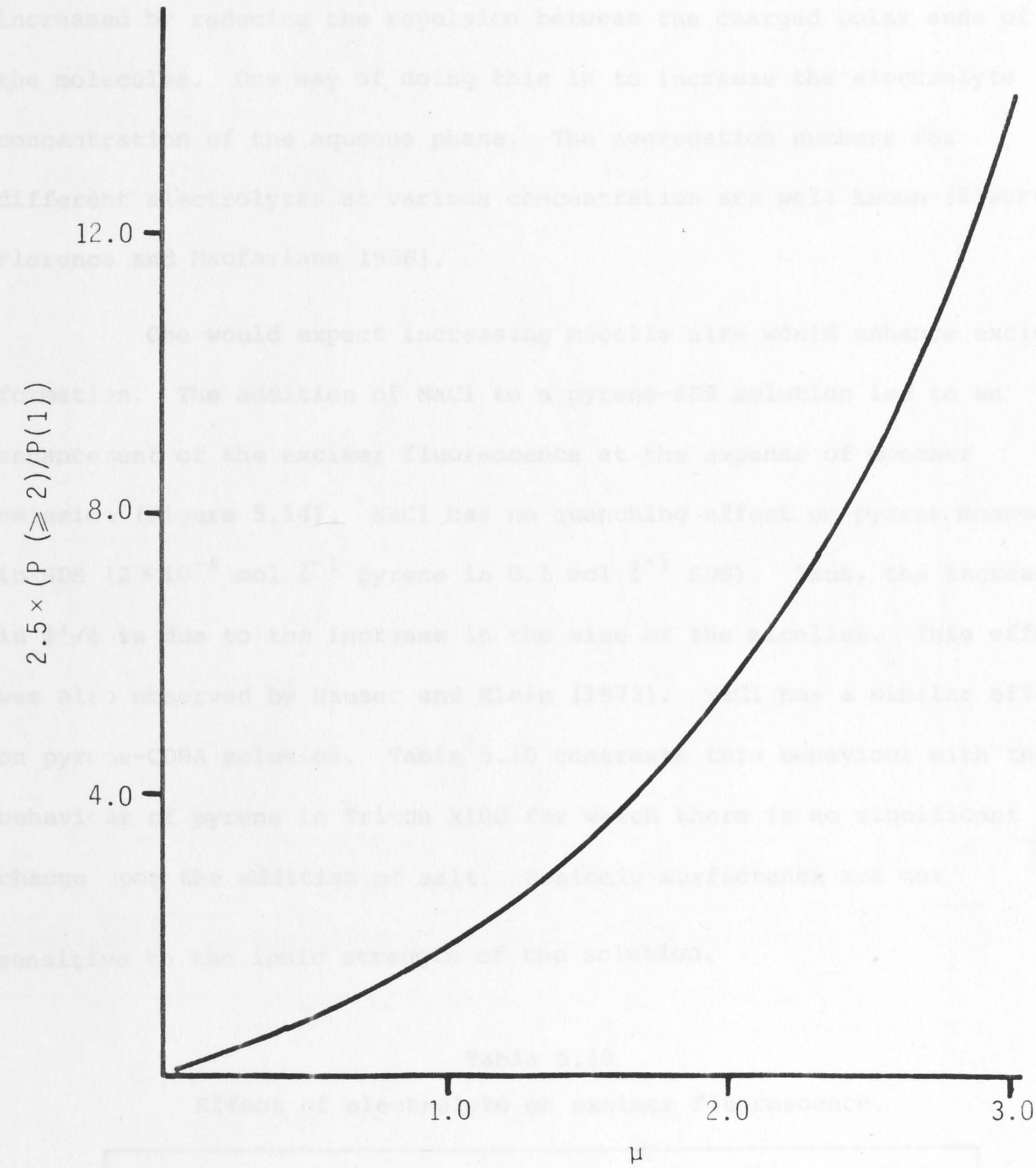

Figure 5.13. Plot of $2.5 \times (P (\geq 2)/P(1))$ against μ.

5.1.3.1 Effect of electrolyte on micelle size

With ionic surfactants, the micellar aggregate can be increased by reducing the repulsion between the charged polar ends of the molecules. One way of doing this is to increase the electrolyte concentration of the aqueous phase. The aggregation numbers for different electrolytes at various concentration are well known [Elworthy, Florence and Macfarlane 1968].

One would expect increasing micelle size would enhance excimer formation. The addition of NaCl to a pyrene-SDS solution led to an enhancement of the excimer fluorescence at the expense of monomer emission (Figure 5.14). NaCl has no quenching effect on pyrene monomer in SDS (2×10^{-5} mol l^{-1} pyrene in 0.1 mol l^{-1} SDS). Thus, the increase in ϕ'/ϕ is due to the increase in the size of the micelles. This effect was also observed by Hauser and Klein [1973]. NaCl has a similar effect on pyrene-CDBA solution. Table 5.10 contrasts this behaviour with the behaviour of pyrene in Triton X100 for which there is no significant change upon the addition of salt. Nonionic surfactants are not sensitive to the ionic strength of the solution.

Table 5.10

Effect of electrolyte on excimer fluorescence.

Excimer-Micelle	[NaCl]/mol l^{-1}	ϕ'/ϕ
ANIONIC		
5×10^{-4} mol l^{-1} pyrene	0.0	1.93
in 0.05 mol l^{-1} SDS	0.5	2.84
CATIONIC		
5×10^{-4} mol l^{-1} pyrene	0.0	0.65
in 0.05 mol l^{-1} CDBA	0.5	0.83
NONIONIC		
2×10^{-4} mol l^{-1} pyrene	0.0	0.65
in 1.5% Triton X100	0.5	0.63

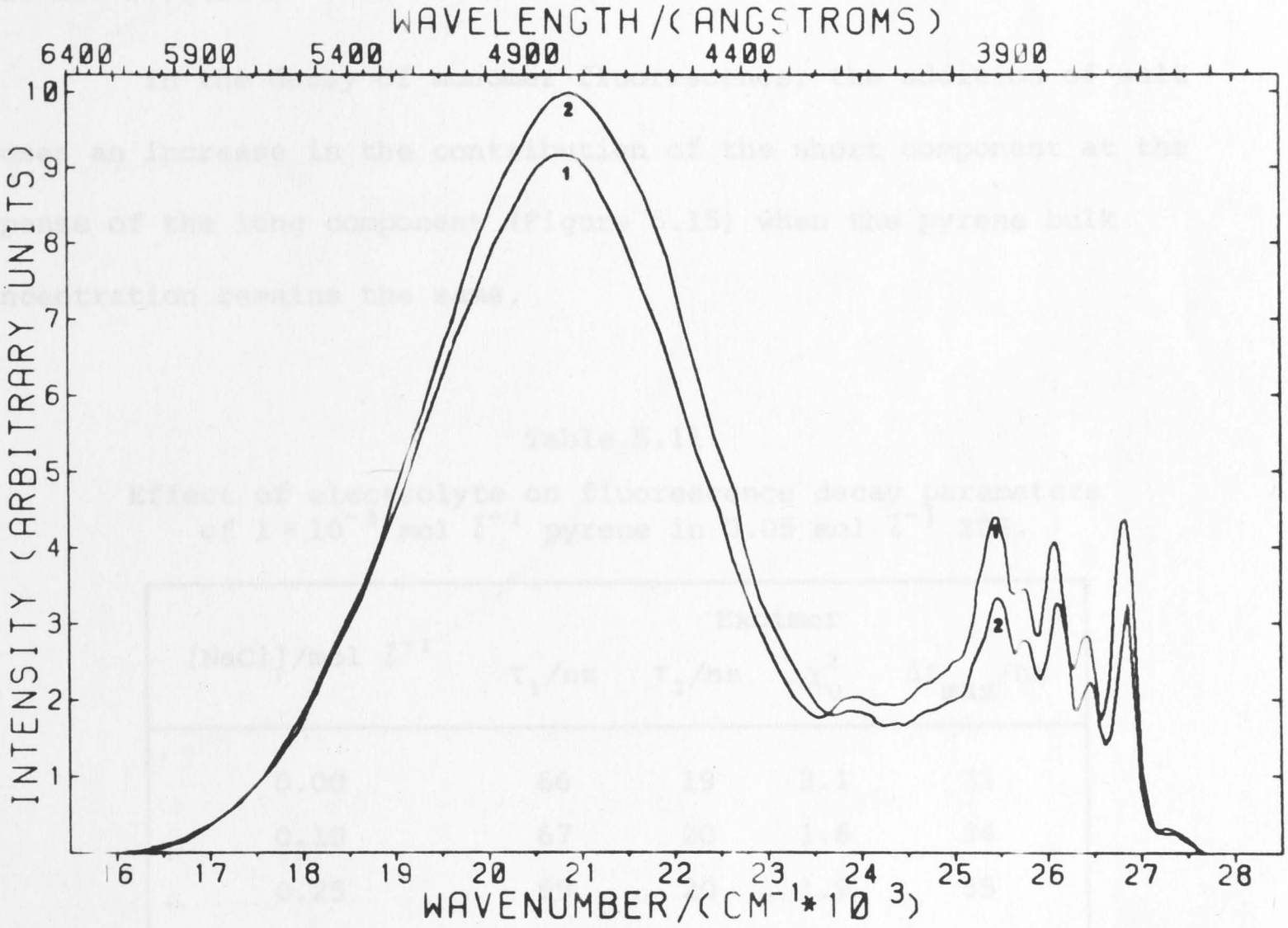

Figure 5.14. Corrected fluorescence spectra of pyrene 1×10^{-3} mol l^{-1} in 0.05 mol l^{-1} SDS. Excitation at 337 nm.

(1) alone;

(2) with addition of 0.5 mol l^{-1} NaCl.

The fluorescence decay curves for pyrene excimer at different electrolyte concentrations have also been obtained. The fitted decay parameters are given in Table 5.11. The time delay Δt_{max} increases with the increase of NaCl concentration as one would expect if the micelle size is increased.

In the decay of monomer fluorescence, the addition of salt causes an increase in the contribution of the short component at the expense of the long component (Figure 5.15) when the pyrene bulk concentration remains the same.

Table 5.11

Effect of electrolyte on fluorescence decay parameters of 1×10^{-3} mol l^{-1} pyrene in 0.05 mol l^{-1} SDS.

[NaCl]/mol l^{-1}	Excimer			
	τ_1/ns	τ_2/ns	χ^2_ν	Δt_{max}/ns
0.00	66	19	2.1	33
0.10	67	20	1.6	34
0.25	69	20	1.9	35
0.50	71	23	2.7	38

To calculate the aggregation numbers of SDS as a function of salt concentration, the fluorescence intensity ratios were corrected by the factors $A_0\tau_0/A\tau$ for both monomer and excimer intensities. The values of $A_0\tau_0/A\tau$ were taken from the decay curves of the monomer fluorescence. Then the aggregation numbers were calculated using the probability curve (Figure 5.13) and the corrected experimental intensity ratios. The results are shown in Table 5.12.

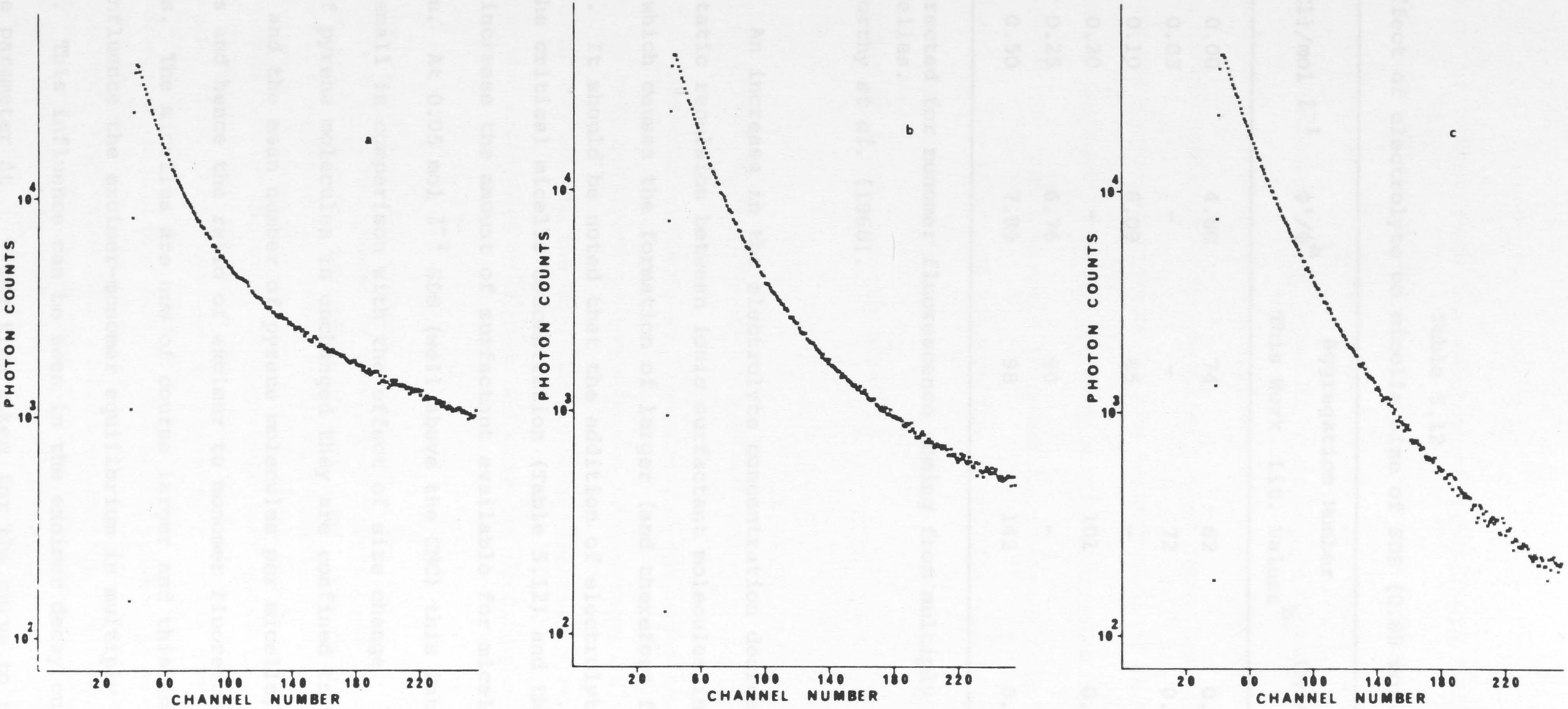

Figure 5.15. Fluorescence decay curves for pyrene monomer in 0.05 mol l^{-1} SDS. (a) 1×10^{-3} mol l^{-1} pyrene; (b) with addition of 0.25 mol l^{-1} NaCl; (c) with addition of 0.50 mol l^{-1} NaCl. The time scale is 2.14 ns per channel.

Table 5.12

Effect of electrolyte on micelle size of SDS (0.05 mol l^{-1}).

[NaCl]/mol l^{-1}	ϕ'/ϕ[a]	Aggregation Number		CMC/mol l^{-1}[b]
		This Work	Lit. Values[b]	
0.00	4.80	74	62	0.00810
0.03	-	-	72	0.00310
0.10	6.09	85	-	-
0.20	-	-	101	0.00090
0.25	6.76	90	-	-
0.50	7.89	98	142	0.00052

[a] Corrected for monomer fluorescence coming from multiply occupied micelles.

[b] Elworthy *et al.* [1968].

An increase in the electrolyte concentration decreases the electrostatic repulsion between ionic surfactant molecules in the micelle which causes the formation of larger (and therefore fewer) micelles. It should be noted that the addition of electrolyte also lowers the critical micelle concentration (Table 5.12) and this will tend to increase the amount of surfactant available for micelle formation. At 0.05 mol l^{-1} SDS (well above the CMC) this latter effect will be small in comparison with the effect of size change. Because the number of pyrene molecules is unchanged they are confined to fewer micelles and the mean number of pyrene molecules per micelle, μ, increases and hence the ratio of excimer to monomer fluorescence increases. The micelles are now of course larger and this in turn should influence the excimer-monomer equilibrium in multiply occupied micelles. This influence can be seen in the excimer decay curves for which the parameter Δt_{max} — the time taken for the curve to reach a

maximum — increases with the addition of salt (Table 5.11). This result is analogous to the effect obtained in homogeneous solutions by lowering the concentration (Figure 3.1) or increasing the viscosity [Speed and Selinger 1969]. That is the mean collision time between excited monomer and partner is increased. Reference to the monomer decay curves obtained in the micellar system shows that the addition of electrolyte causes an increase in the contribution of the short component (monomer fluorescence from multiply occupied micelles) at the expense of the long component (monomer fluorescence from singly occupied micelles). The effect of electrolyte on micelle size, particularly for cationic surfactants, depends on the nature of the electrolyte and is not simply an ionic strength effect.†

5.1.3.2 Effect of temperature on micelle size

Nonionic surfactants form micelles for which the aggregation number is very sensitive to temperature. An increase in temperature causes an increase in the aggregation number because hydrogen bonding between the surfactant molecules and water is decreased.

---

† A number of micellar systems behave as coacervates in that they separate into two phases at a critical electrolyte concentration. This effect becomes operative at much lower concentrations for cationic surfactants than anionic surfactants. Between zero electrolyte concentration and the critical electrolyte concentration, a transition of the micellar aggregate from an essentially isotropic to an anisotropic particle may occur over an electrolyte transition range. This is believed to be true when micellar dissociation is critically supressed. CDBA has been suggested to be such a case [Cohen and Vassiliades 1961]. For those systems in which micellar dissociation increases with the addition of electrolyte to a relatively high value, the micelle grows to a limiting spherical value. It is considered that micelle size changes in cationic surfactants deserve more detailed studies.

The effect of temperature on the fluorescence of pyrene in Triton X100 is shown in Figure 5.16. An increase in temperature results in enhanced excimer emission at the expense of the monomer emission, for larger but fewer micelles form. Both an increase in temperature and the formation of larger micelles should favour increased monomer emission, but both these effects are outweighed by the fact that there are now fewer micelles to hold all the pyrene solute and so μ increases.

A quantitative evaluation of the micelle size change upon change in temperature is not possible without first determining the temperature dependence of the kinetics of excimer formation. The results of an approximate evaluation using fluorescence intensity ratios and the probability curve of Figure 5.13 are given in Table 5.13.

Table 5.13

Effect of temperature on micelle size of Triton X100 (40%).

Temperature °C	ϕ'/ϕ	Aggregation Number
23	0.71	63
25	0.81	71
33	1.06	90
38	1.39	114
43	1.67	132
53	2.19	163

5.1.3.3 Effect of ethylene oxide chain length on micelle size

Generally, the CMC's of nonionic surfactants (typically of the order of 10^{-4} mol l^{-1}) are lower than those of the ionic surfactants. Micelle size increases with increasing temperature and with decreasing

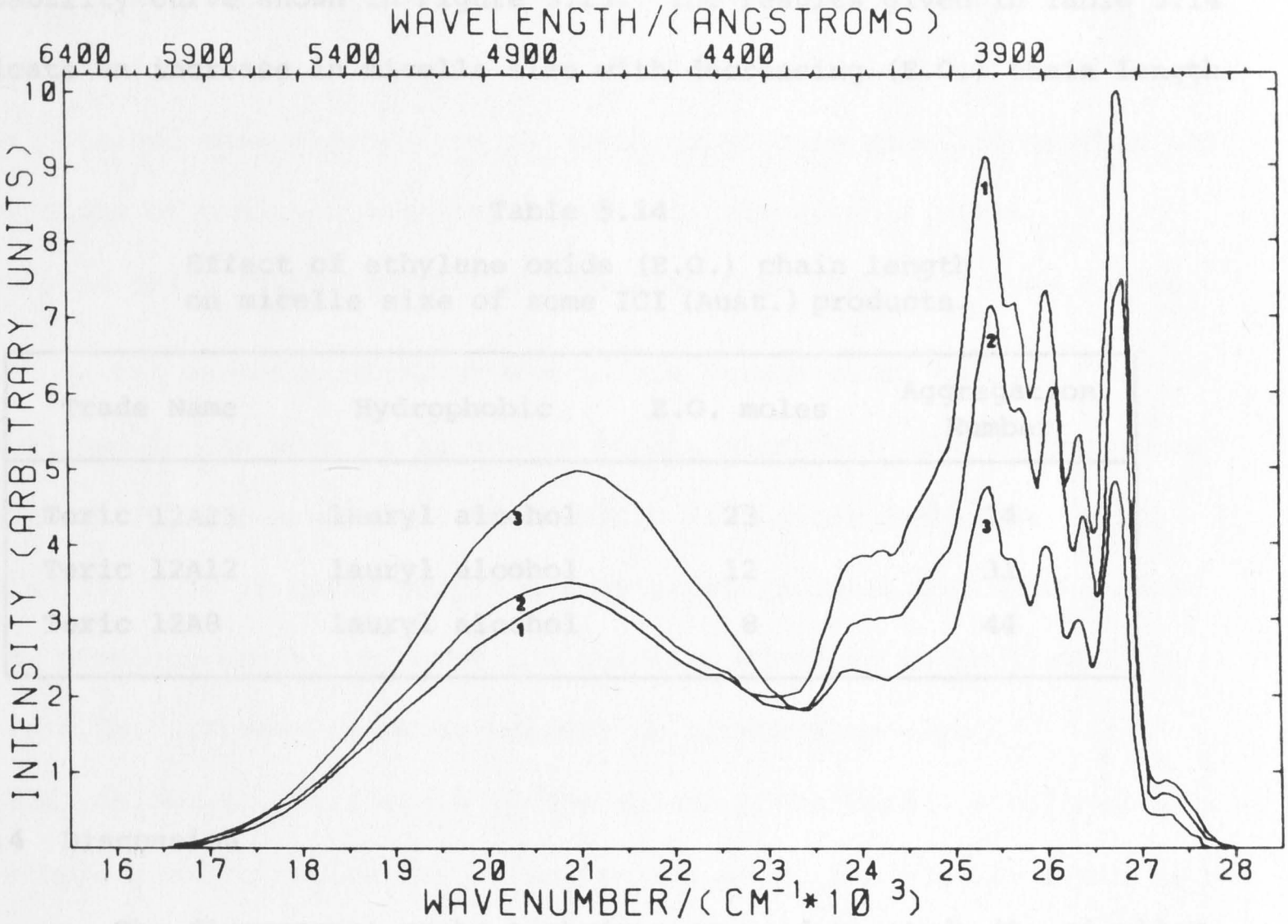

Figure 5.16. Corrected fluorescence spectra of pyrene 3.54×10^{-3} mol l^{-1} in 40% Triton X100 at

(1) 25 °C

(2) 33 °C

(3) 53 °C.

Excitation at 337 nm.

ethylene oxide chain length. The effect of ethylene oxide chain length on micelle size has been studied for some polyoxyethylene alcohols. The micelle sizes were obtained from the combination of corrected fluorescence spectra of pyrene in these surfactant solutions and the probability curve shown in Figure 5.13. The results given in Table 5.14 indicate an increase in micelle size with decreasing (E.O.) chain length.

Table 5.14

Effect of ethylene oxide (E.O.) chain length on micelle size of some ICI (Aust.) products.

Trade Name	Hydrophobic	E.O. moles	Aggregation Number
Teric 12A23	lauryl alcohol	23	24
Teric 12A12	lauryl alcohol	12	31
Teric 12A8	lauryl alcohol	8	44

5.1.4 Discussion

The fluorescent probe technique as used to study the micellar aqueous system involves the insertion of the probe into the required region of the system studied. Pyrene is very insoluble in water and is solubilised in the interior of the ionic micelles. Thus the excimer of pyrene offers a possibility of studying the interior of ionic micelles. With the pyrene excimer as a fluorescent probe, a method has been developed to calculate the micelle size. Ideally, the fluorescent probe should not interact with the surfactant molecule or perturb its properties. This ideal situation, however, does not always prevail in practice. The presence of the solutes in the micelles distorts the micelle size, normally making it bigger, and so the micelle size

calculated from pyrene excimer measurements is the size of a micelle which contains the solute probe. However, the low occupancy of solute pyrene minimises this distortion. It has been assumed in each experiment that the shape of the micelle remains spherical. The pyrene excimer, used as a fluorescent probe, does not seem to be sensitive to the shape of micelles. For the case of the bigger micelles, such as those obtained when electrolyte is added to anionic micelles or when the temperature of nonionic micelles is raised, the micelle sizes calculated using pyrene excimer are smaller than the literature values.

For nonionic micelles the solute pyrene seems to be solubilised in the more polar region of the micelles. The fluorescence lifetime of pyrene monomer in Teric G9A10 is shorter than that in SDS (Table 5.7). It is quite possible that pyrene solutes are solubilised in the ethylene oxide region of the nonionic micelles as indicated in Figure 4.3c. (Pyrene is quite soluble in triethylene glycol $(CH_2OCH_2.CH_2OH)_2$). Here again if the solute probe were solubilised in the ethylene oxide region the effective volume of the micelle would be quite different from that obtained assuming a spherical solubilising micelle. The probe will then predict a much smaller micelle, again underestimating the true micelle volume. The micelle sizes of the Teric 12A series with different ethylene oxide chain lengths given in Table 5.14, are also as a whole smaller than the literature values. However, the micelle size of nonionic surfactant solutions is quite dependent on the surfactant purity and the actual number of ethylene oxide units in the chain.

5.2 EXCIPLEX FORMATION IN SURFACTANT MICELLES

Weller [1967] found that the emission maximum of some arylamine-aromatic hydrocarbon exciplexes was red shifted by up to 4000 cm^{-1} if the solvent were changed from hexane to acetone. This red shift of the exciplex emission band in polar solvents has been shown to be quite general for exciplexes and is evidence of their dipolar nature. It is in this context that an investigation of the polarity dependence of the exciplex emission from within the micelles formed by various surfactants has been undertaken. After an exciplex has been formed in a polar solvent, a non-fluorescent solvated ion pair may be formed by the excited electron donor and acceptor pair. The significance of this process occurring in polar solvent is that the fluorescence of the exciplex is reduced, and in the limit many exciplexes do not fluoresce in polar solvents. There are, therefore, a limited number of exciplexes suitable for use as fluorescent probes to examine the polarity of the interior of micelles.

The exciplex formed by 1-cyanonaphthalene (donor) and naphthalene (acceptor) is suitable as such a fluorescent probe. The red shift of its fluorescence maximum has been measured in polar solvents [Selinger and McDonald 1972]. The exciplex emission has been observed with each surfactant used. The shift in the maximum of the exciplex emission, relative to the exciplex emission in cyclohexane, is as shown in Table 5.15.

This investigation has shown that the order of polarities of the fluorescence site for the three classes of surfactants is as follows:

nonionics > methanol > anionic > cationic.

Table 5.15

Shift in position of 1-cyanonaphthalene-naphthalene exciplex relative to cyclohexane.

Solvents	Micelle	Red Shift/cm^{-1}
Cyclohexane		0*
Ethyl propionate		710*
Methanol		1660*
SDS	anionic	1526
CDBA	cationic	1415
Teric LA8	nonionic	1852
Teric 12A23	nonionic	1852

* Selinger and McDonald [1972].

If the region of solubilisation in the nonionic micelles is the ethylene oxide region (indicated in Figure 4.3c) then the high polarity of non-ionic micelles, as shown by the exciplex probe, would be explained.

5.3 FLUORESCENCE QUENCHING IN SURFACTANT MICELLES

In recent years there has been an expanding interest in the study of surfactant micelles using the fluorescence quenching techniques. Hautala, Schore and Turro [1973] used the variation in the fluorescence lifetime of naphthalene upon addition of quenchers to explore the distribution of naphthalene in aqueous solutions of ionic surfactants. They concluded that the fluorescence quenching of naphthalene in cationic micelles by Br^- ions was due to the electrostatic attraction between the cations of the micelles and the Br^- ions. More recently, Chen, Grätzel and Thomas [1974] measured the quenching rate by I^- ions of pyrene in micelles. They analysed their results in terms of the rate

of entry of quencher into the micelles. In addition, they studied mixed micelles formed between sodium taurocholate (TCHA, $RCONH(CH_2)SO_3^-Na^+$) and sodium dodecyl sulphate (SDS) using pyrene as a fluorescent probe. From the results of their experiments using triethylamine and I^- ions as quenchers, they suggested that the separation of the negative polar groups in the TCHA micelles was larger than in SDS micelles, because the rate of entry of I^- ions increased with TCHA concentration. From the slower entry rate of triethylamine they were able to predict the viscosity of the mixed micelles formed at different concentrations of TCHA.

In the present work, the quenching effects of metal ions and neutral quenchers on the fluorescence of hydrocarbon molecules in micelles have been examined and the influence of the charge of a micelle has also been investigated.

5.3.1 Effect of Electrostatic Charge on Fluorescence Quenching

The extent of fluorescence quenching by added quenchers has been studied using Stern-Volmer plots. The parameter C_h, the concentration of quencher which halves the intensity of fluorescence from the primarily excited molecules, is used as a measure of the extent of fluorescence quenching.

The different values of C_h obtained from the Stern-Volmer plots for excited naphthalene when quenched by Mn^{2+} and Co^{2+}, are shown in Table 5.16. The lower C_h values in anionic micelles (SDS) indicate that the electrostatic attraction force between the positive ions of the quenchers and the negative ions of SDS micelles facilitate the quenching of excited naphthalene inside the micelles.

Table 5.16

Quenching of 10^{-4} mol l^{-1} naphthalene fluorescence by metal ions.

Quencher	Solvent/Micelle	C_h/mol l^{-2}
$MnCl_2$	Water	6.60×10^{-2}
$MnCl_2$	SDS (anionic)	2.45×10^{-3}
$CoCl_2$	Water	3.50×10^{-2}
$CoCl_2$	SDS (anionic)	1.31×10^{-3}

The influence of the charged micelles upon quenching efficiency has also been demonstrated by the Mn^{2+} ion quenching of pyrene fluorescence in different micelles. The results are presented in Table 5.17. The high C_h value for the cationic micelle is due to the repulsion between the ions of opposite charge. The Stern-Volmer plot for pyrene quenched by Mn^{2+} ions is given in Figure 5.17.

Table 5.17

Quenching of 10^{-5} mol l^{-1} pyrene fluorescence in different solvents by Mn^{2+} ions.

Solvent/Micelle	Lifetime of Pyrene/ns	C_h/mol l^{-1}
SDS (anionic)	388	5.1×10^{-4}
Water	207	8.8×10^{-3}
CDBA (cationic)		~ 1.35

5.3.2 Selective Fluorescence Quenching

Selective fluorescence quenching is the technique developed in the course of the present work, in which the location of fluorescent

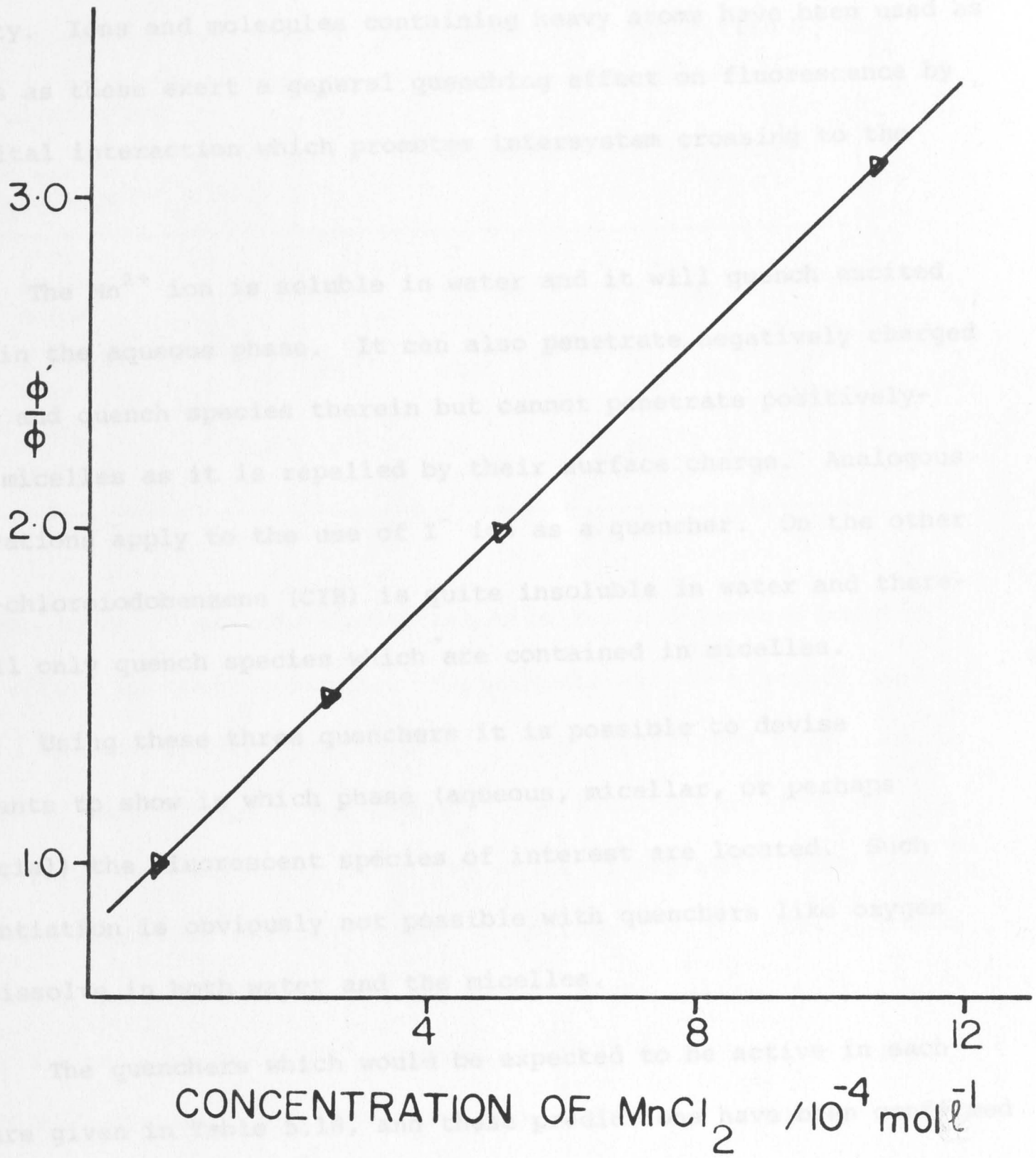

Figure 5.17. Stern-Volmer plot for quenching of 10^{-5} mol ℓ^{-1} pyrene in 0.05 mol ℓ^{-1} SDS by Mn^{2+}.

species is deduced by means of quenchers of the appropriate charge and solubility. Ions and molecules containing heavy atoms have been used as quenchers as these exert a general quenching effect on fluorescence by spin-orbital interaction which promotes intersystem crossing to the triplet.

The Mn^{2+} ion is soluble in water and it will quench excited species in the aqueous phase. It can also penetrate negatively charged micelles and quench species therein but cannot penetrate positively-charged micelles as it is repelled by their surface charge. Analogous considerations apply to the use of I^- ion as a quencher. On the other hand, p-chloroiodobenzene (CIB) is quite insoluble in water and therefore will only quench species which are contained in micelles.

Using these three quenchers it is possible to devise experiments to show in which phase (aqueous, micellar, or perhaps interfacial) the fluorescent species of interest are located. Such differentiation is obviously not possible with quenchers like oxygen which dissolve in both water and the micelles.

The quenchers which would be expected to be active in each phase are given in Table 5.18, and these predictions have been confirmed using pyrene in surfactant solutions and naphthalene in water. The effectiveness of the quenchers is measured by the mean quenching concentration C_h. The value of C_h for Mn^{2+} quencher of the fluorescence of pyrene monomer in anionic surfactant (SDS) is 5.1×10^{-4}, in water it is 8.8×10^{-3} and in cationic surfactant CDBA it is about 1.35 (ineffective) (Table 5.17). For naphthalene, with its shorter lifetime, the values of C_h are higher than for pyrene (Table 5.16). Thus cation quenchers are present in higher concentration in the double layer and

Table 5.18

Effectiveness of quenchers in each phase of a surfactant system.

Quench Territory \ Surfactant	Anionic	Cationic	Nonionic
Aqueous phase	I^- Mn^{2+}	I^- Mn^{2+}	I^- Mn^{2+}
Micellar interior	CIB Mn^{2+}	CIB I^-	CIB Mn^{2+} I^-
Both phases	Mn^{2+}	I^-	Mn^{2+} I^-

Gouy-Chapman layer of anionic surfactant micelles and exert a boosted quenching effect on their contents. Experiments with 2-naphthol also show that a charged species does not exert any significant effect on an excited ion of like charge. For example, the fluorescence from an aqueous solution of 2-naphthol at pH 5-6 shows fluorescence from both ROH^* and RO^{-*} (detailed studies follow in Section 5.4.3). The addition of I^- causes a uniform decrease in the fluorescence intensity from both species as I^- quenches only ROH^*, from which RO^{-*} is formed, and does not quench RO^{-*} directly. On the other hand with Mn^{2+} as quencher there is a greater decrease of RO^{-*} intensity than of the ROH^* intensity because the RO^{-*} emission is quenched directly, in addition to the diminution due to quenching of ROH^* (Figure 5.18).

5.4 PROTOLYTIC REACTIONS IN SURFACTANT MICELLES

Weller [1952] made quantitative studies of the acid-base reactions of naphthols. He established their pK and pK^* values at different temperatures. Tong and Glesman [1957] examined the

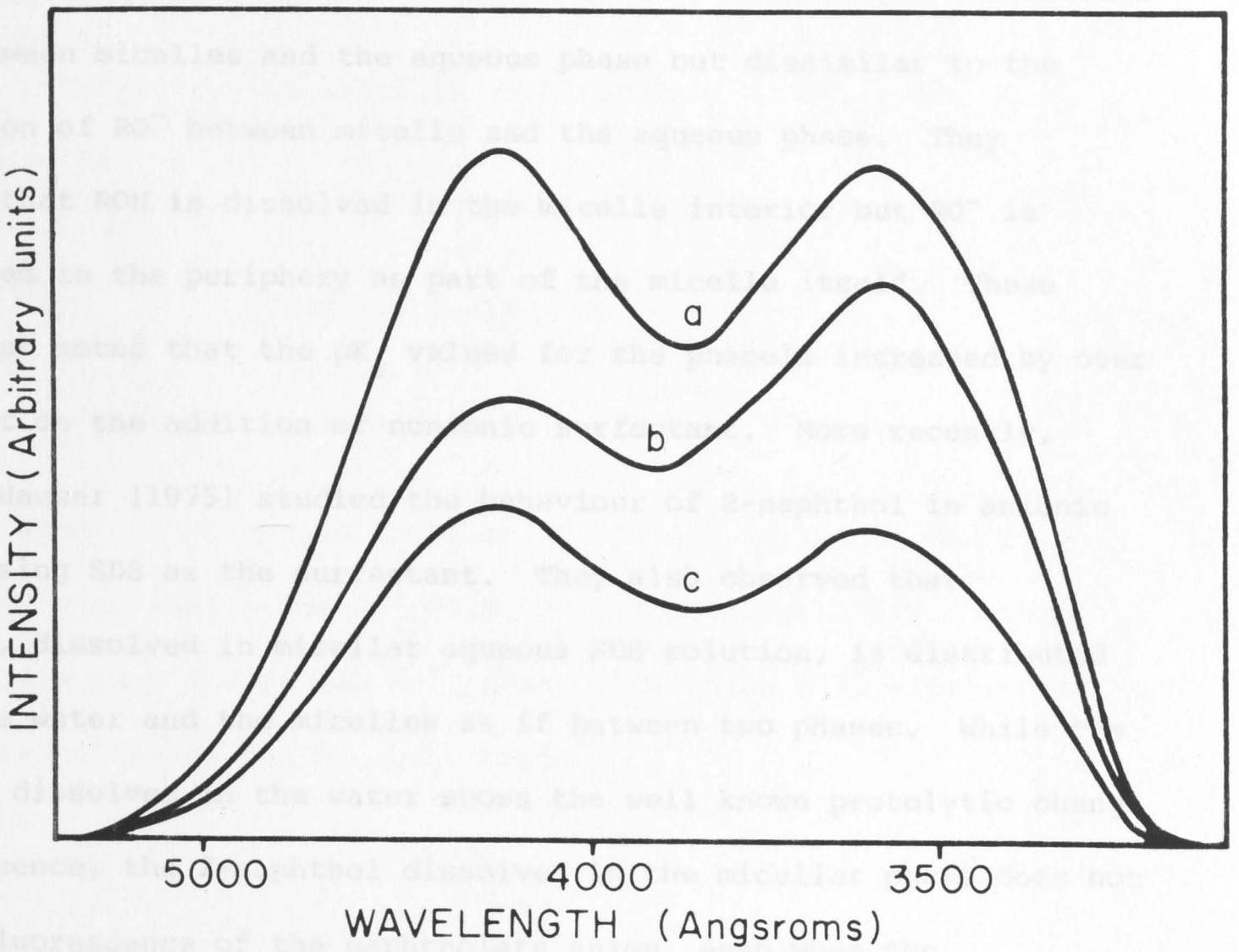

Figure 5.18. Uncorrected fluorescence spectra of 1.5×10^{-4} mol l^{-1} 2-naphthol in water:

(a) alone at pH 6;

(b) with addition of 0.26 mol l^{-1} of $MnCl_2$;

(c) with addition of 0.05 mol l^{-1} of NaI.

interaction of a number of phenols including 1-naphthol with the non-ionic surfactant Triton X100 at different pH and constant ionic strength. They determined the distribution coefficient of ROH between water and n-octanol and showed that it was similar to the distribution coefficient of ROH between micelles and the aqueous phase but dissimilar to the distribution of RO^- between micelle and the aqueous phase. They concluded that ROH is dissolved in the micelle interior but RO^- is incorporated in the periphery as part of the micelle itself. These workers also noted that the pK_a values for the phenols increased by over one pH unit on the addition of nonionic surfactant. More recently, Klein and Hauser [1975] studied the behaviour of 2-naphthol in anionic micelles using SDS as the surfactant. They also observed that 2-naphthol, dissolved in micellar aqueous SDS solution, is distributed between the water and the micelles as if between two phases. While the 2-naphthol dissolved in the water shows the well known protolytic change in fluorescence, the 2-naphthol dissolved in the micellar phase does not show the fluorescence of the naphtholate anion, even when the surrounding water is basic.

2-Naphthol has a pK_a (in water) of 9.49, but in the first excited singlet state the pK_a^* drops to 2.8 [Weller 1952]. It is a much stronger acid in the excited state. The equilibrium is however not completely established during the lifetime of the electronically excited state. Klein *et al.* [1975] have observed that in the presence of anionic surfactant micelles it is not established at all.

Excited state protolytic reactions have been studied because the distribution of solutes across the micellar interface could be a model for ion transport across biological membranes in that the micellar

system is virtually two phases separated (in the case of ionic surfactants) by a charged interface.

5.4.1 The Decay of 2-Naphthol Fluorescence

The protolytic reaction of 2-naphthol in water can be represented as

$$ROH + H_2O \underset{\overleftarrow{k}}{\overset{\vec{k}}{\rightleftharpoons}} RO^- + H_3O^+$$

The pK_a value in the ground state at 25 °C is 9.49 and in the first excited singlet state, the pK_a^* drops to 2.82 [Weller 1952]. At an intermediate pH value of say 5-7, after excitation ROH^* will attempt to dissociate according to the equilibrium:

$$ROH^* + H_2O \underset{\overleftarrow{k}}{\overset{\vec{k}}{\rightleftharpoons}} RO^{-*} + H_3O^+$$

After excitation, the fluorescence of both ROH^* and RO^{-*} will occur according to the following reaction scheme:

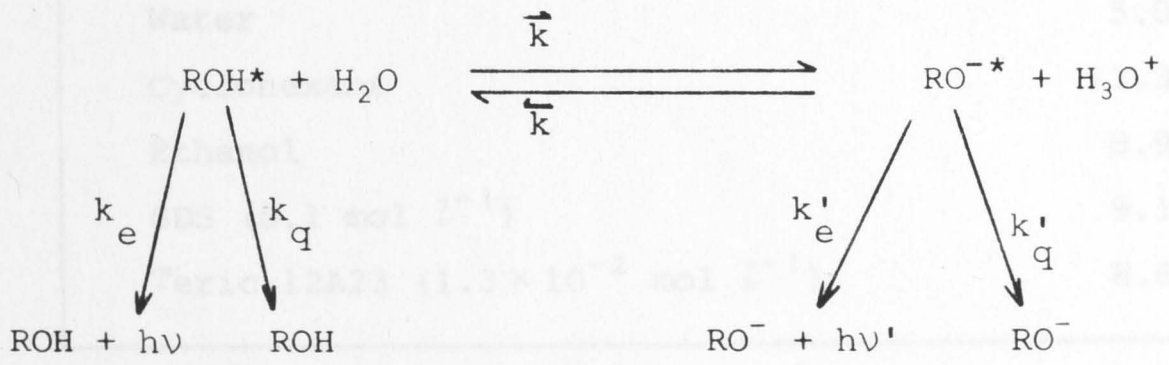

where k_e and k'_e are radiative rate constants and k_q and k'_q are

non-radiative rate constants.

The fluorescence spectrum of 2-naphthol in water at pH 6 is shown in Figure 5.19. The fluorescence of ROH^* occurs to the short wavelength side and RO^{-*} to the long wavelength side of the spectrum. This fluorescence spectrum has been obtained by exciting ROH in the ground state. As RO^{-*} fluorescence is emission from a species formed indirectly according to the above reaction scheme, the decay of RO^{-*} fluorescence requires an interval of time to build up to a maximum before it starts to decay. However, as ROH^* has been excited directly from the ground state, the fluorescence decay of ROH^* shows no time delay. The fluorescence decay curves of the two species are given in Figure 5.20. The fluorescence lifetimes of 2-naphthol (as ROH) in different solvents are given in Table 5.19 and the fluorescence decay parameters of 2-naphtholate anion (RO^-) in water and in Teric 12A23 are given in Table 5.20. At higher pH values only the RO^- species is present in the ground state, and after excitation only RO^{-*} fluorescence is observed, according to the reaction scheme:

Table 5.19

Fluorescence lifetimes of 2-naphthol in different solvents.

Solvent	Lifetime, τ/ns
Water	5.0
Cyclohexane	13.3*
Ethanol	8.9*
SDS (0.1 mol l^{-1})	9.1
Teric 12A23 (1.3×10^{-2} mol l^{-1})	8.6

* Berlman [1971].

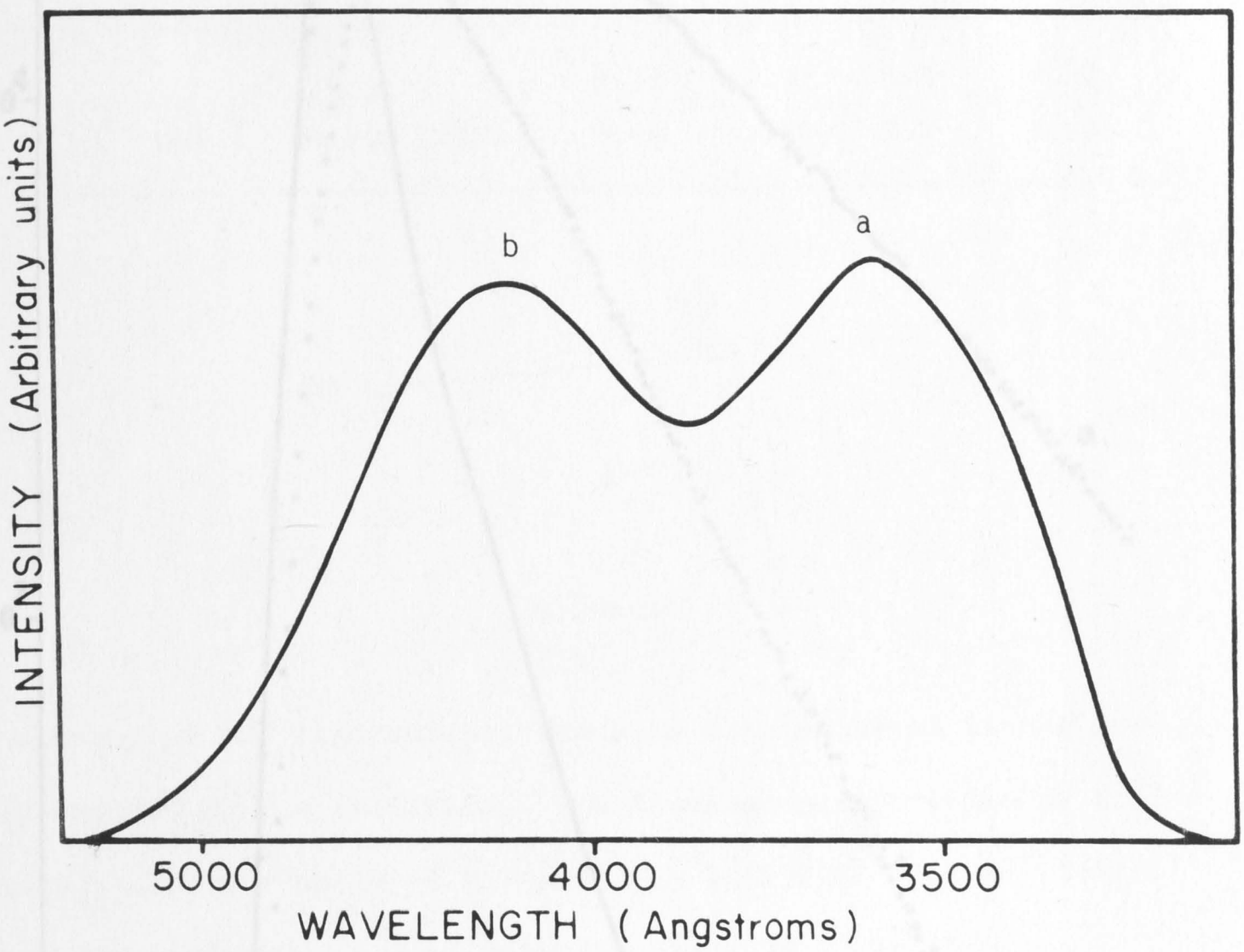

Figure 5.19. Uncorrected fluorescence spectrum of 1.5×10^{-4} mol l^{-1} 2-naphthol in water at pH 6 (room temperature). Excitation at 316 nm.

(a) ROH^* emission.

(b) RO^{-*} emission.

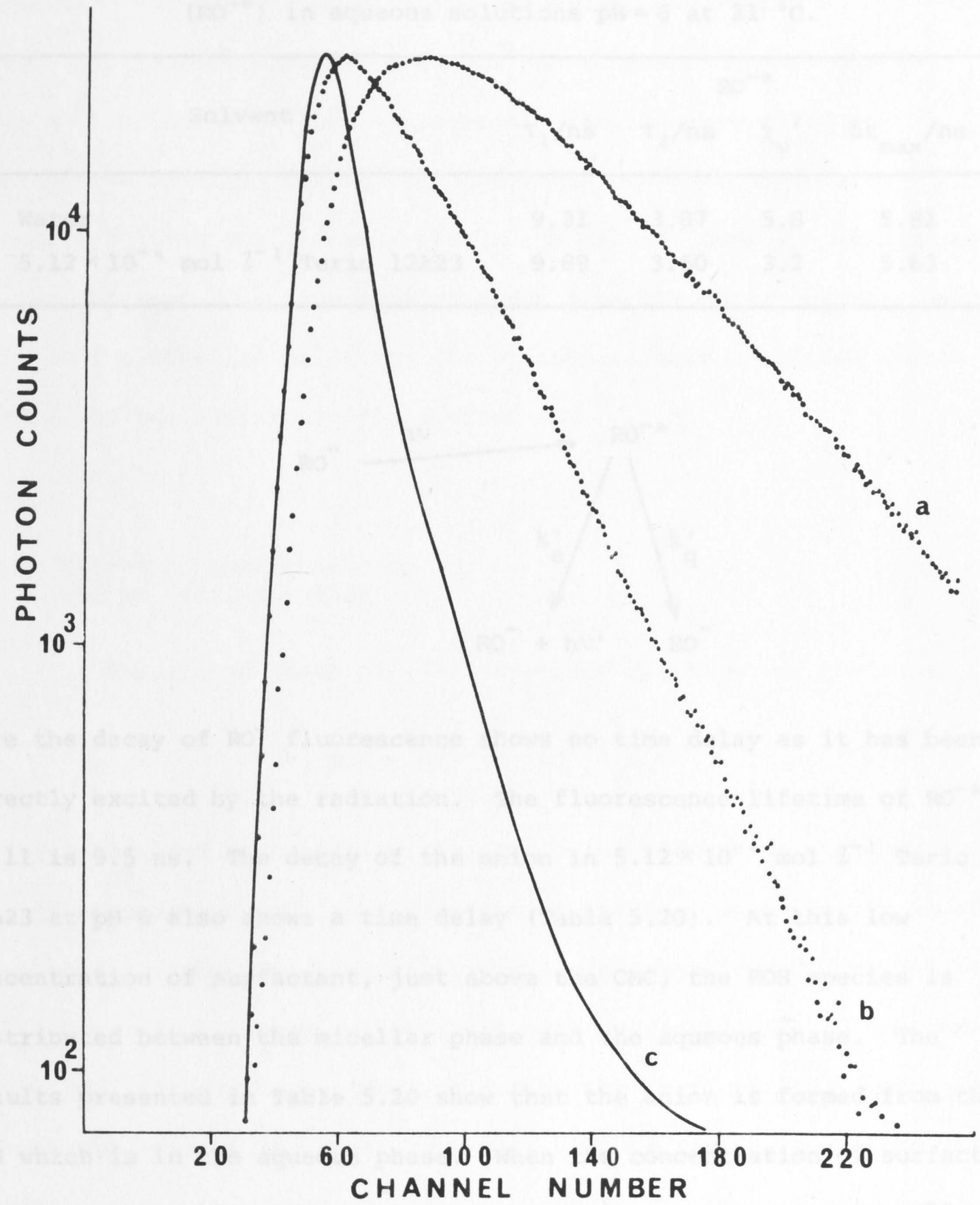

Figure 5.20. Fluorescence decay of 2-naphthol in water at pH 6. Excitation at 316 nm (2 nm band pass). (a) decay curve of RO^{-*} (observed at 450 nm); (b) decay curve of ROH^{*} (observed at 350 nm); (c) decay curve of the air flash lamp. The time scale is 0.21 ns per channel.

Table 5.20

The fluorescence decay parameters of 2-naphtholate anion (RO^{-*}) in aqueous solutions pH = 6 at 21 °C.

Solvent	RO^{-*} τ_1/ns	τ_2/ns	χ_ν^2	Δt_{max}/ns
Water	9.31	3.87	5.8	5.81
5.12×10^{-4} mol l^{-1} Teric 12A23	9.89	3.50	3.2	5.63

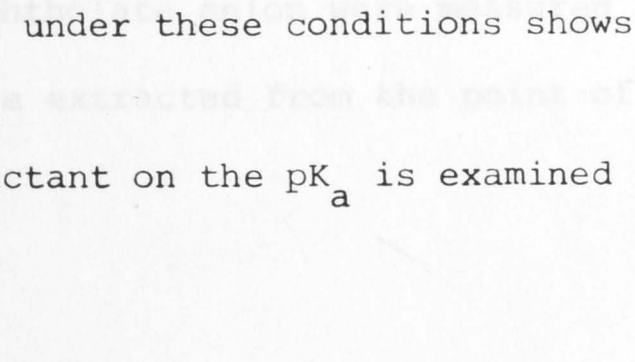

Here the decay of RO^- fluorescence shows no time delay as it has been directly excited by the radiation. The fluorescence lifetime of RO^{-*} at pH 11 is 9.5 ns. The decay of the anion in 5.12×10^{-4} mol l^{-1} Teric 12A23 at pH 6 also shows a time delay (Table 5.20). At this low concentration of surfactant, just above the CMC, the ROH species is distributed between the micellar phase and the aqueous phase. The results presented in Table 5.20 show that the anion is formed from the ROH which is in the aqueous phase. When the concentration of surfactant is increased all the ROH is solubilised in the micelles and no RO^{-*} fluorescence is detected. However, the RO^{-*} fluorescence can be observed by setting the pH of the solution approximately equal to the pK_a of the solute in the particular surfactant used.† The fluorescence decay of RO^{-*} observed under these conditions shows no time delay. For

† The effect of surfactant on the pK_a is examined in Section 5.4.2.

example, the fluorescence decay is shown in Figure 5.21. A single exponential was convoluted with the lamp pulse and fitted to the decay curve. The fluorescence decay of ROH^* under these conditions also shows no time delay. These experimental results show that the fluorescence emission of the acid and anion are photophysically unconnected. The ROH^*, formed within the micelle does not dissociate and the observed RO^{-*} fluorescence comes from the direct excitation of RO^-. In the micellar solutions the dissociation is inhibited within the lifetime of the electronically excited ROH.

5.4.2 Effect of Surfactants on the pK_a of 2-Naphthol

The ground state pK_a for acid-base reactions of the type:

$$ROH + OH^- \rightleftharpoons RO^- + H_2O$$

can be determined by measuring the absorption spectra as a function of pH. pH measurements are an indication of the OH^- concentration in the above equilibrium. For 2-naphthol, as can be seen from Figure 3.6, the RO^{-*} fluorescence intensity increases with increasing pH, at the expense of the ROH^* fluorescence. This is due to the shift of the ground state equilibrium towards the right. In this high pH region, therefore, it is possible to determine the pK_a of the 2-naphthol acid-base reaction by fluorescence spectroscopy. The effect of surfactants on the ground state pK_a of the 2-naphthol reaction was studied by absorption and fluorescence techniques. The absorbances and the fluorescence intensities of the naphtholate anion were measured as a function of pH and the pK_a values were extracted from the point of inflexion of the titration curves.

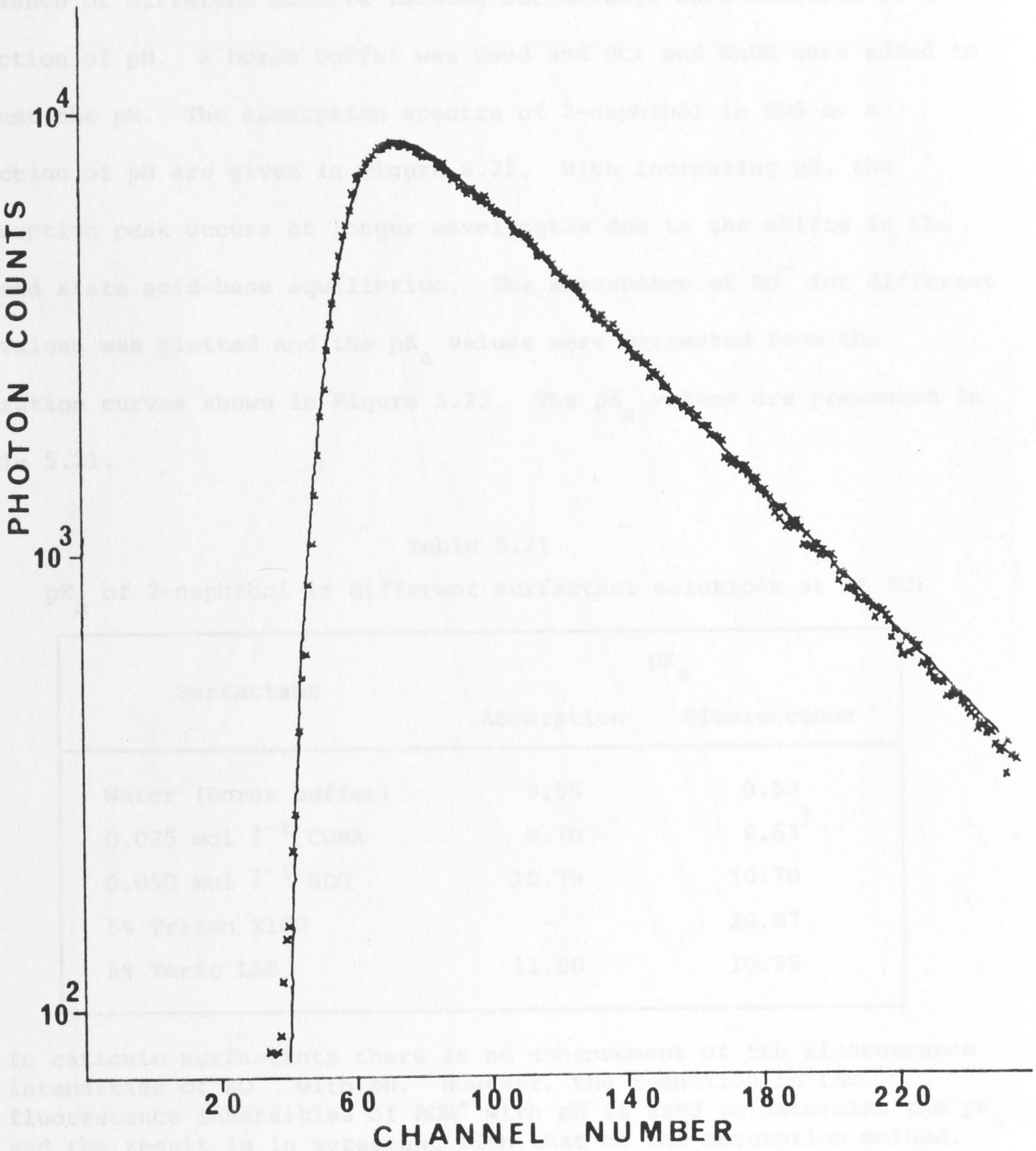

Figure 5.21. Fluorescence decay of 2-naphtholate anion in 0.1 mol l^{-1} SDS at pH = 10.6 at 21 °C. (———) the resultant fitted to the experimental data (x) after convolution.

τ = 10 ns; χ_{ν}^{2} = 3.08.

The absorption spectra of 2-naphthol in water and in the presence of different micelle forming surfactants were measured as a function of pH. A borax buffer was used and HCl and NaOH were added to adjust the pH. The absorption spectra of 2-naphthol in SDS as a function of pH are given in Figure 5.22. With increasing pH, the absorption peak occurs at longer wavelengths due to the shifts in the ground state acid-base equilibrium. The absorbance of RO^- for different pH values was plotted and the pK_a values were extracted from the titration curves shown in Figure 5.23. The pK_a values are presented in Table 5.21.

Table 5.21

pK_a of 2-naphthol in different surfactant solutions at 21 °C.

Surfactant	pK_a	
	Absorption	Fluorescence
Water (Borax buffer)	9.55	9.50
0.025 mol l^{-1} CDBA	8.70	8.63†
0.050 mol l^{-1} SDS	10.70	10.70
5% Triton X100	-	10.97
5% Teric LA8	11.00	10.95

† In cationic surfactants there is no enhancement of the fluorescence intensities of RO^{-*} with pH. However, the reduction in the fluorescence intensities of ROH^* with pH is used to determine the pK_a and the result is in agreement with that of the absorption method.

The fluorescence spectrum of 2-naphthol in water and in the presence of different surfactants was also measured as a function of pH. The fluorescence spectrum of 2-naphthol in Triton X100 for different pH values is given in Figure 5.24. The fluorescence intensities of RO^{-*} at 430 nm were plotted against pH (Figure 5.25) and the pK_a values obtained using this method are also given in Table 5.21.

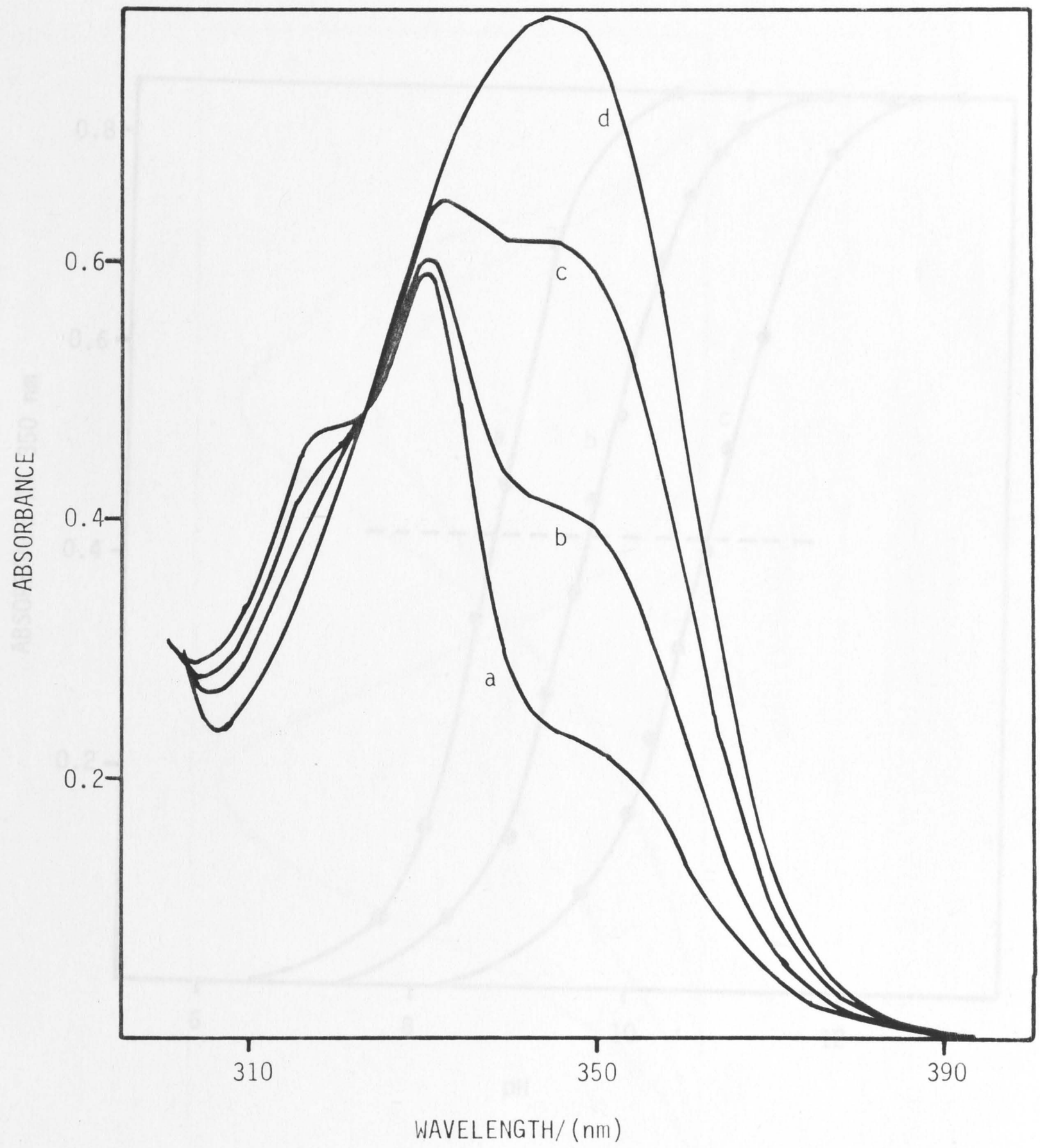

Figure 5.22. Absorption spectra in 1.5×10^{-4} mol l^{-1} 2-naphthol in 0.05 mol l^{-1} SDS at 21 °C.

(a) pH = 10.2; (b) pH = 10.7; (c) pH = 11.2; (d) pH = 11.8.

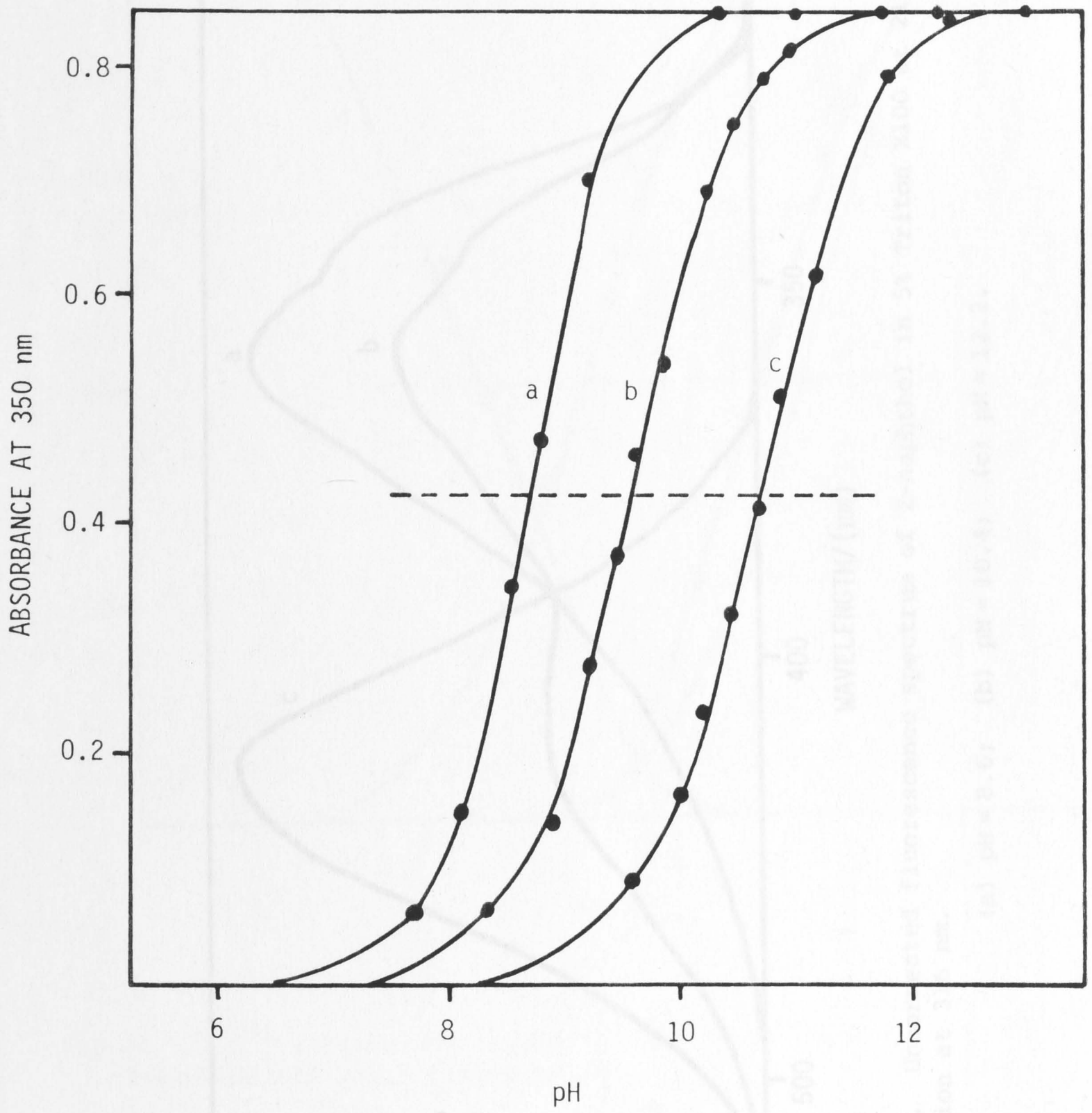

Figure 5.23. Absorbance of 2-naphtholate anion versus pH in:

(a) 0.025 mol l^{-1} CDBA;

(b) Water;

(c) 0.05 mol l^{-1} SDS.

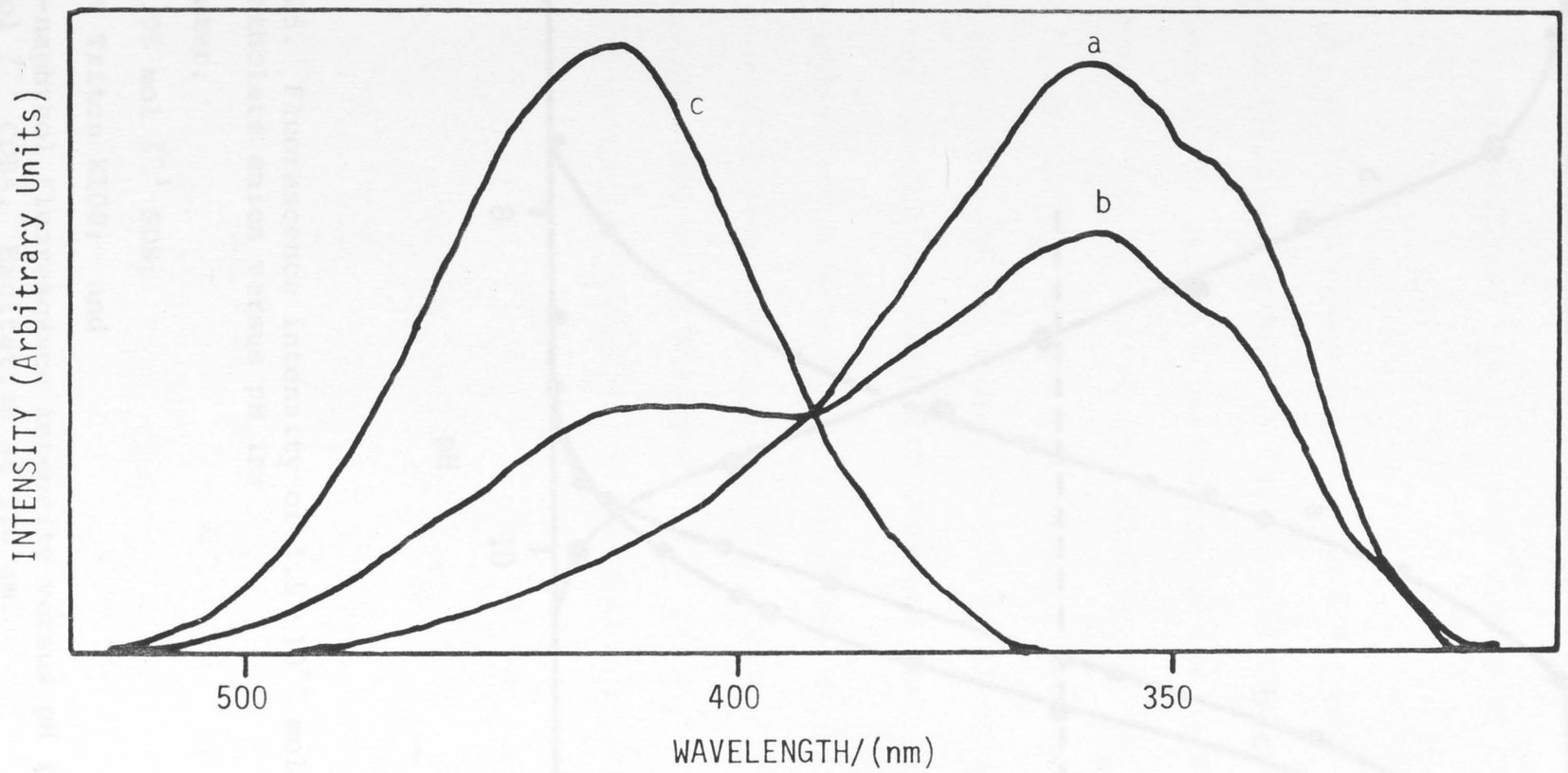

Figure 5.24. Uncorrected fluorescence spectrum of 2-naphthol in 5% Triton X100 at 21 °C. Excitation at 316 nm.

(a) pH = 8.6; (b) pH = 10.4; (c) pH = 12.2.

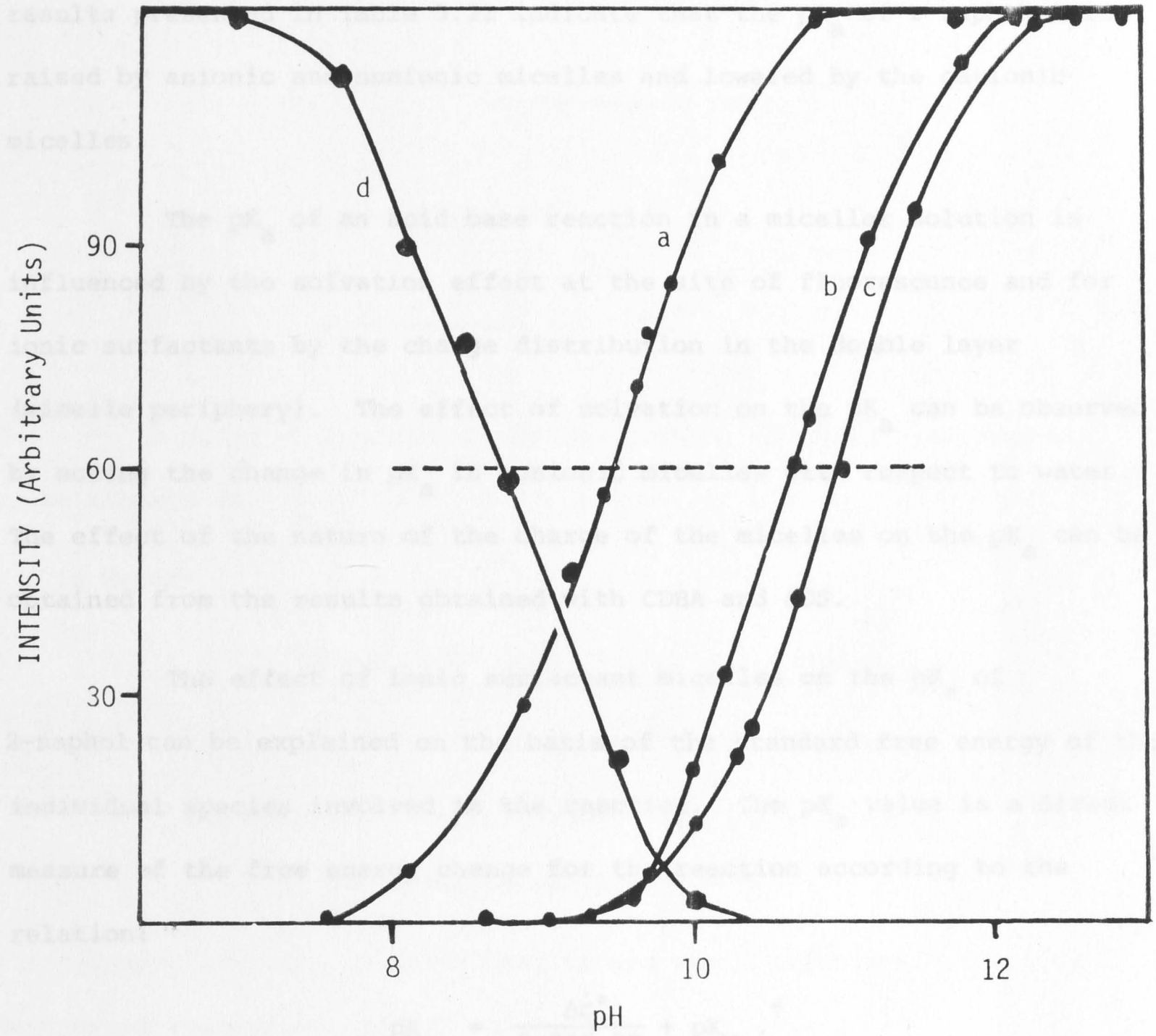

Figure 5.25. Fluorescence intensity of 1.5×10^{-4} mol ℓ^{-1} 2-naphtholate anion versus pH in:

(a) water;

(b) 0.05 mol ℓ^{-1} SDS;

(c) 5% Triton X100; and

(d) 2-naphthol fluorescence intensity versus pH in 0.025 mol ℓ^{-1} CDBA. Excitation at 316 nm.

I_{RO^-*} observed at 430 nm.

I_{ROH^*} observed at 350 nm.

The pK_a obtained by the absorption and the fluorescence techniques are in good agreement within the experimental error. The results presented in Table 5.21 indicate that the pK_a of 2-naphthol is raised by anionic and nonionic micelles and lowered by the cationic micelles.

The pK_a of an acid base reaction in a micellar solution is influenced by the solvation effect at the site of fluorescence and for ionic surfactants by the charge distribution in the double layer (micelle periphery). The effect of solvation on the pK_a can be observed by noting the change in pK_a in nonionic micelles with respect to water. The effect of the nature of the charge of the micelles on the pK_a can be obtained from the results obtained with CDBA and SDS.

The effect of ionic surfactant micelles on the pK_a of 2-naphol can be explained on the basis of the standard free energy of the individual species involved in the reaction. The pK_a value is a direct measure of the free energy change for the reaction according to the relation:

$$pK_a = \frac{\Delta G^\circ}{2.303\ RT} + pK_W \ .^{\dagger}$$

---

† For the reaction

$$ROH + OH^- \rightleftharpoons RO^- + H_2O$$

$$K' = \frac{[RO^-]}{[ROH][OH^-]}$$

$$K_a = \frac{[RO^-][H_3O^+]}{[ROH]}$$

$$\therefore \quad K' = \frac{K_a}{K_W} \ ,$$

where $K_W = [H_3O^+][OH^-] \approx 10^{-14}$.

ΔG° is the energy gap between the ground state energies of ROH and RO^- as illustrated below.

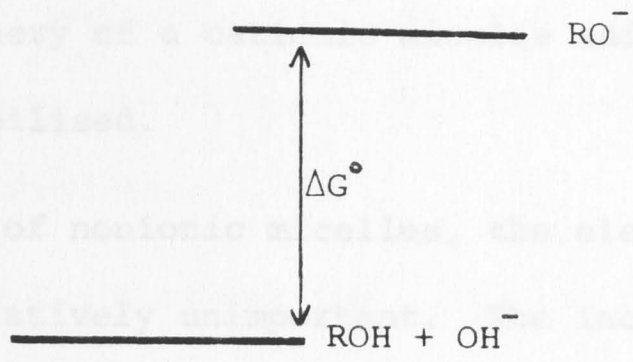

In order to explain the charge effect, the acid-base reaction may be assumed as:

In water:

$$ROH(aq) + OH^-(aq) \rightarrow RO^-(aq) + H_2O \ .$$

In micellar systems:

$$ROH \text{ (micelle interior)} + OH^- \text{ (micelle periphery)} \rightarrow RO^- \text{ (micelle periphery)} + H_2O \ .$$

Cationic micelles with positive head groups would effectively stabilise the charged species RO^- and OH^- so that

$$\Delta G^{\circ} \text{ (cationic micelles)} < \Delta G^{\circ} \text{ (water)} \ .$$

Anionic micelles with negative head groups would, on the other hand, destabilise the charged species so that

$$\Delta G^{\circ} \text{ (anionic micelles)} > \Delta G^{\circ} \text{ (water)} \ .$$

The essential difference is that it requires energy for an OH^- to

---

Using $\Delta G^{\circ} = - RT \ln K'$

then, $pK_a = \frac{\Delta G^{\circ}}{2.303\ RT} + pK_W \ .$

approach to the periphery of an SDS micelle and that RO^-, if it remains in the periphery of the micelle, is destabilised. Both effects are due to electrostatic interaction. It requires much less energy for an OH^- to approach the periphery of a cationic micelle and RO^- which remains in the periphery, is stabilised.

In the case of nonionic micelles, the electrostatic factors just mentioned are relatively unimportant. The increase measured in the pK_a may arise primarily from the difference in the environment of the solubilised species. The ROH molecules which are in the micelles would be stabilised more effectively than those in the aqueous phase so that

$$\Delta G \text{ (nonionic micelles)} > \Delta G \text{ (water)} .$$

Hence, the pK_a measured with a nonionic surfactant is higher than that measured in water. For ionic micelles this solvation effect is much smaller than the charge effect.

5.4.3 Distribution of Hydrophilic Solutes in Micelles

In the study of acid-base reaction in surfactant solutions it is important to know the solubilisation site of the species. The selective fluorescence quenching technique described in Section 5.3.2 is used to examine the distribution of 2-naphthol and 2-naphtholate anion in micellar aqueous systems.

5.4.4 Results and Discussion

At neutral pH in water 2-naphthol shows fluorescence from ROH^* and RO^{-*}. The addition of small amounts of anionic surfactant (just

above the CMC) causes a marked increase in the fluorescence intensity of ROH^*. This is because the anionic micelles raise the pK_a of those 2-naphthol molecules which are solubilised. It was under these conditions of a small number of micelles, when fluorescence from both solubilised and free solute is seen, that the selective quenching experiments were carried out.

The iodide ion quenches ROH^* emission from the aqueous phase (and also reduces RO^{-*} emission equally) leaving the ROH^* fluorescence from the micelles unaltered (Figure 5.26). CIB quenches the ROH^* emission from within the micelles but leaves unaltered the ROH^* (and RO^{-*}) emission from the aqueous phase. When the pH of the micellar solution is raised above the pK_a of the solute for a given surfactant, the 2-naphthol in the ground state is converted totally to the RO^- species and the fluorescence is totally that from RO^{-*}. We now find that CIB no longer exerts any quenching effect and so under these conditions no RO^- is present in the interior of the micelle.

In cationic micelles the pK_a of 2-naphthol is lowered to such an extent that in neutral solution some RO^- is already present in the ground state and hence is detected in fluorescence. Otherwise analogous arguments hold allowing for the change in sign of the micellar charge.

The addition of nonionic surfactant also causes a marked increase in the fluorescence intensity of ROH^*. The ROH^* fluorescence increases at the expense of RO^{-*} fluorescence as the concentration of the nonionic surfactant increases (Figure 5.27). In nonionic micelles the absence of a charged interface means that the only selective quenching experiment that can be carried out relies on the insolubility of CIB in water (Figure 5.28). CIB quenches ROH^* fluorescence in the

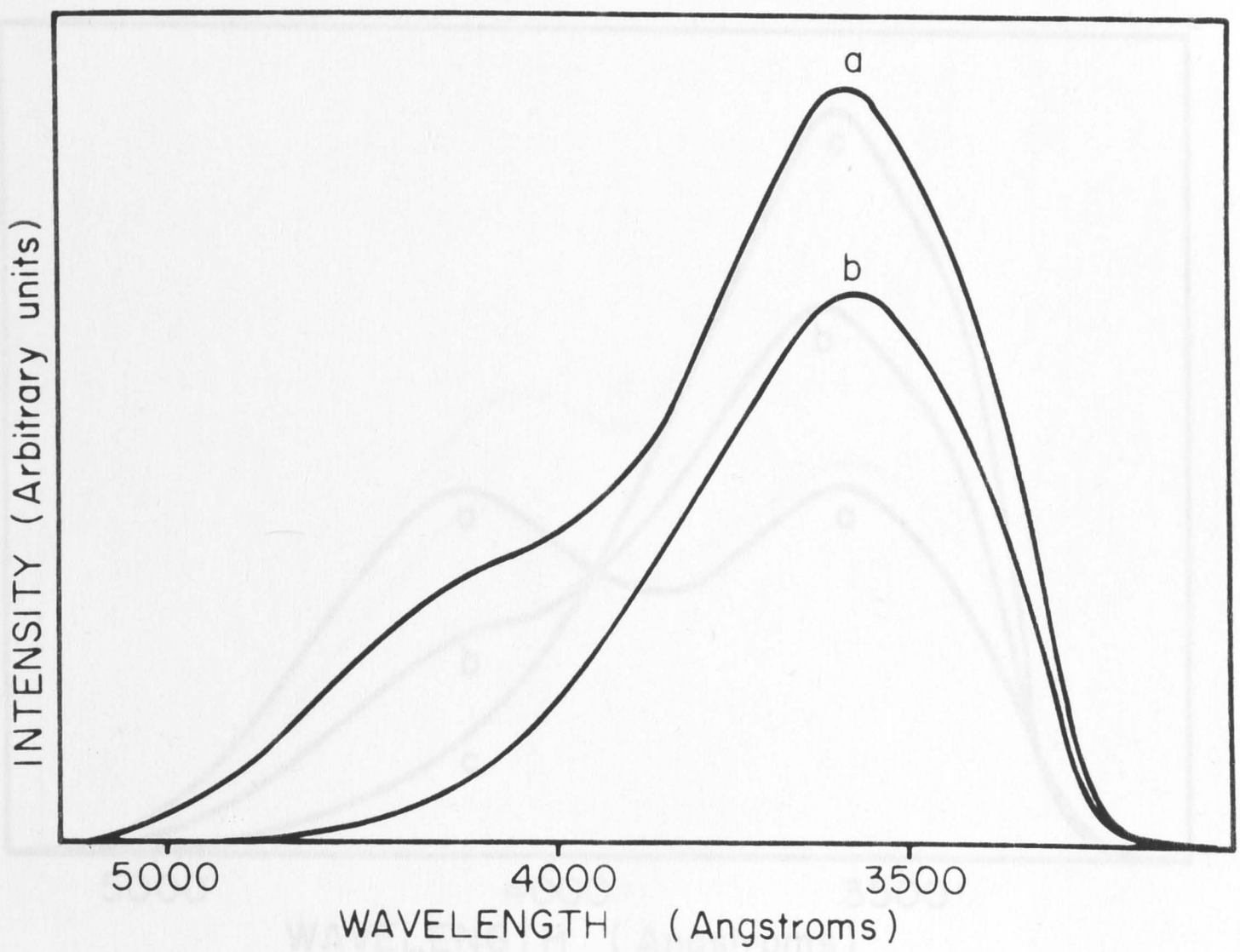

Figure 5.26. Uncorrected fluorescence spectra of 1.5×10^{-4} mol l^{-1} 2-naphthol in 1.0×10^{-2} mol l^{-1} SDS:

(a) alone;

(b) with addition of 0.4 mol l^{-1} of NaI.

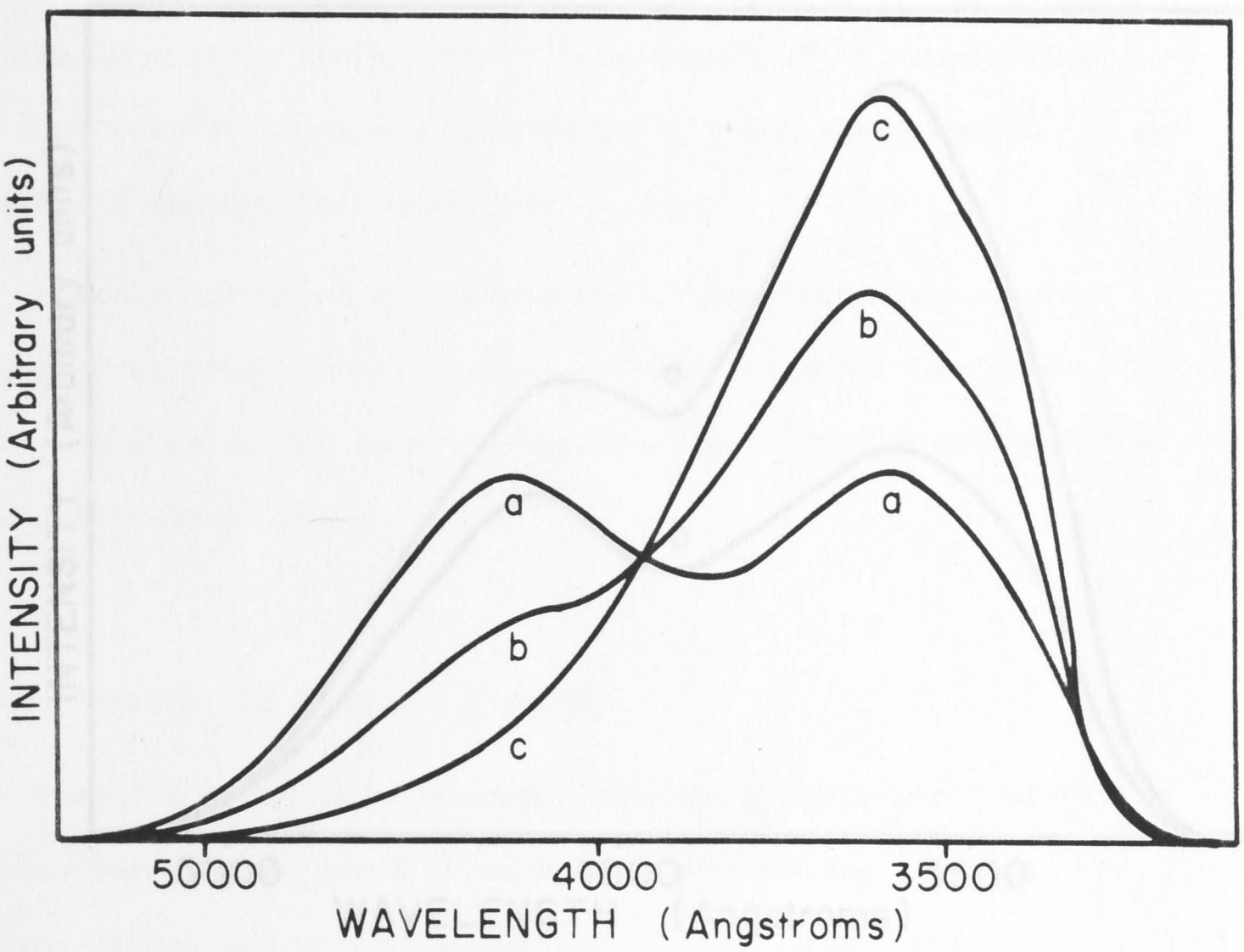

Figure 5.27. Uncorrected fluorescence spectra of 1.5×10^{-4} mol l^{-1} 2-naphthol in water:

(a) alone;

(b) with addition of 1.0×10^{-3} mol l^{-1} Teric 12A23;

(c) with addition of 2.56×10^{-2} mol l^{-1} Teric 12A23.

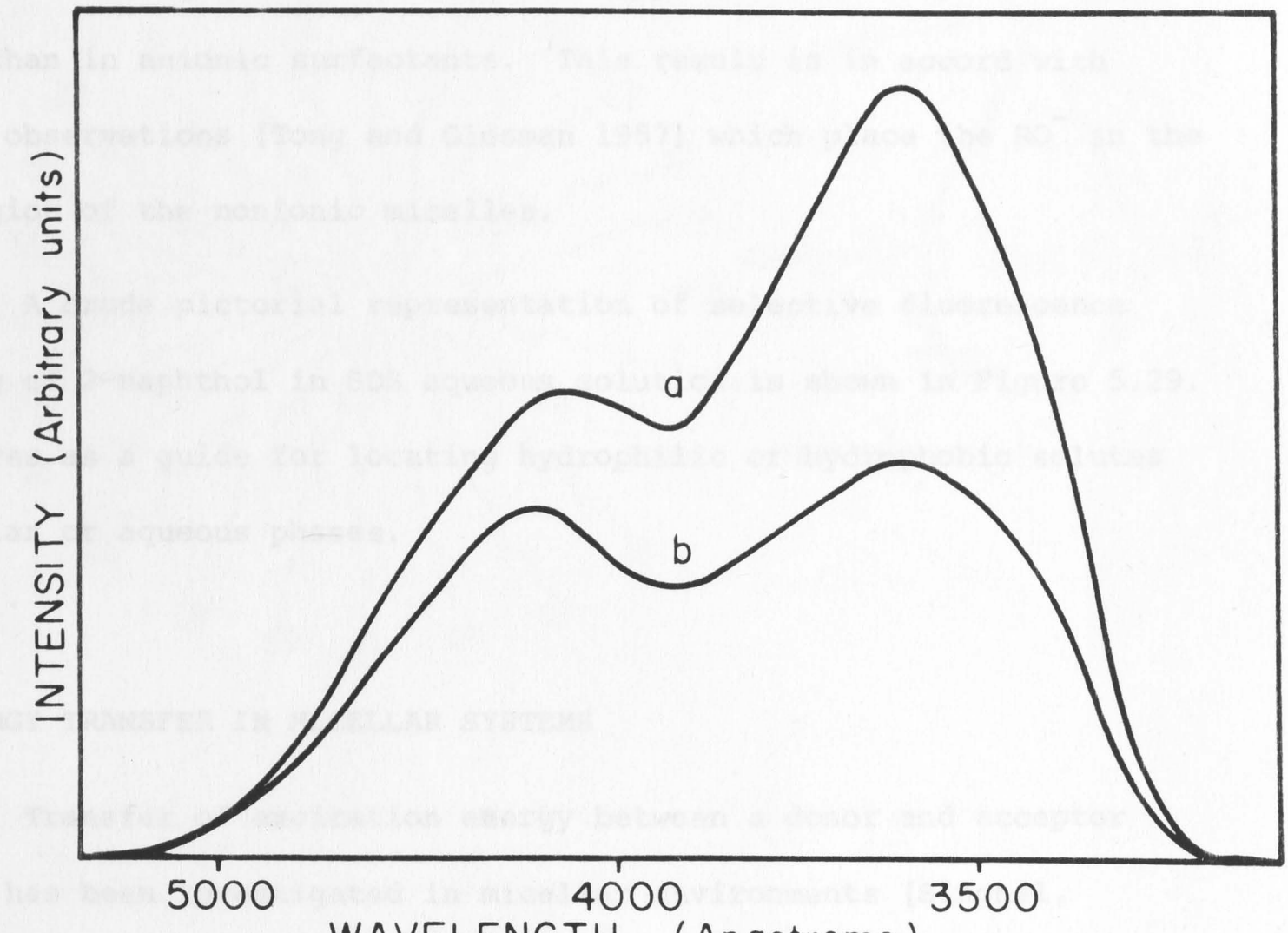

Figure 5.28. Uncorrected fluorescence spectra of 1.5×10^{-4} mol l^{-1} 2-naphthol in 5.12×10^{-4} mol l^{-1} Teric 12A23.

(a) alone;

(b) with addition of CIB.

interior of the micelles. At pH = 11 the fluorescence is totally RO^{-*} and CIB quenches some of the RO^{-*} fluorescence. This quenching effect shows that RO^{-*} fluorescence comes in part from a region of the micelle accessible to the quencher — so that RO^{-} appears to be deeper in the micelle than in anionic surfactants. This result is in accord with previous observations [Tong and Glesman 1957] which place the RO^{-} in the outer region of the nonionic micelles.

A crude pictorial representation of selective fluorescence quenching of 2-naphthol in SDS aqueous solution is shown in Figure 5.29. This serves as a guide for locating hydrophilic or hydrophobic solutes in micellar or aqueous phases.

5.5 ENERGY TRANSFER IN MICELLAR SYSTEMS

Transfer of excitation energy between a donor and acceptor molecule has been investigated in micellar environments [Singhal, Robinowitch, Hevesi and Srinivasan 1970; Almgren 1972; Shinitzky 1973; Wallace and Thomas 1973; Kenney-Wallace, Flint and Wallace 1975]. Locations of solutes in the micellar aqueous systems and information on micellar structures can be derived from investigations of energy transfer processes in micellar systems.

The transfer of excitation energy from thionine to methylene blue in micellar SDS has been reported [Singhal *et al.* 1970]. The extent of the energy transfer from thionine to methylene blue on the SDS surface decreases with increasing SDS concentration. This effect has been attributed to the decrease in the average number of dye molecules per micelle with increasing surfactant concentration at a given dye concentration. At the optimum transfer efficiency each micelle was

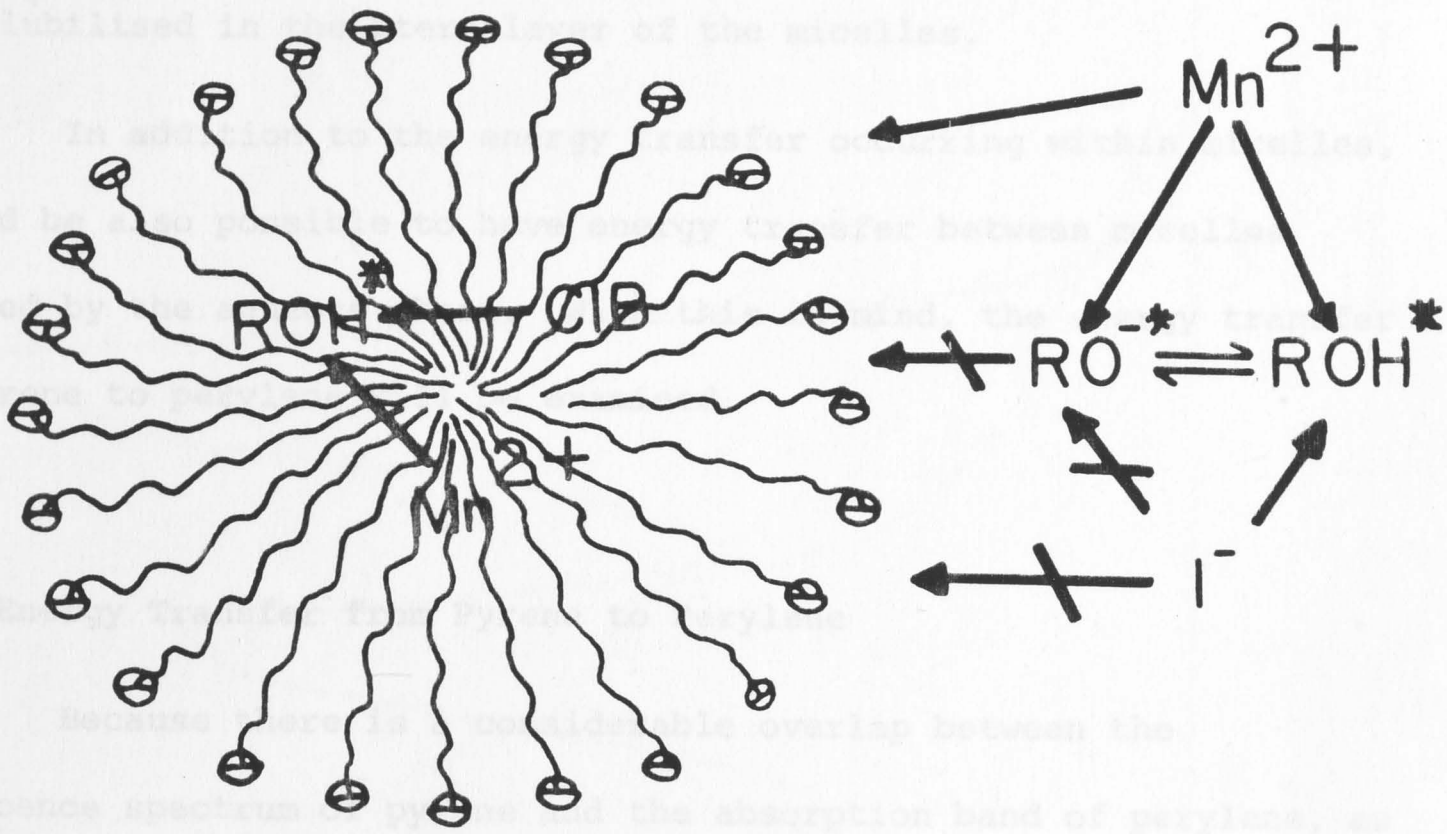

Figure 5.29. A crude representation of "selective fluorescence quenching". Fluorescence of 2-naphthol in SDS aqueous solution quenched by CIB, Mn^{2+} and I^-.

calculated to be associated with 10 - 14 dye molecules [Singhal *et al.* 1970].

Energy transfer from sodium phenyl undecanoate to naphthalene has been used to calculate the aggregation number and the CMC of the surfactant [Almgren 1972]. He reported the CMC and the aggregation number to be 9.1×10^{-3} mol l^{-1} and 75, respectively.

Energy transfer from pyrene to rhodamine 6G has been investigated using the laser photolysis technique [Kenney-Wallace *et al.* 1975]. From the fluorescence lifetime of a solution of pyrene in the presence of rhodamine 6G in SDS, the rate constant for energy transfer

was determined. From this result they calculated the distance between the donor and the acceptor molecules to be 28 Å. Assuming pyrene to be in the interior of the micelles they concluded that the dye molecules were solubilised in the Stern-layer of the micelles.

In addition to the energy transfer occurring within micelles, it would be also possible to have energy transfer between micelles separated by the aqueous phase. With this in mind, the energy transfer from pyrene to perylene will be examined.

5.5.1 Energy Transfer from Pyrene to Perylene

Because there is a considerable overlap between the fluorescence spectrum of pyrene and the absorption band of perylene, as shown in Figure 5.30, excitation energy transfer between these molecules can be expected. Excitation energy transfer from excited pyrene to ground state perylene occurs by means of the very weak dipole-dipole interaction mechanism [Mataga, Kobashi and Okada 1967]. Theoretical studies of energy transfer have been mainly developed by Förster and the mechanisms of energy transfer have been reviewed by him [Förster 1967]. In our study, these molecules are chosen because selective excitation of pyrene at 3371 Å is favoured by the minimum extinction coefficient of perylene at that wavelength (Figure 5.30). Pyrene and perylene are solubilised in the interior of the micelles and thus there is no complication by emission from the aqueous phase.

The concentrations of pyrene, perylene and the surfactant (Teric G9A10) are chosen such that the probability of having multiply occupied micelles is very low [7.2×10^{-5} mol l^{-1} pyrene 2×10^{-5} mol l^{-1} perylene in 0.4 mol l^{-1} Teric G9A10 the probability ($P \geqslant 2$) is very

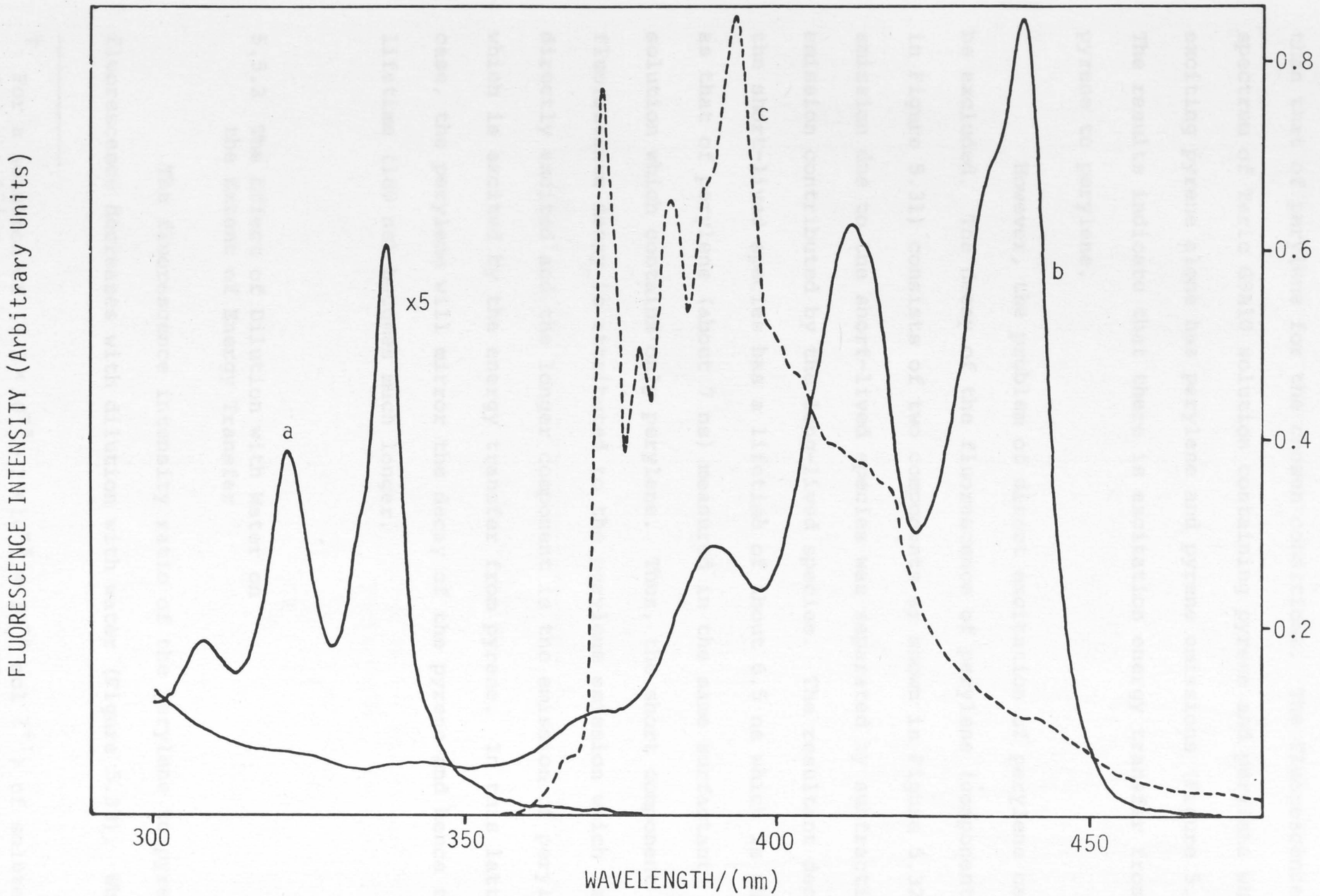

Figure 5.30. Absorption spectra of (a) pyrene; (b) perylene; and (c) fluorescence spectrum of pyrene in Teric G9A10.

low].† In this condition the micelles can be assumed to be singly occupied. The absorbance of pyrene at 3371 Å is a hundred-fold higher than that of perylene for the chosen conditions. The fluorescence spectrum of Teric G9A10 solution containing pyrene and perylene when exciting pyrene alone has perylene and pyrene emissions (Figure 5.31). The results indicate that there is excitation energy transfer from pyrene to perylene.

However, the problem of direct excitation of perylene can not be excluded. The decay of the fluorescence of perylene (component (b) in Figure 5.31) consists of two components as shown in Figure 5.32. The emission due to the short-lived species was separated by subtracting the emission contributed by the long-lived species. The resultant decay of the short-lived species has a lifetime of about 6.5 ns which is the same as that of perylene (about 7 ns) measured in the same surfactant solution which contains only perylene. Thus, the short component of the fluorescence decay is attributed to the perylene emission which is directly excited and the longer component is the emission of perylene which is excited by the energy transfer from pyrene. In this latter case, the perylene will mirror the decay of the pyrene and hence the lifetime (180 ns) becomes much longer.

5.5.2 The Effect of Dilution with Water on the Extent of Energy Transfer

The fluorescence intensity ratio of the perylene to pyrene fluorescence decreases with dilution with water (Figure 5.33). When the

---

† For a solution of $(7.2 \times 10^{-5} + 2 \times 10^{-5} \approx 10^{-4}$ mol $l^{-1})$ of solutes in 0.4 mol l^{-1} Teric G9A10 (aggregation number 50), average molecule per micelle is 0.0125. Using Poisson distribution, P $(\geqslant 2) \cong 0$.

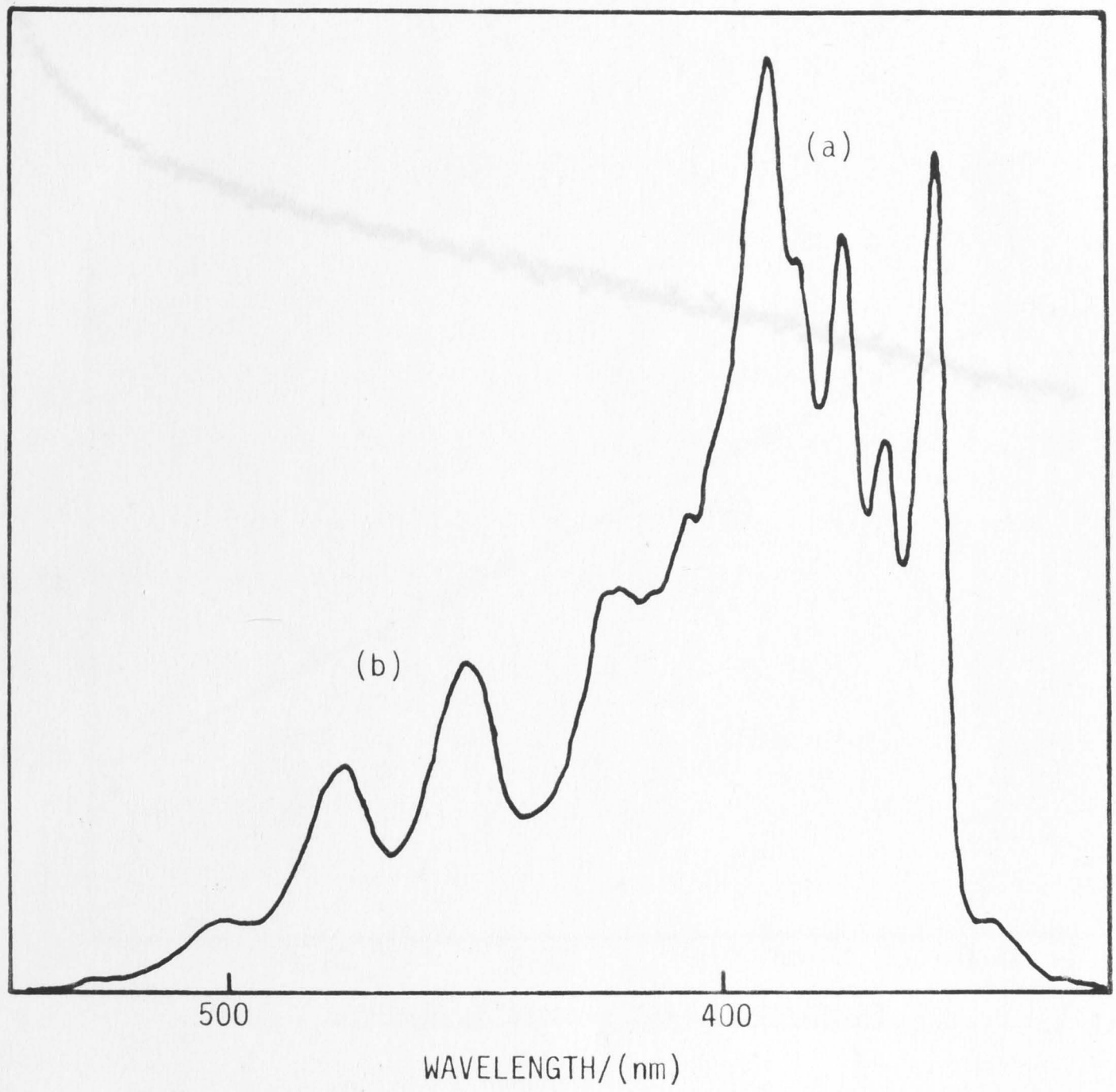

Figure 5.31. Fluorescence spectrum of (a) pyrene and (b) perylene in 0.4 mol l^{-1} Teric G9A10. Excitation at 337 nm.

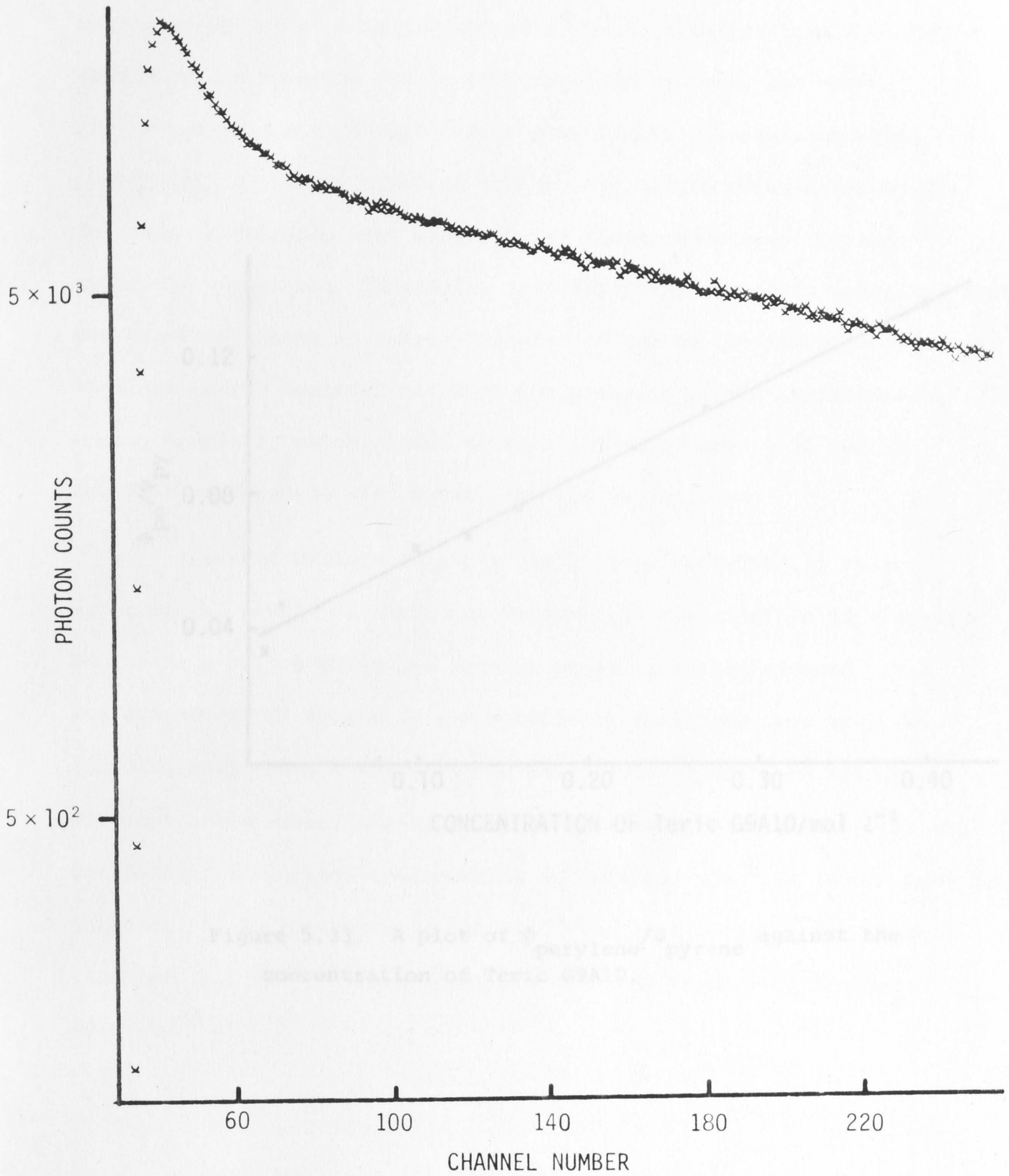

Figure 5.32. The decay of perylene fluorescence in a surfactant solution of 0.4 mol l^{-1} Teric G9A10 containing 7×10^{-5} mol l^{-1} pyrene and 2×10^{-5} mol l^{-1} perylene. The time scale is 0.8 ns/channel. Excitation at 337 nm (2 nm band pass). The emission was observed at 500 nm with a 10 nm band pass.

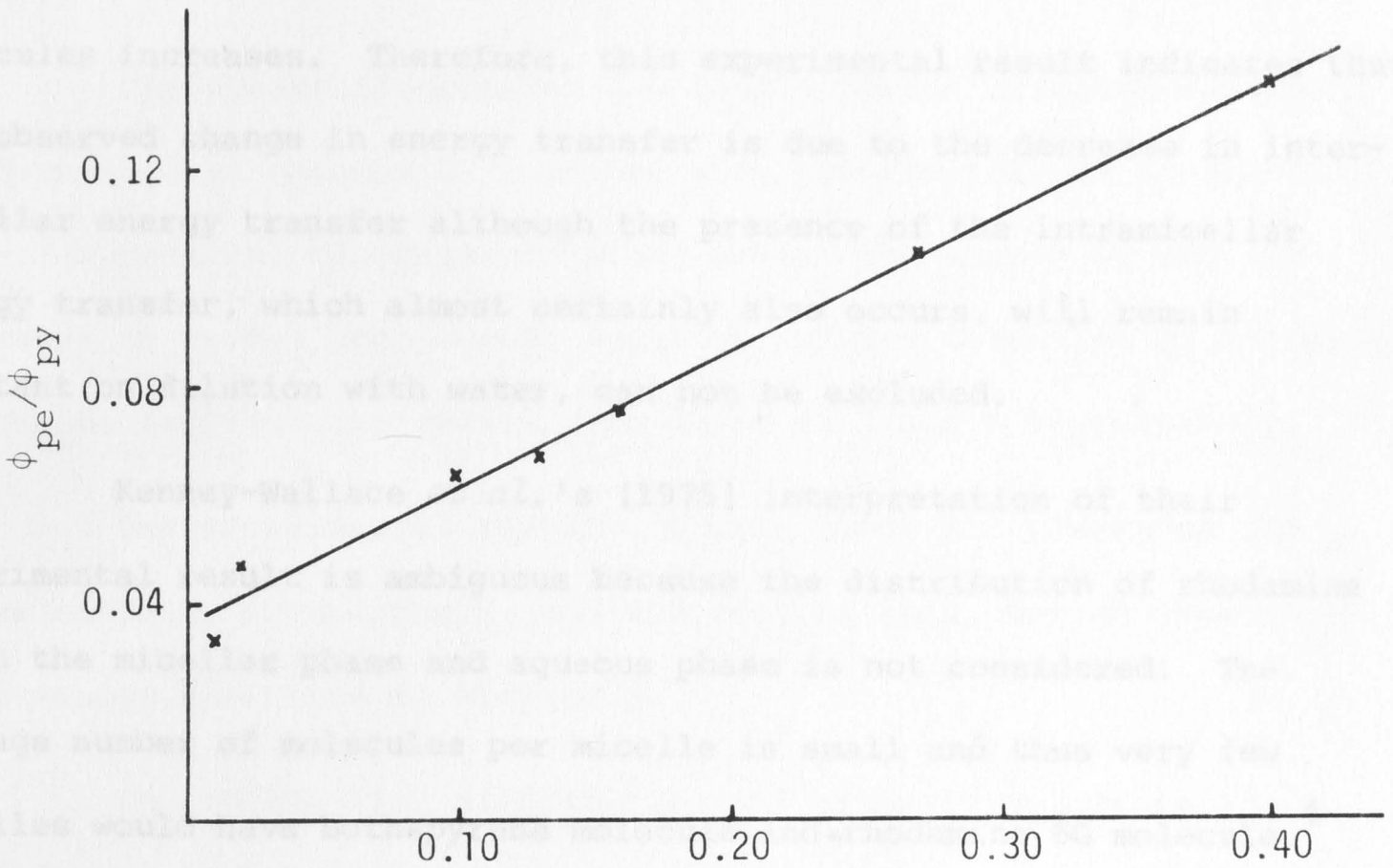

Figure 5.33. A plot of $\phi_{perylene}/\phi_{pyrene}$ against the concentration of Teric G9A10.

solution is diluted with water, the micelles are further apart while the ratios of pyrene to micelles and perylene to micelles remain unchanged. Thus perylene emission due to *intra*micellar transfer and direct excitation will not be expected to change with dilution. However, the probability of energy transfer between two neighbouring micelles will decrease on dilution with water as the distance between the two molecules increases. Therefore, this experimental result indicates that the observed change in energy transfer is due to the decrease in intermicellar energy transfer although the presence of the intramicellar energy transfer, which almost certainly also occurs, will remain constant on dilution with water, can not be excluded.

Kenney-Wallace *et al.*'s [1975] interpretation of their experimental result is ambiguous because the distribution of rhodamine 6G in the micellar phase and aqueous phase is not considered. The average number of molecules per micelle is small and thus very few micelles would have both a pyrene molecule and a rhodamine 6G molecule.† The excitation energy transfer may occur from pyrene (which is in the interior of a micelle) to a rhodamine 6G molecule which is in the aqueous phase or in a neighbouring micelle. The rate constant for energy transfer (1.2×10^7 s^{-1}) was very low compared to that in organic solvents.‡

---

† For a solution of 10^{-5} mol l^{-1} pyrene in 10^{-2} mol l^{-1} SDS with an assumed micelle aggregation number of 60, the average number of molecules per micelle is 0.06.

‡ The rate constant for energy transfer takes the values $10^{10} \sim 10^{11}$ litre/mole.sec in its order of magnitude in organic solvents [Mataga and Kubota 1970].

solution is diluted with water, the micelles are further apart while the ratios of pyrene to micelles and perylene to micelles remain unchanged. Thus perylene emission due to *intra*micellar transfer and direct excitation will not be expected to change with dilution. However, the probability of energy transfer between two neighbouring micelles will decrease on dilution with water as the distance between the two molecules increases. Therefore, this experimental result indicates that the observed change in energy transfer is due to the decrease in intermicellar energy transfer although the presence of the intramicellar energy transfer, which almost certainly also occurs, will remain constant on dilution with water, can not be excluded.

Kenney-Wallace *et al.*'s [1975] interpretation of their experimental result is ambiguous because the distribution of rhodamine 6G in the micellar phase and aqueous phase is not considered. The average number of molecules per micelle is small and thus very few micelles would have both a pyrene molecule and a rhodamine 6G molecule.† The excitation energy transfer may occur from pyrene (which is in the interior of a micelle) to a rhodamine 6G molecule which is in the aqueous phase or in a neighbouring micelle. The rate constant for energy transfer (1.2×10^7 s^{-1}) was very low compared to that in organic solvents.‡

---

† For a solution of 10^{-5} mol l^{-1} pyrene in 10^{-2} mol l^{-1} SDS with an assumed micelle aggregation number of 60, the average number of molecules per micelle is 0.06.

‡ The rate constant for energy transfer takes the values $10^{10} \sim 10^{11}$ litre/mole.sec in its order of magnitude in organic solvents [Mataga and Kubota 1970].

5.6 SUMMARY

This thesis has explored the use of fluorescent species as probes to study the behaviour and properties of surfactant micelles. Use has been made of excimers, exciplexes, protolytic reactions and energy transfer systems as probes.

The spectrofluorimeter and single photon counting equipment are described in chapter 2 together with the analysis of exponential and nonexponential fluorescence decay data. The theory of excited processes in normal homogeneous solution and the formation of micelles in aqueous solution are reviewed in chapters 3 and 4 respectively.

The experimental results of this study are presented and discussed fully in chapter 5, and the rest of this section summarises the findings described in chapter 5.

The statistical distribution of aromatic molecules in micelles has been examined using excimers as fluorescent probes. The ratio of the intensities of excimer to monomer fluorescence (ϕ'/ϕ) increases with the addition of a quencher. The time delay (Δt max) for the excimers decreases as the concentration of solutes increases. The fluorescence decay of pyrene monomer in some surfactant solutions is nonexponential. These three experimental results have been explained on the basis of the statistical distribution of solutes in micelles. The Poisson distribution is found suitable for describing the statistical distribution of solutes in micelles.

From the ratio $(A_o\tau_o/A\tau)$ obtained from the monomer decay curves, the ratio of multiply occupied micelles to singly occupied micelles has been obtained. Then the size of micelles has been calculated from the experimental values of (ϕ'/ϕ) and $(A_o\tau_o/A\tau)$ and the

theoretical curve of $f \times \frac{P(\geq 2)}{P(1)}$ using a Poisson distribution. The application of this technique has been demonstrated by studying the change in fluorescence quantum yield ratios and decay parameters with the ionic strength, temperature and length of surfactant molecules.

Some work has been carried out on the polarity of the micelles. The polarity of the solubilisation site of the 1-cyano-naphthalene*-naphthalene exciplex has been found to increase in the order: SDS, CDBA, methanol and nonionic micelles.

In the protolytic reactions of 2-naphthol in surfactant solutions, it has been found that the ROH^* and RO^{-*} species are photophysically unconnected during the lifetime of the excited state. The ROH^* species solubilised in the micelles does not dissociate at all. The pKa of the reaction increased in the presence of cationic micelles. The pKa is affected by the charge of the micelles and, in the case of nonionic micelles, the effect is caused by the solvation properties of the micelles.

Using fluorescence quenchers having different charges and different solubilities in water and in micelles, a method has been developed for locating the position of various solutes. Applying this method to the 2-naphthol-naphtholate equilibrium, it has been found that the naphtholate ion is located in the Stern layer of anionic micelles.

In a study of energy transfer from pyrene to perylene (both solubilised in micelles), it has been found that the probability of energy transfer decreases upon dilution with water. This result indicates that the energy transfer takes place by inter-micellar as well as intra-micellar processes.

REFERENCES

Almgren, M., 1972. *Photochem. Photobiol.* 15, 297.

Anacker, E.W., 1958. *J. Phys. Chem.* 62, 41.

Anacker, E.W., 1970. *Cationic Surfactants* (Jungermann, E., Ed., Marcel Dekker: New York), p.224.

Balmbra, R.R., Clunie, J.S., Corkill, J.M., and Goodman, J.F., 1962. *Trans. Faraday Soc.* 58, 1661.

Balmbra, R.R., Clunie, J.S., Corkill, J.M., and Goodman, J.F., 1964. *Trans. Faraday Soc.* 60, 979.

Beens, H., Knibbe, H., and Weller, A., 1967. *J. Chem. Phys.* 47, 1183.

Beens, H., and Weller, A., 1968. *Acta Phys. Polon.* 34, 593.

Berlman, I.B., 1971. *Handbook of Fluorescence Spectra of Aromatic Molecules* (Academic Press: New York).

Berrnett, M.K., and Zisman, W.A., 1959. *J. Phys. Chem.* 63, 1911.

Birks, J.B., 1967. *Nature* 214, 1187.

Birks, J.B., 1970a. *Photophysics of Aromatic Molecules* (Wiley-Interscience: London).

Birks, J.B., 1970b. *Prog. in Reaction Kinetics* 4, 181.

Birks, J.B., Dyson, D.J., and Munro, I.H., 1963. *Proc. Roy. Soc. A* 275, 575.

Blaustein, R.P., and Gant, K.S., 1973. *Photochem. Photobiol.* 18, 347.

Chapman, J.H., Förster, Th., Kortüm, G., Lippert, E., Melhuish, W.H., Nebbia, G., and Parker, C.A., 1963. *Appl. Spectry.* 17, 171.

Chen, M., Grätzel, M., and Thomas, J.K., 1974. *Chem. Phys. Letts.* 24, 65.

Cohen, M., and Selinger, B.K., 1969. *Mol. Photochem.* 1, 371.

Cohen, I., and Vassiliades, A.E., 1961. *J. Phys. Chem.* 65, 1781.

Corrin, M.L., and Harkins, W.D., 1946a. *J. Chem. Phys.* 14, 216.

Corrin, M.L., and Harkins, W.D., 1946b. *J. Chem. Phys.* 14, 481.

Döller, E., 1961. Ph.D. Thesis: Von der Technischen Hochschule, Stuttgart.

Döller, E., and Förster, Th., 1962. *Z. physik. Chem. N.F.* 34, 132.

Dorrance, R.C., and Hunter, T.F., 1972. *J. Chem. Soc. Faraday Trans. I* 68, 1312.

Dorrance, R.C., and Hunter, T.F., 1974. *J. Chem. Soc. Faraday Trans. I* 70, 1572.

Eigen, M., Kruse, W., Maass, G., and de Maeyer, L., 1964. *Prog. in Reaction Kinetics*, Vol. 2, Ch. 6 (Pergamon Press: London).

Elworthy, P.H., Florence, A.T., and Macfarlane, C.B., 1968. *Solubilization by Surface-Active Agents* (Chapman & Hall: London).

Elworthy, P.H., and McDonald, C., 1965. *Kolloid-Z.* 195, 16.

Eriksson, J.C., 1963. *Acta Chem. Scand.* 17, 1478.

Eriksson, J.C., and Gillberg, G., 1966. *Acta Chem. Scand.* 20, 2019.

Evans, H.C., 1956. *J. Chem. Soc.* Part 1, 579.

Fendler, E.J., and Fendler, J.H., 1970. *Adv. Phys. Org. Chem.* 8, 271.

Fendler, J.H., and Fendler, E.J., 1975. *Catalysis in Micellar and Macromolecular Systems* (Academic Press: New York).

Ferguson, L.N., 1955. *J. Amer. Chem. Soc.* 77, 5288.

Förster, Th., 1950a. *Z. Elektrochem.* 54, 42.

Förster, Th., 1950b. *Z. Elektrochem.* 54, 531.

Förster, Th., 1959. *Discussions Faraday Soc.* 27, 7.

Förster, Th., 1960. *Photochemistry in the Liquid and Solid States* (Daniels, F., Ed., John Wiley & Sons: New York), p.9.

Förster, Th., 1963. *Pure and Applied Chemistry* 7, 73.

Förster, Th., 1967. *Comprehensive Biochemistry* 22, 61 (Florkin, M., and Stotz, E.G., eds., Elsevier: Amsterdam).

Förster, Th., 1969. *Angew. Chem. internat. Edit.* 8, 333.

Förster, Th., and Kasper, K., 1955. *Z. Electrochem., Ber. Bunsenges Physik. Chem.* 59, 976.

Förster, Th., and Selinger, B.K., 1964. *Z. Naturforsch.* 19a, 38.

Geer, R.D., Eylar, E.H., and Anacker, E.W., 1971. *J. Phys. Chem.* 75, 369.

Geiger, M.W., and Turro, N.J., 1975. *Photochem. Photobiol.* 22, 273.

Goddard, E.D., and Benson, G.C., 1957. *Can. J. Chem.* 35, 986.

Goodwin, A., and Nichols, R.J., 1972. Unpublished data: Australian National University, Canberra.

Grätzel, M., and Thomas, J.K., 1972. *J. Amer. Chem. Soc.* 95, 6885.

Griffith, O.H., and Waggoner, A.S., 1969. *Acc. Chem. Res.* 1, 17.

Hamilton, C.L., and McConnell, 1968. *Structural Chemistry and Molecular Biology* (Rich, A., and Davidson, N., Eds., Freeman and Co.: San Francisco), p.115.

Harris, C.M., 1975. B.Sc. Honours Thesis: Australian National University, Canberra.

Harris, C.M., 1976. Private communication.

Hartley, G.S., 1936. *Aqueous Solutions of Paraffin Chain Salts* (Hermann et Cie: Paris).

Hauser, M., and Klein, U., 1972. *Z. Phys. Chem.* 78, 32.

Hauser, M., and Klein, U., 1973. *Acta Phys. Chem.* XIX(4), 363.

Hautala, R.R., Schore, N.E., and Turro, N.J., 1973. *J. Amer. Chem. Soc.* 95, 5508.

Hautala, R.R., and Turro, N.J., 1972. *Mol. Photochem.* 4, 545.

Heckman, K.D., 1958. *Discussions Faraday Soc.* 25, 71.

Hinde, A., 1975. Private communication.

Horrocks, D.L., and Brown, W.G., 1970. *Chem. Phys. Letts.* 5, 117.

Hyde, A.J., and Robb, D.J.M., 1964. Proceedings 4th International Congress on Surface Active Substances, Brussels, 1964 (Gordon and Breach: New York, 1967), p.743.

Jaffé, H.H., and Orchin, M., 1962. *Theory and Application of Ultraviolet Spectroscopy* (John Wiley and Sons: New York), p.556.

Jaycock, M.J., and Ottewill, R.H., 1964. Proceedings 4th International Congress on Surface Active Substances, Brussels, 1964 (Gordon and Breach: New York, 1967), p.545.

Jungermann, E., 1970. *Cationic Surfactants* (Marcel Dekker: New York).

Kenney-Wallace, G.A., and Flint, J.H., 1975. *Chem. Phys. Letts.* 32, 71.

Klein, U.K.A., and Hauser, M., 1975. *Z. Phys. Chem. N.F.* 96, 139.

Klevens, H.B., 1948. *J. Phys. Chem.* 52, 130.

Klevens, H.B., 1953. *J. Amer. Oil Chemists Soc.* 30, 74.

Knibbe, H., 1969. Ph.D. Thesis: Vrije Universiteit te Amsterdam.

Knibbe, H., Röllig, K., Schäfer, F.P., and Weller, A., 1967. *J. Chem. Phys.* 47, 1184.

Knight, A.E.W., and Selinger, B.K., 1971. *Spectrochimica Acta* 27A, 1223.

Knight, A.E.W., and Selinger, B.K., 1973. *Aust. J. Chem.* 26, 1.

Kuriyama, K., 1962. *Kolloid-Z.* 180, 55.

Leonhardt, H., and Weller, A., 1963. *Ber. der Bunsenges. Phys. Chem.* 67, 791.

Maclay, W.N., 1956. *J. Colloid Science* 11, 272.

Mataga, N., Kobashi, H., and Okada, T., 1967. *Chem. Phys. Letts.* 1, 133.

Mataga, N., and Kubota, T., 1970. *Molecular Interactions and Electronic Spectra* (Marcel Dekker: New York), p.182.

Mataga, N., Okada, T., and Yamamoto, N., 1967. *Chem. Phys. Letts.* 1, 119.

McBain, J.W., 1913. *Trans. Faraday Soc.* 9, 99.

McBain, M.E.L., and Hutchinson, E., 1955. *Solubilization and Related Phenemona* (Academic Press: New York).

McBain, J.W., and McHan, H., 1948. *J. Amer. Chem. Soc.* 70, 3838.

McDonald, R.J., 1972. Ph.D. Thesis: Australian National University, Canberra.

McDonald, R.J., and Selinger, B.K., 1971a. *Mol. Photochem.* 3(2), 99.

McDonald, R.J., and Selinger, B.K., 1971b. *Aust. J. Chem.* 24, 249.

Mukerjee, P., 1967. *Adv. Colloid Interface Sci.* 1, 241.

Mysels, K.J., and Princen, L.H., 1959. *J. Phys. Chem.* 63, 1696.

Nakagawa, T., Kuriyama, K., and Inoue, H., 1960. *J. Colloid Science* 15, 276.

Nakagawa, T., and Shinoda, K., 1963. *Colloidal Surfactants* (by Shinoda, K., Nakagawa, T., Tamamushi, B., and Isemura, T., Academic Press: New York), p.140.

Nott, P.R., 1971. B.Sc. Honours Thesis: Australian National University, Canberra.

Nott, P.R., and Selinger, B.K., 1972. *J. Luminescence* 5, 138.

Osborne, A.D., and Porter, G., 1965. *Proc. Roy. Soc. A* 284, 9.

Parker, C.A., 1968a. *Photoluminescence of Solutions*, §4D (Elsevier: Amsterdam).

Parker, C.A., 1968b. *Photoluminescence of Solutions*, §4C (Elsevier: Amsterdam).

Patterson, L.K., and Vieil, E., 1973. *J. Phys. Chem.* 77, 1191.

Pinion, J.P., Minn, F.L., and Filipescu, N., 1971. *J. Luminescence* 3, 245.

Pownall, H.J., and Smith, L.C., 1973. *J. Amer. Chem. Soc.* 95, 3136.

Riegelman, S., Allawala, N.A., Hrenoff, M.K., and Strait, L.A., 1958. *J. Colloid Science* 13, 208.

Schick, M.J., 1962. *J. Colloid Science* 17, 801.

Schick, M.J., 1967. *Nonionic Surfactants* (Marcel Dekker: New York).

Schick, M.J., Atlas, S.M., and Eirich, F.R., 1962. *J. Phys. Chem.* 66, 1326.

Seidell, A., 1952. *Solubility of Inorganic and Organic Compounds*, Supplement to 3rd Edn. (Van Nostrand: London).

Seidel, H.P., 1963. Ph.D. Thesis, Stuttgart.

Selinger, B.K., 1966. *Aust. J. Chem.* 19, 825.

Selinger, B.K., and McDonald, R.J., 1972. *Aust. J. Chem.* 25, 897.

Shinitzky, M., 1973. *Chem. Phys. Letts.* 18, 247.

Shinitzky, M., Dianoux, A.C., Gitler, C., and Weber, G., 1971. *Biochemistry* 10, 2106.

Shinoda, K., 1955. *J. Phys. Chem.* 59, 432.

Shinoda, K., 1963. *Colloidal Surfactants* (by Shinoda, K., Nakagawa, T., Tamamushi, B., and Isemura, T., Academic Press: New York), Chapter 1.

Shinoda, K., 1967. *Solvent Properties of Surfactant Solutions* (Marcel Dekker: New York).

Shinoda, K., Nakagawa, T., Tamamushi, B., and Isemura, T., 1963. *Colloidal Surfactants* (Academic Press: New York).

Singhal, G.S., Rabinowitch, E., Hevesi, J., and Srinivasan, U., 1970. *Photochem. Photobiol.* 11, 531.

Smoluchowski, M., 1917. *Z. Phys. Chem.* 92, 129.

Speed, R., and Selinger, B.K., 1969. *Aust. J. Chem.* 22, 9.

Stevens, B., and Ban, M.I., 1964. *Trans. Faraday Soc.* 60, 1515.

Stevens, B., and Dubois, J.T., 1966. *Trans. Faraday Soc.* 62, 1525.

Stevens, B., and Hutton, E., 1960. *Nature* 186, 1045.

Stigter, D., 1975. *J. Phys. Chem.* 79, 1008; *ibid.* 1045.

Tanford, C., 1973. *The Hydrophobic Effect: Formation of Micelles and Biological Membranes* (John Wiley & Sons: New York).

Tong, L.K.J., and Glesmann, M.C., 1957. *J. Amer. Chem. Soc.* 79, 4305.

van der Donckt, E., 1970. *Prog. in Reaction Kinetics*, Vol. 2, Ch. 5 (Pergamon Press: London).

Walker, M.S., Bednar, T.W., and Lumry, R., 1966. *J. Chem. Phys.* 45, 3455.

Wallace, S.C., and Thomas, J.K., 1973. *Radiat. Res.* 54, 49.

Weber, K., 1931. *Z. Physik. Chem. (Leipzig)* B15, 18.

Weller, A., 1952. *Z. Elektrochem.* 56, 662.

Weller, A., 1954. *Z. Elektrochem.* 58, 849.

Weller, A., 1961. *Prog. in Reaction Kinetics*, Vol. 1, Ch. 7 (Pergamon Press: London).

Weller, A., 1967. Proc. 5. Nobel Symposium (Claesson, S., ed.), p.413.

Wilairat, P., 1966. B.Sc. Honours Thesis: Australian National University, Canberra.

Wright, K.A., Abbott, A.D., Sivertz, V., and Tartar, H.V., 1939. *J. Amer. Chem. Soc.* 61, 549.

Yoshihara, K., and Kasuya, T., 1971. *Chem. Phys. Letts.* 9, 469.